MELANOMA MAINTENANCE BY THE AP1 TRANSCRIPTION FACTOR FOSL1

DISSERTATION ZUR ERLANGUNG DES

NATURWISSENSCHAFTLICHEN DOKTORGRADES

DER JULIUS-MAXIMILIANS-UNIVERSITÄT WÜRZBURG

VORGELEGT VON

KATJA MAURUS

GEBOREN IN MEMMINGEN

WÜRZBURG 2016

EINGEREICHT AM: _____

MITGLIEDER DER PROMOTIONSKOMMISSION:

VORSITZENDER: _____

1. GUTACHTER: Prof. Dr. rer. nat. S. Meierjohann
2. GUTACHTER: Prof. Dr. rer. nat. C. Stigloher

TAG DES PROMOTIONSKOLLOQUIUMS: _____

DOKTORURKUNDE AUSGEHÄNDIGT AM: _____

Erklärungen

nach §4 Abs. 3 Satz 3, 5, 8 der Promotionsordnung

der Fakultät für Biologie

Hiermit erkläre ich ehrenwörtlich, die vorliegende Dissertation eigenständig, d. h. insbesondere selbständig und ohne Hilfe eines kommerziellen Promotionsberaters, angefertigt und keine anderen, als die von mir angegebenen Quellen und Hilfsmittel verwendet zu haben.

Ich erkläre außerdem, dass die Dissertation weder in gleicher noch in ähnlicher Form bereits in einem anderen Prüfungsverfahren vorgelegen hat.

Würzburg, August 2016 _____

Katja Maurus

Content

Summary

Identifying novel driver genes in cancer remains a crucial step towards development of new therapeutic approaches and the basic understanding of the disease.

This work describes the impact of the AP1 transcription activator component FOSL1 on melanoma maintenance. FOSL1 is strongly upregulated during the progression of melanoma and the protein abundance is highest in metastases. I found that the regulation of FOSL1 is strongly dependent on ERK1/2- and PI3K- signaling, two pathways frequently activated in melanoma. Moreover, the involvement of p53 in FOSL1 regulation in melanoma was investigated. Elevated levels of the tumor suppressor led to decreased FOSL1 protein levels in a miR34a/miR34c- dependent manner.

The benefit of elevated FOSL1 amounts in human melanoma cell lines was analyzed by overexpression of FOSL1 in cell lines with low endogenous FOSL1 levels. Enhanced levels of FOSL1 had several pro-tumorigenic effects in human melanoma cell lines. Besides increased proliferation and migration rates, FOSL1 overexpression induced the colony forming ability of the cells. Additionally, FOSL1 was necessary for anchorage independent growth in 3D cell cultures. Microarray analyses revealed novel downstream effectors of FOSL1. On the one hand, FOSL1 was able to induce the transcription of different neuron-related genes, such as *NEFL*, *NRP1* and *TUBB3*. On the other hand, FOSL1 influenced the transcription of *DCT*, a melanocyte specific gene, in dependence of the differentiation of the melanoma cell line, indicating dedifferentiation.

Furthermore, FOSL1 induced the transcription of *HMGA1*, a chromatin remodeling protein with reprogramming ability, which is characteristic for stem cells. Consequently, the influence of HMGA1 on melanoma maintenance was investigated. In addition to decreased proliferation and reduced anoikis resistance, *HMGA1* knockdown reduced melanoma cell survival. Interestingly, the FOSL1 induced pro-tumorigenic effects were demonstrated to be dependent on the HMGA1 level. HMGA1 manipulation reversed FOSL1 induced proliferation and colony forming ability, as well as the anchorage independent growth effect.

In conclusion, I could show that additional FOSL1 confers a clear growth benefit to melanoma cells. This benefit is attributed to the induction of stem cell determinants, but can be blocked by the inhibition of the ERK1/2 or PI3K signaling pathways.

Zusammenfasssung

Die Identifizierung von neuen onkogenen Mutationen in Tumoren ist nach wie vor ein unerlässlicher Schritt für die Entwicklung neuer Therapieansätze und für das grundlegende Verständnis der Tumorerkrankungen.

Die vorliegende Arbeit beschreibt den Einfluss der AP1-Transkriptionskomplexkomponente FOSL1 auf die Tumorigenität des humanen Melanoms. FOSL1 wird im Verlauf der Melanomentwicklung stark hochreguliert und ist in Metastasen am stärksten exprimiert. Darüber hinaus konnte gezeigt werden, dass FOSL1 Expression stark von ERK1/2- und PI3K- vermittelten Signalen abhängig ist, welche im Melanom sehr häufig übermäßig aktiviert sind. Auch p53 ist an der Regulierung von FOSL1 im Melanom beteiligt. Durch eine Erhöhung der Proteinmenge dieses Tumorsuppressors konnte ich die Verminderung des FOSL1-Levels beobachten und konnte weiterhin zeigen, dass dieser Regulation ein miR34a/c- vermittelter Mechanismus unterliegt.

Weiterhin untersuchte ich den Vorteil einer erhöhten FOSL1- Menge in menschlichen Melanomzellen, indem FOSL1 in Zellen mit niedrigem endogenen FOSL1- Gehalt konstitutiv überexprimiert wurde. Erhöhte FOSL1- Mengen hatten unterschiedliche protumorigene Effekte auf humane Melanomzellen. Neben deutlich gesteigerter Proliferation und Migration konnte ich auch die FOSL1- induzierte Koloniebildung der Zellen demonstrieren. Ergänzend konnte gezeigt werden, dass FOSL1- Expression für Anoikisresistenz von Zellen notwendig ist.

Des Weiteren konnte mit Hilfe einer Microarrayanalyse neue FOSL1- regulierte Effektoren identifiziert werden. Zunächst konnte demonstriert werden, dass FOSL1 zahlreiche neuronale Gene in ihrer Expression beeinflusst. Im Speziellen wurde *NEFL*, *NRP1* und *TUBB3* validiert. Zusätzlich nahm FOSL1 Einfluss auf die Expression von *DCT*, einem melanozytenspezifisch exprimierten Gen. Die Regulierung von *DCT* durch FOSL1 war abhängig vom Differenzierungsgrad der untersuchten Melanomzelllinien und wies, zusammen mit der Induktion von neuronal-assoziierten Genen, auf Dedifferenzierungsvorgänge hin.

Neben den neuronalen Genen wurde auch die Expression von *HMGA1*, einem Chromatin-Remodeling-Faktor mit Reprogrammierungseigenschaften, durch FOSL1 induziert, was unter anderem charakteristisch für Stammzelligkeit ist. Infolge dieser Beobachtungen wurde der Einfluss von HMGA1 auf das humane Melanom untersucht. Die Herabregulierung von *HMGA1* hatte unterschiedliche antitumorigene Effekte auf Melanomzellen. Zusätzlich zu stark verminderter Proliferation und Anoikisresistenz zeigten die Melanomzellen auch reduzierte Überlebensraten. Interessanterweise waren die FOSL1- induzierten, protumorigenen Effekte stark abhängig vom HMGA1- Gehalt der Zellen. Die Manipulation der *HMGA1*- Level machte die FOSL1- induzierte Proliferation, die Fähigkeit zur Koloniebildung und die Anoikisresistenz rückgängig.

Zusammenfassend konnte ich darstellen, dass zusätzliches FOSL1 einer Melanomzelle einen klaren Wachstumsvorteil verschafft. Dieser Vorteil ist der Induktion von Stammzelldeterminanten zu verdanken und kann durch die spezifische Inhibierung von ERK1/2- und PI3K- Signalkaskaden verhindert werden.

1 Introduction

1.1 Malignant melanoma

1.1.1 Occurrence and incidence of melanoma

Melanoma is a form of skin cancer, which arises from pigment producing cells, the melanocytes. Consequently, melanoma can occur in pigment cell containing tissues, meaning in the skin, in the uvea, and in the different mucosal areas of our body. Malignant melanoma constitutes one of the rarest, but also one of the most aggressive types of skin cancers. Skin cancer in general is the most commonly diagnosed cancer in Germany and the U.S. Worldwide, more than 3 million new cases are diagnosed annually, but only 4% are classified as melanoma. For 2014, 19700 new patients are estimated for Germany [1] and 76100 new cases for the U.S. [2]. Malignant melanoma is responsible for 75% of skin cancer related deaths. Moreover, regarding the last three decades, melanoma shows an increasing incidence. The average age of melanoma diagnosis is 61 years, but it is also a common cancer in young adults [2].

1.1.2 Melanocyte function and melanoma development

Under normal conditions, the homeostasis of melanocytes is strictly controlled by factors secreted by neighboring keratinocytes. The keratinocytes are also involved in the most important function of the melanocytes, the production of melanin, a pigment which protects our skin from carcinogenic UV irradiation and thereby preventing DNA damage and mutagenesis. The synthesis of melanin in melanocytes is UV induced. In response to UV, keratinocytes produce the melanocyte-stimulating hormone (α-MSH), which binds the melanocortin-1 receptor (MC1R) of melanocytes, resulting in the activation the cAMP pathway. Subsequently, cAMP signaling induces the transcription of MITF (microphthalmia-associated transcription factor), the crucial melanocytic transcription factor, thereby activating melanin production [3].

The tight control by the keratinocytes can be disrupted when melanocytes acquire growth autonomy, e.g. caused by mutations in growth regulatory genes. Consequently, the melanocytes can gain proliferative and dispersive features, leading to the development of a mole or nevus, generally classified as benign lesions, but sometimes containing morphologically atypic melanocytes. These nevi are able to further advance to radial growth phase (RGP) melanoma which show local micro-invasion to the dermis. A following progression to the vertical growth phase (VGP) cells has severe consequences. The cells in this phase already possess metastatic potential and form nests from where they invade the dermis and infiltrate the vascular and lymphatic systems (Figure 1) [4]. However, it is

important to note that only roughly 30% of all occurring melanoma tumors are derived from pre-existing nevi [5, 6]. It has also been reported that single melanocytes can give rise to RGP or VGP growth. Furthermore, isolated melanocytes or nevi can directly progress to the metastatic stage [4].

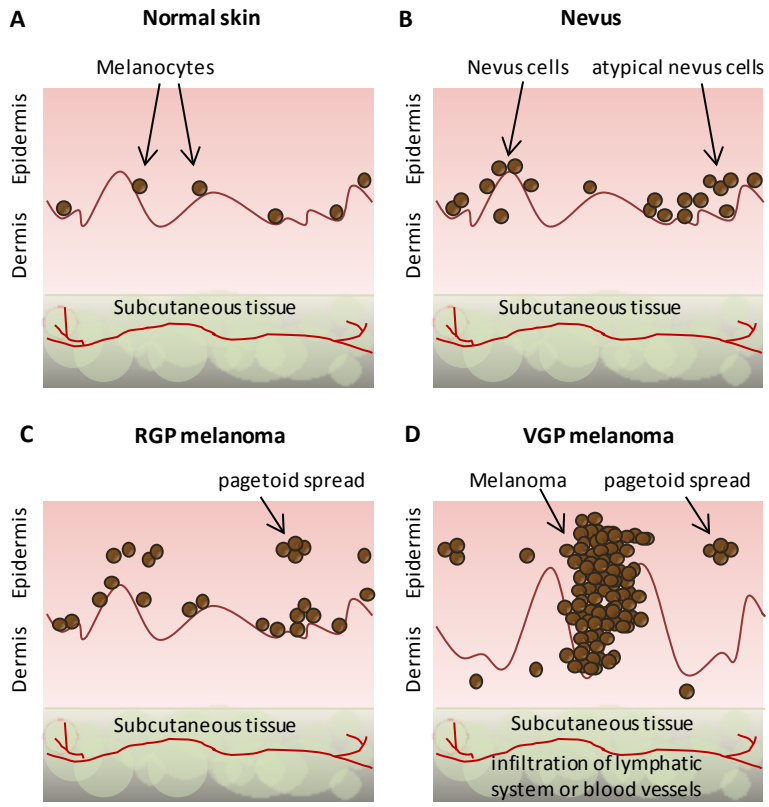

Figure 1: Melanocyte transformation
A. Normal skin. Melanocytes are located in the basal layer of the epidermis. **B**. Nevi and atypical nevi. Here, the number of melanocytes is increased. They form benign lesions. Some of them contain atypical melanocytes. **C**. Radial growth phase (RGP) melanoma. Primary malignant stage of melanoma with pagetoid spread of atypical melanocytes. **D**. Vertical growth phase (VGP) melanoma. This stage has malignant potential and can lead directly to metastatic malignant melanoma by infiltrating the lymphatic or vascular system. Adapted from [4].

For the survival of affected patients it is critical, at which stage the melanoma lesion is diagnosed. Different stages at diagnosis involve different therapy strategies and strongly affect survival rates. Generally, the earlier a melanoma lesion is detected the less severe the impact is on the patients' health. Patients with a local lesion show a 5-survival rate of 98.1% if the lesion is surgically removed. If the melanoma has already spread to regional lymph nodes 62.6% of the patients survive this time span. A tumor which has already metastasized to distant lymph nodes or organs at the time of diagnosis lowers the 5-year survival rate to 16.1%. In 3% of all melanoma cases the stage remains unknown. Patients of this group show a 5-year survival of 78.3% (Figure 2) [7].

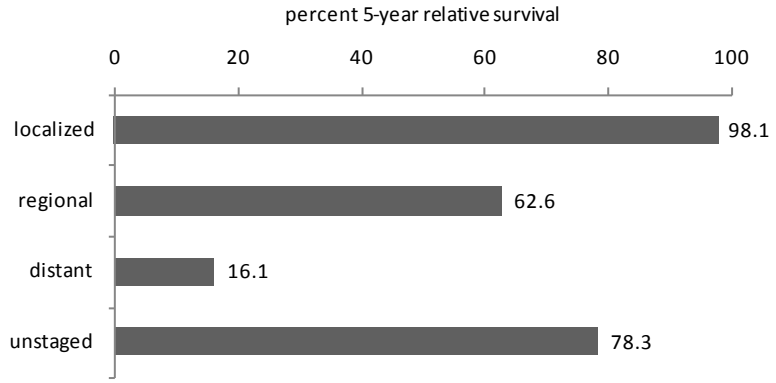

Figure 2: 5-year-survival of patients depending on the stage at diagnosis of cutaneous melanoma
Based on data from SEER 2004-2010 (The Surveillance, Epidemiology, and End Results), all races, both sexes in the U.S.[7]

Cutaneous melanoma is the most frequent form of melanoma. It is divided into four subtypes. The most frequent one is the superficial spreading melanoma (SSM), which accounts for 57.4% of cutaneous melanomas. Furthermore, the nodular melanoma (NM) type accounts for 21.4% of the cases and the lentigo maligna melanoma (LMM) is diagnosed in 8.8% of all cutaneous melanoma patients. The less common form of cutaneous melanoma is the acral lentiginous melanoma (ALM), which accounts for 4% among the German population [8].

5% of all occurring melanomas develop in the ocular and adnexal structures of patients. With 85% the majority of theses tumors arise in the uvea, whereas conjunctival and orbital melanomas are rare [9]. Besides malignant melanomas of the skin and the eye, melanoma can occur on mucosal surfaces. These cases constitute approximately 1% of all melanomas and occur in the head and neck region, the anorectal region and the female genital tract, as well as in the esophagus, gallbladder, bowel, and urethra [10].

1.2 Melanoma pathogenesis and effector pathways

In general, it has to be distinguished between familial and sporadic melanoma. Both are related to different subsets of oncogenic mutations. Familial melanoma constitutes only 10% of all occurring cases, whereas sporadic melanomas represent the other 90%.

1.2.1 Familial melanoma

In familial melanoma, *CDKN2A* (cyclin-dependent kinase inhibitor 2A) plays a major role [11]. A large scale comparison of studies from Europe, North America, the Middle East and Australia displayed that

38% of families prone to melanoma show mutations within the *CDKN2A* gene [12]. The *CDKN2A* gene locus encodes two proteins, P14ARF (alternative reading frame) and P16INK4A (inhibitor of cyclin dependent kinase 4). Both proteins act as tumor suppressors. In non-transformed cells, P14ARF blocks the p53 inhibitor MDM2 (murine double minute homolog), thereby inducing G1 and G2 checkpoints arrests. P16INK4A inhibits the catalytic activity of CDK4 and CDK6 enzymes and consequently the phosphorylation of RB, resulting in blocked G1- to S-phase transition [13, 14].

In affected families, the loss-of-heterozygosity or mutations within this locus were highly linked to enhanced melanoma susceptibility [11, 15]. Furthermore, deletions in this locus were found in several cancer cell lines and somatic mutations in the gene were also discovered to a certain extent in sporadic melanoma [16]. In addition, certain inherited variants of the *MC1R* (melanocortin 1 receptor) gene also enhance melanoma risk. Generally, MC1R mediates the generation of the black/brown eumelanin, whereas reduced receptor activity leads to prevailing synthesis of the red/yellow pheomelanin [17]. Hence, inactivating polymorphisms within the gene are causative for the red hair/fair skin phenotype in humans. Persons with this phenotype have an enhanced melanoma risk, as the pheomelanin is less protective against UV radiation than eumelanin. Moreover, pheomelanin was described to reinforce UVA-induced reactive oxygen species production [18]. Mice harboring an inactivating mutation within the *Mc1r* gene as well as the melanoma promoting $Braf^{V600E}$ mutation showed a phenotype similar to red hair/fair skin humans and a highly increased incidence of invasive melanoma. Interestingly, this way was independent of UV exposure [19].

1.2.2 Sporadic melanoma

Besides genetic risk factors, melanomagenesis is affected by environmental risk factors, the most important one being repeated exposure to UV light. Development of melanoma is enhanced by severe sunburns, especially in early childhood and during adolescence [2].

In these melanoma cases, most of the causative mutations are involved in the regulation of two major pathways, the ERK1/2-pathway and the PI3K-signaling pathway. They are constitutively activated in more than 90% and 60% of all cutaneous melanoma cases, respectively [4]. Furthermore, p53-signaling plays a crucial role in melanomagenesis, as the prominent tumor suppressor is frequently mutated or downregulated in melanoma.

1.2.3 The ERK1/2-pathway

The ERK1/2 (extracellular-signal-regulated kinase) signaling pathway is the best characterized of all MAPK pathways and is involved in the regulation of a variety of different cellular processes.

Furthermore, it is implicated in tumorigenic processes in many human tumor types as well as melanoma. This pathway is hyperactivated in up to 90% of all melanoma patients and affects central tumor driving processes such as differentiation, proliferation, survival, anchorage independent growth, EMT and metastasis, and immune evasion [20-22].

In non-transformed cells, the ERK1/2 pathway is embedded into a signaling cascade, which converts extracellular stimuli to transcriptional regulators with a receptor tyrosine kinase (RTK) at its top. This RTK is activated by extracellular growth factor ligand binding, resulting in a phosphorylation cascade. The activated RTKs transmit their signaling to the RAS (rat sarcoma) protein, which is membrane bound and activated in the GTP-bound state. In addition to SH2-domain harboring adaptor proteins (for example GRB2), guanine-nucleotide exchange factors (GEFs, for example SOS) are required for this activation. Activated RAS subsequently recruits cytosolic RAF (rapidly accelerated fibrosarcoma) to the membrane where it gets phosphorylated. P-RAF then phosphorylates MEK1/2, finally resulting in the phosphorylation of ERK1/2 directly by MEK1/2. ERK1/2 is phosphorylated at specific threonine and tyrosine residues (for example Thr202/ Tyr204). Consequently, ERK1/2 is translocated to the nucleus, where it is responsible for activation of downstream transcription factors and complexes such as MYC, FOS, AP1, and ELK and many others (Figure 3) [23].

The mutations within this pathway which, are found in malignant melanoma, are distributed throughout almost any level of this signaling cascade, but all lead to hyperactivation of ERK1/2. The predominant mutation in cutaneous melanoma affects the BRAF protein, which is encoded by one of the three *RAF* genes (besides *ARAF* and *CRAF*), and is found in around 60% of all melanoma cases [24]. The most common mutation in this case results in an amino acid exchange from valine to glutamic acid at position 600 (V600E). This alteration leads to a conformational change of BRAF due to the phospho-mimetic glutamic acid, localized between two phosphorylation residues (Thr598/Ser601) which are involved in the activation of wiltype BRAF. Thus the $BRAF^{V600E}$ results in hyperactivation of the kinase, as it is no longer dependent on signal transmission through RAS to propagate its signal to MEK1/2. Wan et al. found that this mutation leads to an approximately 500 fold increased kinase activity [25]. Certainly, the role of CRAF is also relevant in melanomas. It is the main isoform that is activated by mutated and hyperactivated RAS [26]. The second, most commonly mutated gene that results in hyperactivation of the ERK1/2-signaling pathway is the *NRAS* gene. Mutations of NRAS are found in 20% of cutaneous melanomas, whereas HRAS and KRAS, two other well described RAS- oncogenes, are only mutated in 1% and 2%, respectively. The most frequently mutated position constitutes codon 61. Amino acid substitutions at this position from glutamine to arginine or lysine result in impaired GTPase activity. Less frequent mutational events occur at position 12 and 13, leading to the transcription of a RAS protein which is insensitive to the inactivation by RAS GTPase-activating proteins (GAPs). All mentioned mutations render RAS constitutively activated and thereby cause elevated ERK1/2 signaling

[27]. NRAS and BRAF mutations are mutually exclusive in malignant melanoma, which is a strong indication for the similar role in ERK1/2 signaling induction [28].

Moreover, oncogenic RAS also activates further downstream signaling pathways such as the PI3K/AKT pathway. In the context of melanoma, this pathway plays an important role and will be explained separately in the next chapter. In addition to NRAS and BRAF, activation of the MAPK pathway can be reached by mutations in RTKs, which are further upstream. Activating mutations in cutaneous melanoma were only described for KIT (mast/stem cell growth factor receptor) [29]. Mutations in the *KIT* gene are displayed in 23% of samples of acral, mucosal or frequently sun-damaged skin sites [30]. For MET (hepatocyte growth factor receptor) and EGFR (epidermal growth factor receptor), overexpression of the protein was observed in late-stage melanomas, which was due to genomic amplifications of the encoding genomic regions [31, 32]. A study from 2009 revealed that *ERBB4* (V-Erb-B2 avian erythroblastic leukemia viral oncogene homolog 4), another RTK, is mutated in 19% of a panel of 79 melanomas, leading to enhanced kinase activity and transforming ability [33].

For uveal melanomas, mutation in *GNAQ* (guanine nucleotide-binding protein G (q) subunit alpha) and *GNA11* (guanine nucleotide-binding protein subunit alpha-11) are found as the most common tumor contributing oncogenes. In 83% of all uveal melanomas, either *GNAQ* or *GNA11* carry activating mutations. The two proteins act as the alpha subunits of heterotrimeric G proteins. The mutations occur in most cases at either position R183 or Q209 in the *GNA11* gene and at position Q209 in the *GNAQ* gene and lead to diminished GTPase activity, which in turn results in constitutive activation and upregulation of ERK1/2 signaling through PKC (protein kinase C) [34, 35].

1.2.4 The PI3K/AKT-pathway

The phosphatidylinositide 3-kinase can be activated by RTKs as well as RAS proteins (Figure 3). RAS is capable of recruiting the catalytic subunit of PI3K (p110α, β, γ or δ) to the membrane. These subunits get into contact with the regulatory subunit (p85, p65, p55 or p101) and the substrate phosphatidylinositol-3,4-biphosphate (PIP2), which is subsequently phosphorylated, thereby forming the second messenger PIP3 (phosphatidylinositol-3,4,5- triphosphate). The antagonist of the PI3K is the tumor suppressor and lipid phosphatase PTEN (phosphatase and tensin homolog), as PTEN catalyzes the dephosphorylation of PIP3 to PIP2. The next signal transmission events within this cascade are the stimulation of PDK1 by PIP3 and the following phosphorylation and partial activation of AKT. Complete AKT activation demands a further phosphorylation for example by mTOR-complex2 (mechanistic target of rapamycin, formerly mammalian target of rapamycin) or AKT itself [36, 37]. Accordingly, AKT modulates a broad spectrum of effector molecules including the pro-apoptotic protein BAD, different forkhead transcription factors, such as FOXO1/3a and mTOR (involved in the

mTOR-complex1). PI3K/AKT signaling is involved in the modulation of cell survival, cell growth, cell proliferation, angiogenesis, cellular metabolism as well as migration and invasion (reviewed in [38, 39]).

This PI3K/AKT signaling pathway is hyperactivated in up to 60% of sporadic melanomas, due to the already mentioned RAS activating mutation and different other mutations occurring within the pathway [40]. In 19% of melanomas PTEN is strongly reduced or absent, leading to enhanced levels of PIP3 and thereby to increased levels of P-AKT [41]. PTEN loss-of-function mutations are found in around 20% of BRAF mutated melanomas [42]. Less common are mutations concerning *PIK3CA*. In comparison to other tumor entities, where alterations in this gene are found in up to 57% e.g. in uterine tumors, alterations in the p110α catalytic subunit was detected in 3-5% of melanomas [43]. For AKT, mutation events were found to be rare. However, AKT3, the predominant AKT isoform in melanoma, was identified to be amplified in 6-7% of the melanoma patients [28].

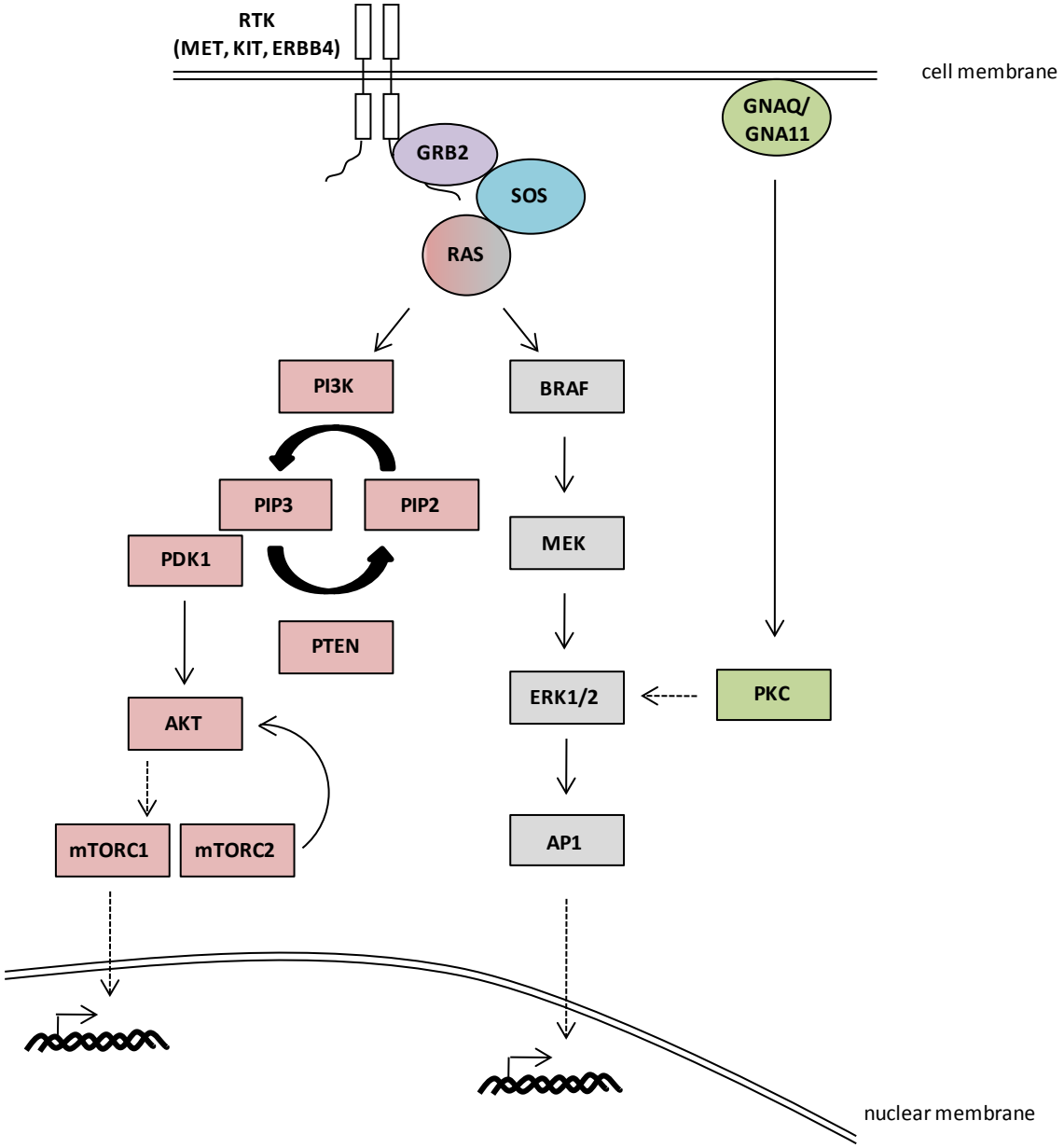

Figure 3: Relevant signaling pathways in human melanoma
Schematic overview of the ERK1/2- and PI3K/AKT- signaling cascades, which promote protumorigenic effects in the vast majority of cutaneous melanoma tumors. Moreover, the GNAQ/GNA11 signaling axis is shown, which plays a crucial role in uveal melanoma. The single components of the signaling pathways are described and explained in the continuous text.

1.2.5 The MDM/p53-pathway

P53 is one of the best investigated tumor suppressors and was first described thirty-five years ago. It is implicated in many biological processes including cell cycle arrest, apoptosis, DNA-repair, differentiation, angiogenesis and metabolism. P53 acts as a universal stress sensor and the regulation of distinct target genes depends on the nature of the stimuli, activating p53 signaling. Thus, p53 regulates different subsets of genes, which either induce apoptosis or cell cycle arrest (reviewed in [44,

45]). *TP53* is mutated in 50% of all human cancer cases [46]. In melanoma, mutations within the *TP53* gene are detected in 10-20% of all cases [47].

One important regulator of p53 is MDM2 (mouse double minute 2 homolog). MDM2 binds the p53 protein and acts as a ubiquitin E3 ligase to destabilize p53 through degradation by the proteasome [48].

Moreover, MDM2 acts as a transcriptional inhibitor of p53. It binds to the N-terminal transcription domain of p53 and thereby avoids transcriptional target gene induction [49, 50]. A more important MDM protein in the context of melanoma is MDM4 (mouse double minute 4 homolog), which acts similar to MDM2 as a transcriptional inhibitor of p53 by binding to the transcription domain. MDM4 is overexpressed in approximately 65% of investigated melanoma cases. This in turn leads to strongly downregulated or even absent p53 in this tumor type. MDM2 is upregulated to a lesser extent in melanoma, however enhanced levels of MDM2 or MDM4 result in the lack of cell cycle control and thereby favoring tumor growth [51]. An additional and crucial regulator of p53 is the p14ARF protein encoded by the *CDKN2A* gene locus. As mentioned above, this locus is strongly associated with familial melanoma, but altogether it is deleted or mutated in 44% of cutaneous melanoma cases, irrespective of the familial or sporadic origin [28]. In somatic cells, p14ARF binds to MDM2 and precludes the MDM2-dependent p53 degradation [52]. Hence, the lack of p14ARF in melanoma causes p53 destabilization and disrupted cell cycle control.

The tumor suppressive features of p53 strongly depend on the transcriptional activity of p53. Classically, p53 is stabilized after genotoxic stress through a variety of posttranslational modifications, then translocated to the nucleus and finally p53 binds as a tetramer to defined response elements close to the promoter regions of its target genes [53].

For transcription initiation, diverse histone modifications are necessary to open the chromatin in a more accessible configuration. In this context, it has been described, that after p53 binding, histone acetyltransferases are recruited in a p53-dependent manner. The best examined transferases in this regard, constitute the p300/ CBP complex forming transferases. They connect transcription factors to the POLII holoenzyme, acetylate histones in the proximity of target gene promoters and assist thereby in the activation of transcription [54]. Moreover, these histone acetyltranferases are found to also acetylate p53 itself correlating with an enhanced transactivative property of p53 [55, 56].

1.3 The AP1 complex and its component FOSL1

One prominent ERK1/2 signaling- dependent transcription regulator, which is implicated in tumorigenesis, is the activator protein 1 (AP1). The AP1 transcription factor complex binds to heptamer 12-O-tetradecanoylphorbol-13-acetate (TPA) response elements (TRE, 5'TGA(C/G)TCA3') or to octamer cAMP responsive elements (CRE) with a specific 5'TGACGCTA3' consensus sequence [57, 58].

The exact transcriptional effect of an AP1 transcription factor complex depends on the composition of the complex [59, 60]. AP1 acts as a dimeric transcription factor complex, which is composed of JUN, FOS and ATF family members. The JUN family of transcription factors consists of JUN, JUNB and JUND. They can form homodimers and activate transcription. The family of FOS proteins includes the proteins c-FOS, FOSB, FOSB2, FOSL1 and FOSL2. All members contain a bZIP domain for dimerization and DNA-binding. Additionally, c-FOS and FOSB harbor a C-terminal transactivation domain. FOS proteins alone are not able to form homodimers and to activate gene expression on their own, thus they have to form heterodimers to induce transcription [61]. ATF proteins harbor also a bZIP region for DNA-binding and dimerization. Due to the bZIP domain, they are able to form homodimers and additionally heterodimers with either the JUN or the FOS family members [60].

1.3.1 FOSL1- the FOS-related antigen 1

The cellular immediate early gene *Fos-related antigen 1* (*FOSL1*) encodes for the FOSL1 protein. *FOSL1* is located on chromosome 11q13.1, contains four exons and five transcript variants are described. Transcript variant FOSL1-001 constitutes the main isoform and is translated into the FOSL1 protein existing of 271 amino acids [62]. The best described dimerization partners for FOSL1 are the members of the JUN protein family. Dimers are mainly observed between FOSL1 and JUN, but also, to a lesser extent, JUNB and JUND, especially in the context of tumorigenensis [63]. Although the JUN proteins are the main dimerization partners of FOSL1, FOSL1 can form dimeric AP1 complexes with ATF4 (activating transcription factor 4) [64].

Moreover, USF (upstream stimulating factor) is reported to interact with FOSL1. Whereas ATF-complexes preferentially bind to octamer cAMP responsive elements (CRE), USF interaction with FOSL1 indirectly inhibits AP1 activating function by interacting with FOSL1 [65].

1.3.2 FOSL1 and its biological function

Mice with a constitutive *Fosl1* knockout are not viable. They already die *in utero* between embryonic stage E10 and E10.5 due to placental defects. The placental labyrinth layer of *Fosl1* knockout mice shows a clearly reduced size and a diminished number of vascular endothelial cells leading to strong vascularisation defects in this tissue. Mutant embryos are severely retarded in growth. Interestingly, this growth effect is no cell-autonomous effect, as proliferation of primary ES and MEF cells derived from these mice is unaltered compared to primary cells of wildtype mice [66]. The placental defects of the *Fosl1*-/- mice can be avoided by injection of *Fosl1*-/- ES cells into tetraploid wild-type blastocyts resulting in mice without apparent phenotypic defects and a survival up to two days after birth.

To study the impact of FOSL1 on development, Eferl et al. generated a mouse model with a conditional floxed *Fosl1* version crossed to *Mox2-cre* knock-in mice (mesenchyme homeobox 2), which leads to deletion during gastrulation. Thus, the depletion of FOSL1 is restricted to the embryo and the lethal placenta-phenotype is avoided. The embryos lacking *Fosl1* develop osteopenia. The authors uncovered several FOSL1 regulated target genes, which contribute to bone matrix formation, mainly collagen1a2 and matrix GLA protein. These proteins are produced by osteoblasts and chondrocytes [67]. In contrast to this mouse model, Jochum et al. investigated mice with ectopic expression of *Fosl1* under the major histocompatibility complex class I antigen H2-K^b promoter. In these transgenic mice, FOSL1 was overexpressed in a variety of organs, such as bone, liver, heart, spleen, thymus, kidney, brain, testis, and lung. The transgenic mice suffer from osteosclerosis, as well as lipodystrophy [68, 69]. The osteosclerosis phenotype relies on FOSL1 overexpression induced progressive bone mass production and goes with the findings of Eferl et al., who observed reduced bone mass formation in *Fosl1* knockout mice [67].

1.3.3 Tumorigenic features of FOSL1

Although *Fosl1* transgenic mice do not show a tumorigenic phenotype, FOSL1 was soon considered to be implicated in cancer progression. The ectopic overexpression of FOSL1 in established rat fibroblasts was found to be sufficient to induce anchorage independent growth of these cells and moreover to transfer the capability to form tumors in athymic mice [70]. Additionally, it was demonstrated that FOSL1 was highly upregulated in RAS-transformed fibroblasts and essential for a transformed phenotype in wildtype mouse fibroblasts, if overexpressed together with JUN [71]. Furthermore, FOSL1 was also shown to play crucial role in malignant processes in RAS-transformed thyroid cells [72]. A study from Kustikova et al. investigated the different expression levels of FOSL1 of a highly metastatic and a non-metastatic cell line derived from the same ancestral mouse mammary adenocarcinoma. FOSL1 expression was elevated in the metastatic cell line, but almost absent in the non-metastatic epithelial like cell line. If FOSL1 was overexpressed in the non-metastatic cell line, cells showed a more mesenchymal morphology and enhanced motility and invasiveness *in vitro* [73]. Bakiri et al. recently demonstrated enhanced proliferation, motility and invasiveness after ectopic expression of FOSL1 in non-transformed, mouse mammary epithelial cells. Furthermore, these cells showed a mesenchymal phenotype as well as tumorigenic potential, as they invaded mouse lungs upon transplantation experiments. As FOSL1- targets and molecular regulators for the described invasive phenotype, they uncovered the prominent epithelial- to- mesenchymal- transition- inducing (EMT) transcription factors ZEB1, ZEB2 and SLUG [74].

In humans, FOSL1 is often upregulated in different tumors of epithelial tissue, such as thyroid, breast, lung, nasopharynx, esophagus, endometrium, and the prostate, as well as in glioblastomas, mesotheliomas, colon and head and neck squamous cell carcinomas [63, 75]. The role of FOSL1 is best understood in breast cancer. In a study of 2001, it was described that the level of FOSL1 in primary breast cancers directly correlates with an aggressive phenotype [76]. Four years later, Belguise et al. found that in breast cancer cell lines FOSL1 levels positively influenced cell proliferation, cell motility and invasiveness. In addition, they showed that FOSL1- dependent *MMP1* and *MMP9* transcription went along with increased malignant features of the cells [77]. Recently, Zhao et al gained more insight into the invasive phenotype of triple-negative breast cancer. They identified FOSL1 as direct inducer of ZEB2 expression. This led to the repression of *CDH1* (epithelial cadherin), leading to an EMT comparable phenotype as a basis for the invasive behavior [78]. In epithelial cells, E-cadherin mediates cell-cell contact at the basolateral membrane in adherens junctions [79]. Consequently, downregulation of E-cadherin leads to decreased adhesion and enhanced cellular motility. Moreover, FOSL1 is considered to have prognostic relevance in human breast cancers, as FOSL1 overexpression highly correlates with the progression of tumors [80, 81].

Taken together, FOSL1 was shown to enhance malignancy of different tumor entities by regulating migration- and invasion-relevant genes.

1.4 Aim of the thesis

To better understand processes, which determine the onset and the progression of human tumors such as melanoma, it is inevitable to detect novel driver proteins and to characterize their specific functions during tumorigenesis. Furthermore, it is important to uncover, how potential drivers are regulated and how they influence the tumor relevant cellular processes. FOSL1 belongs to the genes, which are strongly upregulated during melanoma development and progression.

So far, the role of FOSL1 has been characterized in epithelial tumors, where it is strongly linked to EMT processes and metastasis. As the function and tumorigenic relevance of FOSL1 in melanoma is entirely unknown, one aim of this thesis was to analyze the role of FOSL1 in human melanoma. Moreover, I was interested in the regulation and stabilization of FOSL1 in human melanoma cell lines and in identifying novel target genes of the transcription factor.

2. Material and methods

2.1 Material

2.1.1 Cell lines

Table 1: Cell lines

Cell line	Supplier	Type
A375	ATTC	human melanoma derived from metastatic site
HCT116	A. Paschen (Essen)	human colon carcinoma
HEK 293T	M. Gessler (Würzburg)	human embryonic kidney
M14	NCI/NIH	human melanoma derived from metastatic site
M19Mel	NCI/NIH	human melanoma derived from metastatic site (axillary node)
MelHo	A. Bosserhoff (Regensburg)	human melanoma derived from primary tumor
NHEM	Promocell	normal human epidermal melanocytes
SkMel2	NCI/NIH	human melanoma derived from metastatic site
SkMel28	ATCC	human melanoma derived from metastatic site
UACC257	NCI/NIH	human melanoma
UACC62	NCI/NIH	human melanoma

2.1.2 Plasmids

Table 2: Plasmids

Backbone	Insert
P201-iEP	-
p201-iEP	FOSL1wt
p201-iEP	FOSL1flag
pPAX2	-
CMV-VSVg	-

2.1.3 Inhibitors and compounds

Table 3: Inhibitors and compounds

Compound	Manufacturer	Catalog number
PD184352	Axon Medchem	1368
Nutlin3a	Axon Medchem	1880
Puromycin	Calbiochem	32438
SN-38	Tocris	2684

X-tremeGene siRNA Transfection Reagent	Roche	04476093001
GDC 0941	Selleck Chem	S1065
Sodium butyrate	Sigma Aldrich	B5887
PEI Polyethylenimine	Eurogentech	-

2.1.4 siRNAs

Table 4: siRNAs

siRNA	manufacturer	Catalog number
ON-Target plus Non-Targeting pool	Thermo scientific	D-001810-10-20
siGENOME SMARTpool FOSL1	Thermo scientific	M-004341-04
siGENOME SMARTpool HMGA1	Thermo scientific	M-004597-02

2.1.5 Antibodies

Table 5: Primary antibodies for western blot

Primary antibodies	Manufacturer	Catalog number	Applied dilution
β-Actin	Santa Cruz	sc-47778	1:10000
FOSL1	Santa Cruz	sc-605	1:500
FOSL1	Cell Signaling	5281	1:1000
P53	Santa Cruz	Sc-126	1:500
P-FOSL1$_{SER265}$	Cell Signaling	3880	1:1000
P-ERK p42/44 $_{Thr202/Tyr204}$	Cell Signaling	9101	1:5000
P-p53$_{Ser15}$	Cell Signaling	9284	1:2000
tubulin	Sigma-Aldrich	T6074	1:5000
vinculin	Sigma-Aldrich	V9131	1:10000
P-AKT$_{SER473}$	Cell Signaling	9271	1:1000
HMGA1	Cell Signaling	12094S	1:2000
MITF	C.Goding (Ludwig Institute for Cancer Research, University of Oxford)		1:2500

Table 6: Secondary antibodies for western blot

Secondary antibodies	Manufacturer	Catalog number	Applied dilution
Goat Anti-mouse IgG+IgM (H+L) (POD)	Thermo Scientific	31444	1:3000

Goat Anti-rabbit IgG (H+L) (POD)	Bio-Rad	170-6515	1:3000

2.1.6 Kits

Table 7: Kits

KIT	Manufacturer	Catalog number
Bradford Reagent	Sigma-Aldrich	B6916
GenElute PCR Clean-Up Kit	Sigma-Aldrich	NA1020-1KT
GenElute™ HP Plasmid Miniprep Kit	Sigma-Aldrich	NA0160-1KT
TRIzol® Reagent 200 ml	Life technologies	15596018
PureYield Plasmid Midiprep System	Promega	A2495
RevertAid First Strand cDNA Kit	Fermentas	K1622
RNeasy® Mini-Kit	Quiagen	74106
SuperSignal West Pico Chemiluminescent Su.	Thermo Scientific	LH146987

All kits were used according to the manufacturer`s instructions.

2.1.7 Buffers

Table 8: Buffers

Buffer	
EDTA	3.42 mM; adjusted to pH 7.4
Laemmli	312,5 mM Tris pH 6.8; 10% SDS, 50% glycerine 0.005% bromo-phenol-blue; 25% ß-mercaptoethanol
Lysis buffer	20 mM HEPES (pH 7.8), 500 mM NaCl, 5 mM $MgCl_2$, 5 mM KCl, 0.1% deoxycholate, 0.5% Nonidet-P40, 10 mg/ml aprotinin, 10 mg/ml leupeptin, 200 mM Na_3VO_4, 1 mM phenylmethanesulphonyl- fluoride and 100 mM NaF
PBS	137 mM NaCl; 2.7 mM KCl; 4.3 mM Na_2HPO_4; 1.47 mM KH_2PO_4; adjusted to pH 7.4
Reprofast PCR Buffer	100 mM $(NH4)_2SO_4$; 200 mM Tris pH 8.8; 100 mM KCl 20 mM $MgSO_4$; 1% Triton; 1% BSA
SDS running buffer	250 mM Tris; 192 mM glycine; 0.5% SDS
TBST	10 mM Tris pH 7.9; 150 mM NaCl; 0.1% Tween
Transfer buffer	25 mM Tris; 192 mM glycine; 20% methanole

2.1.8 qPCR oligonucleotides

Table 9: Oligonucleotides used for qPCR

GENE	Oligo forward	Oligo reverse
RPS14	CTCAGGTGGCTGAAGGAGAG	GCAGCCAACATAGCAGCATA
NEFL	AGTTCATGAGCTGCAACACG	GGTCTCTGAGGGTCAAGCAG
NRP1	AGGCCAAGACCCTGGAAATC	CACGTTGAGGAGGTCTTGGT
TUBB3	GACTGGGGCTCAGAATGGAG	ACCTGATTGTATGGTGCTGTCT
HMGA1	TCTCACAAGTACGTGCCTCG	CATCCAGGACCGAATCCACC
DCT	AACCAAAGCCACCAGTGTTC	GGTTCCTTTCTTCCCTCCAG
TYR	CCGCTATCCCAGTAAGTGGA	TACGGCGTAATCCTGGAAAC
FOSL1	AGCTGCAGAAGCAGAAGGAG	GGAGTTAGGGAGGGTGTGGT

2.1.9 Cloning oligonucleotides

Table 10: Oligonucleotides used for cloning procedures

GENE/CONSTRUCT	Oligo forward	Oligo reverse
FOSL1	gcgc**GCTAGC**ATGTTCCGAGACTTCGGGGA	gcgc**GGATCC**TCACAAAGCGAGGAGGGTTG
FOSL1-flag	gcgc**GCTAGC**ATGTTCCGAGACTTCGGGGA	gcgc**GGATCC**TCA*CTTATCGTCGTCATCCTTG TAATC*CAAAGCGAGGAGGGTTGGAG

Small form letters indicate the oligonucleotides' ends, located outside the cloned gene. Fat capital letters highlight the recognition sites of the used restriction enzymes (GCTAGC for NheI/GGATCC for BamHI). Normal capital letters indicate the start and end sequences of the cloned gene. Italic capital letters indicate the flag tag sequence.

2.1.10 ChIP oligonucleotides

Table 11: Oligonucleotides used for ChIP PCR

gDNA binding region (distance from HMGA1 transcriptional start site)	Oligo forward	Oligo reverse
-12577	GCATGAGGCAGCGTGAGT	AGCAGCGTTTCGAACACTTTC
-4808	CCCATGCCAAACACCCTACT	TAATGCCAGCCTGAGGAAGC
+7272	TCATTCCTTGAGCTGAGCCAC	TGCCAGGCACAAACTCCAAA
+7836	TCAGCCCTGACTCATCCCTC	AGTTGTTGGTGTGAGCTCTGG

2.1.11 ChIP buffers

Table 12: ChIP buffers

Buffer	
ChIP dilution buffer	0.01% SDS, 1.1% TritonX-100, 1.1 mM EDTA, 20 mM Tris pH 8.0, 167 mNaCl, 1X Roche Complete protease inhibitor, 50 µg/ml PMSF
Elution buffer	50 mM Tris pH 8.0, 10 mM EDTA, 1% SDS
High salt wash buffer	500 mM NaCl, 2 mM EDTA, 10 mM Tris-HCl pH 8.0, 1% TritonX 100, 0.1% SDS, 1X Roche Complete protease inhibitor, 50 µg/ml PMSF
LiCl wash buffer	250 mM LiCl, 1 mM EDTA, 10 mM Tris-HCl pH 8.0, 0.5% Nonidet P 40, 0.5% SDS, 1X Roche Complete protease inhibitor, 50 µg/ml PMSF
Low salt wash buffer	150 mM NaCl, 2 mM EDTA, 10 mM Tris-HCl pH 8.0, 1 % TritonX-100, 0.1% SDS, 1X Roche Complete protease inhibitor, 50 µg/ml PMSF
Lysis buffer	50 mM Hepes-KOH pH 7.5, 150 mMNaCl, 1 mM EDTA, 1 % TritonX 100, 0.1 % Deoxycholate, 0.1 % SDS, 1X Roche Complete protease inhibitor, 50 µg/ml PMSF
Nuclei lysis buffer	50 mMHepes-KOH pH 7.5, 150 mMNaCl, 1 mM EDTA, 1 % TritonX 100, 0.1 % Deoxycholate, 1 % SDS, 1X Roche Complete protease inhibitor, 50 µg/ml PMSF

2.1.12 Technical equipment

Photo Image Station 4000MM (Kodak)

Mastercycler ep Realplex (Eppendorf)

Mini-PROTEAN Tetra Electrophoresis System (Biorad)

Trans Blot Cell (Biorad)

Cary 50 Spectrophotometer (Varian)

NanoDrop ND-1000 Spectrophotometer (NanoDrop Technologies)

Hera Cell 150i Incubator (Thermo Scientific)

CTR 6000 inverted microscope (Leica)

Cytomics FC 500 flow cytometer (Beckman Coulter)

Bioruptor® Standard sonifier

2.2 Methods

2.2.1 Cell culture methods

2.2.1.1 Maintenance of cells

All cell lines were kept at 37°C and 5% CO_2 in a Hera Cell 150i Incubator (Thermo Scientific). Human colon carcinoma cells were grown in RPMI medium containing 10% FCS (fetal calf serum) and 1x penicillin/streptomycin (Sigma). The human melanoma cell lines were kept in DMEM (high glucose) containing 10% FCS and 1x penicillin/streptomycin. NHEM cells were maintained in Ham's F10 containing 20% FCS, 100 nM TPA (Calbiochem), 200 pM cholera toxin (Calbiochem), penicillin/streptomycin, 100µM 3-isobtyl-1-mthylxanthine and ITS^{TM} Premix (1:1000 BD Bioscience).
Cells were grown regularly treated with 1x trypsin in EDTA (Sigma) and were passaged to avoid confluence. For long term storage the cell lines were frozen in freezing medium, containing DMEM, 20% FCS and 10% dimethylsulfoxide and stored at -80 °C. For long-term storage, cells were kept in liquid nitrogen.

2.2.1.2 Generation of transgenic cell lines

Transgenic cell lines were generated using a lentiviral vector system. For this purpose, 60-70% confluent HEK293T cells were cotransfected with the lentiviral vectors (p201-iEP/ p201-*FOSL1*/ p201-*FOSL1flag,* each 6 µg) and two helper plasmids pPAX2 (4.5 µg) and pCMV-VSVG (3 µg), encoding lentiviral envelop and packaging proteins, respectively. The plasmids were diluted in a total volume of 250 µl DMEM. 1xPEI (Polyethylenimine, 100 mg/ml diluted in 1:100 in 150 mM NaCl) was used as transfection reagent and also prepared in DMEM. After 2 minutes of incubation, the PEI mix was added to the DNA mix and the mixture was vortexed and incubated for 20 minutes. The transfection mix was then added dropwise to the HEK293T cells. 8 hours later medium was exchanged. On day two, virus accumulation was promoted by adding 10 mM sodium butyrate for eight hours to the medium. On day four after transfection, supernatant, containing the virus was harvested, sterile filtered and transferred to the target melanoma cells for eight hours. Remaining virus was shock frozen in liquid nitrogen and stored at -80°C. To select for the stable transgenic cells, puromycin (1-2 µg/ml) was added after two more days for one week.

2.2.1.3 siRNA transfection

Cells were seeded in 6 well dishes and were grown until they reached 70-80% confluence. siRNA transfection was performed using XtremeGene reagent (Roche) according to the manufacturer's

recommendations. If not stated otherwise, 12 µl of a 10 µM siRNA stock together with 5 µl XtremeGene were used per well of a 6-well plate. Firstly, the siRNA was prepared in Opti-MEM reduced serum medium (life technologies) in a total volume of 100µl. Secondly, the XtremeGene was dissolved in 95 µl Opti-MEM and mixed with the siRNA. After 15 minutes of incubation, the transfection mix was added dropwise to the cells, which were kept in 900 µl DMEM containing 10% FCS and 1x penicillin/streptomycin. Eight hours after transfection medium was exchanged. 24 hours after transfection the cells were reseeded to new dishes for the following assays. 24 hours later additional treatments were performed or cells were harvested 48-72 hours after transfection for microarray, RT-qPCR and western blot analyses.

2.2.1.4 Proliferation assay

To determine the influence of overexpression or siRNA mediated knockdown of investigated genes on the proliferative capacity of different cell lines manual cell counting was performed. The cells were seeded in triplicates to six well plates at equal cell numbers (2-4 x 10^4) and were allowed to grow for six days. Afterwards, cells were all harvested, resuspended in PBS (0.05 – 1 ml) and counted at day three and six using a Neubauer hemacytometer.

2.2.1.5 Transwell migration assay

To determine the motility of the cells, cells with 70% confluence were starved in DMEM containing 1% dialyzed FCS. After 24 hours, the transwell inlays (BD Falcon Cell Culture Insert, 24 well format, 8.0µm pore size) were equilibrated in the same medium. Next, 2x 10^4 cells in starving medium were applied to the upper layer of the transwell and DMEM containing 10% FCS was placed in the lower well to attract them. Cells were allowed to migrate between 8 and 24 hours, depending on the cell line. After removal of non migrated cells from the upper membrane layer, cells on the lower layer of the transwell were fixed with methanol and membranes were stained with Hoechst diluted 1:10000 in PBS for ten minutes. After imaging the membranes with an inverse fluorescent microscope, cells were counted.

2.2.1.6 Colony formation assay

To determine the ability of autonomous growth of single cells, cells were seeded in 6 well dishes. The conditions for the single cells were chosen very stringent, thus only 150 to 400 cells per well were seeded. After an incubation time of 12 days cells were fixed with methanol for 10 minutes. Afterwards, the colonies were stained with 2 % crystal violet dissolved in ethanol. After 20 minutes the crystal

violet solution was removed. Several washing steps with PBS were followed by imaging with an inverted microscope.

2.2.1.7 Soft agar assay

To investigate anoikis independent growth of cells, soft agar assays were performed in 6 wells. Initially, the 6 wells were prepared with a lower layer consisting of 0.6% bactoagar (Difco) mixed with D20 medium (DMEM containing 20% FCS and 1x Penicilin/Streptomycin). After solidifying of the first soft agar layer, the second layer was prepared. The second, upper layer contained the $2x\ 10^4$ cells collected in D20 medium, mixed with soft agar with a final concentration of 0.3%. Mixture was poured on the first layer and was also dried. Each of the layers had a final volume of 2ml. Cells were allowed to form colonies for up to 7 days. Every 3 to 4 days D20 was added in small amounts to the soft agar to guarantee adequate maintenance of the cells. The development of the colonies was documented by capturing 5x5 wide range images with an inverted microscope. Afterwards, all colonies consisting of at least 8 cells were counted in a defined, consistent area of 6 representative connected images of the total 25 images.

2.2.1.8 FACS/ cell cycle analysis

After trypsinization, at least $1x\ 10^5$ cells were harvested and washed with PBS. Afterwards, they were fixed with 70-80% of ice-cold ethanol for at least 24 hours. Thereafter, cells were washed twice in PBS and were centrifuged for 5 minutes at 1000 rpm. After repeated centrifugation, cells were resuspended in 500µl of a 38mM sodium citrate solution and were treated with 25 µl RNaseA (10 mg/ml) at 4°C over night. The next day, cells were stained with 8µl propidium iodide (2 mg/ml) and cell cycle profiles were measured with a Cytomics FC 500 flow cytometer (Beckman Coulter). Data were analyzed with the according CXP software (Beckman Coulter).

All cell culture assays were performed at least two times in triplicates.

2.2.2 RNA and DNA methods

2.2.2.1 Vector cloning procedure

To generate FOSL1 overexpressing melanoma cells, the human *FOSL1* gene was amplified by PCR from cDNA derived from the melanoma cell line A375 using primers each containing recognition sites for restriction enzymes (NheI and BamHI from Thermo scientific). Amplificates were cleaned up using

GenElute PCR Clean-Up Kit (Sigma- Aldrich). Additionally to the full length *FOSL1* gene, a second *FOSL1* flag-tagged construct was cloned. For this purpose, a second reverse primer containing the sequence for a flag-tag and the mentioned forward primer were applied for an equivalent *FOSL1* PCR to generate a flag-tagged *FOSL1* version. To achieve a constitutive overexpression of the *FOSL1* and the *FOSL1flag* construct, the CMV promoter containing p201-iEP vector was chosen (Figure 4). This lentiviral vector also contains an IRES site which drives the expression of an EGFP-puromycin cassette.

Double digestion of the p201-iEP vector and the PCR product was performed simultaneously for 1 hour at 37°C. The vector was dephosphorylated for 15 minutes at 37°C with shrimp alkaline phosphatase (Thermo scientific). After another purification step, vector and insert were ligated at 14°C over night with T4 ligase (Thermo Scientific). Reaction mixtures were calculated according to the instructions of the manufacturer. Subsequently, constructs were transformed in $CaCl_2$ competent DH5α E.coli (NEB) according to the manufacturers' high efficiency transformation protocol.

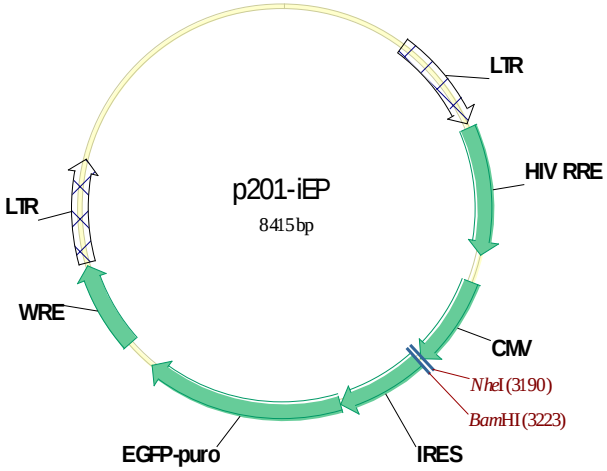

Figure 4 p201-iEP empty vector
Scheme of the lentiviral overexpression vector p201-iEP. Indicated restriction sites for NheI and BamHI mark the integration site for human *FOSL1* and *FOSL1flag*.

2.2.2.2 RNA extraction, cDNA synthesis and RT-qPCR

Cells were harvested by centrifugation, and the pellet was applied to isolate RNA using TRIzol® reagent (life technologies) according to the manufacturer's protocol. DNA digestion was performed afterwards with DNAseI for one hour at 37°C (Thermo Scientific). RNA concentration was measured with a NanoDrop spectrophotometer. Subsequently, 1-4 µg of RNA was reversely transcribed with a RevertAid First Strand cDNA Synthesis Kit from Fermentas. For RT-qPCR 25 ng of total RNA per reaction were applied. According to the manufacturer, mRNA comprises 1-3% of total RNA. All reactions were conducted in triplets. mRNA levels were normalized to the housekeeping gene *RPS14.* PCR reactions were performed and analyzed with a Mastercycler ep Realplex from Eppendorf.

Standard protocol for one reaction:

14.25 µl ddH_2O
2.5 µl 10xBuffer (ReproFast)
0.75 µl forward primer (10 pmol/µl)
0.75 µl reverse primer (10 pmol/µl)
0.3 µl Taq-polymerase
0.7 µl dNTPs
0.75 µl SYBR-GREEN (1:2000)
5 µl cDNA (5 ng/µl)

Table 13: Standard cycling program

Step	Temp.	Time	
1	95°C	pause	
2	95°C	5’	
3	95°C	15’’	x40
4	60°C	15’’	
5	72°C	15’’	
6	95°C	5’	
7	60°C	15’’	
8	60°C-95°C gradient	20’’	
9	95°C	15’’	

All RT-qPCR assays were performed at least two times in triplicates unless stated otherwise. Only from experiments, performed at least three or more times the significance was determined using Student’s t-test (*: $p<0.05$; **: $p<0.01$; ***:$p<0.001$).

2.2.3 Protein methods

2.2.3.1 Protein lysis, SDS-PAGE and Western Blot

To extract proteins from cells, cells of interest were harvested from culture dishes with a silicone rubber or with trypsin/EDTA and were subsequently lysed in lysis buffer. The amount of lysis buffer depended on the size of the pellet and was between 20 and 80 µl. Using one ml Bradford reagent (Sigma–Aldrich) per one µl of lysate, the protein concentration was measured using the Cary 50 Spectrophotometer (Varian).

Afterwards, 40µg of protein, diluted in lysis buffer and denaturing 5 % Laemmli buffer containing β-mercaptoethanol were separated during a SDS-PAGE (sodium dodecyl sulfate polyacrylamide gel electrophoresis) [82]. Polyacrylamide gels contained 12-14% of Rotiphorese®Gel 40 (37, 5:1) (Roth). Subsequently, the proteins were transferred to nitrocellulose membranes (Whatman) in a wet blot procedure at 4°C with 25mA per gel.

To investigate the proteins and their regulation, membranes were sampled with specific antibodies. For this purpose, after blocking the membrane in 5 % BSA (Serva) in TBST for 1 hour at room temperature, membranes were incubated overnight at 4 °C in blocking solution containing the primary antibody in the recommended dilution. Next, membranes were washed several times in TBST and incubated in blocking reagent with the dissolved horseradish peroxidase coupled secondary antibodies for 1 hour at room temperature. Finally, after a new TBST washing cycle, detection of the protein bands was performed using SuperSignal West Pico Chemiluminescent Substrate (Thermo Scientific) and a Photo Image Station 4000MM (Kodak).

2.2.3.2 Chromatin immunoprecipitation (ChIP)

6 x 10^6 of UACC62 empty vector cells and FOSL1-flagtagged overexpressing cells of a subconfluent culture were used for chromatin immunoprecipitation. Chomatin immunoprecipitation was performed as described before [83]. Briefly, cells were fixed with 1% paraformaldehyde for 10 minutes at room temperature. Fixation was stopped by addition of glycine to 0.2 M for 5 minutes. Afterwards, cells were washed three times with ice-cold PBS and were harvested. All following steps were performed at four degrees. Cells were lysed in cell lysis buffer and centrifuged for five minutes. The won pellet of nuclei was lysed in nuclei lysis buffer and sonicated using a Bioruptor® Standard sonifier for 25 minutes (on “high” with 30 seconds pulse and 30 seconds break). The cell debris was removed by centrifugation. For the following immunoprecipitation, chromatin was diluted tenfold with ChIP dilution buffer. 1.5 ml of diluted chromatin was added with 40 µL 1:1 protein G agarose (blocked for four hours in ChIP dilution buffer with 10 µg/ml BSA and 1 µg/ml Salomon sperm DNA) (Pierce), incubated for one hour and centrifuged. The resulting pre-cleared supernatant was then incubated with 4 µg anti-flag-tag antibody (α-flag-M2, Sigma-Aldrich) overnight. Subsequently, 60 µl 1:1 protein G agarose diluted in ChIP buffer was added and the mixture was incubated for two hours. Afterwards, the agarose beads were washed two times with low salt washing buffer, once with high salt washing buffer and four times with LiCl washing buffer. Each washing step was performed for five minutes. The elution was accomplished using 200 µl of the elution buffer at 68°C for 30 minutes. The eluted chromatin was then incubated with 0.8 mg/ml proteinase K and PFA fixation was reversed by 68°C overnight. The gDNA

was purified by performing phenol-chloroform extraction and additionally a Cycle Pure Kit (Omega Bio-Tek). gDNA was eluted in 120 µl.

To check for FOSL1flag binding to the UACC62 gDNA, PCR was performed with primers amplifying 100 bp fragments in case of binding.

Standard protocol for one reaction:

15 µl ddH_2O
2.5 µl 10xBuffer (ReproFast)
0.75 µl forward primer (10pmol/µl)
0.75 µl reverse primer (10pmol/µl)
0.3 µl Taq-polymerase
0.7 µl dNTPs
5 µl gDNA

Table 14: PCR program for ChIP analysis

Step	**Temp.**	**Time**	
1	95°C	pause	
2	95°C	5’	
3	95°C	15’’	x 40
4	60°C	15’’	
6	95°C	5’	

3 Results

3.1 FOSL1 regulation in melanoma

3.1.1 P-ERK1/2- dependent regulation of FOSL1

The RAS/RAF/ERK1/2 pathway plays a central role in development and maintenance of human malignant melanoma. As FOSL1 is regulated by this pathway, I closely investigated the conditions under which MAPK pathway inhibition affects the abundance of this transcription factor [84]. FOSL1 mRNA levels were first analyzed after MEK inhibition with the MEK1/2 inhibitor PD184352 in the human melanoma cell lines UACC62 and MelHo. In both cell lines, FOSL1 mRNA levels were clearly reduced after PD184352 treatment for 24h (Figure 5A). The next question to address to which extent the MEK inhibition affects FOSL1 protein levels. Therefore, a panel of different human melanoma cell lines was treated with PD184352 and western blot analysis was performed (Figure 5B). The different cell lines showed different endogenous levels of FOSL1, but all cell lines responded to the MEK inhibitor treatment and FOSL1 levels were strongly reduced in all of the tested cell lines. To gain further insight into protein stability and dependency on ERK1/2 signaling, FOSL1 levels were also observed after short time treatment with PD184352 (10 minutes to 3 hours) in MelHo cells. Already 10 min after the start of MEK inhibition, FOSL1 levels were visibly reduced (Figure 5C).

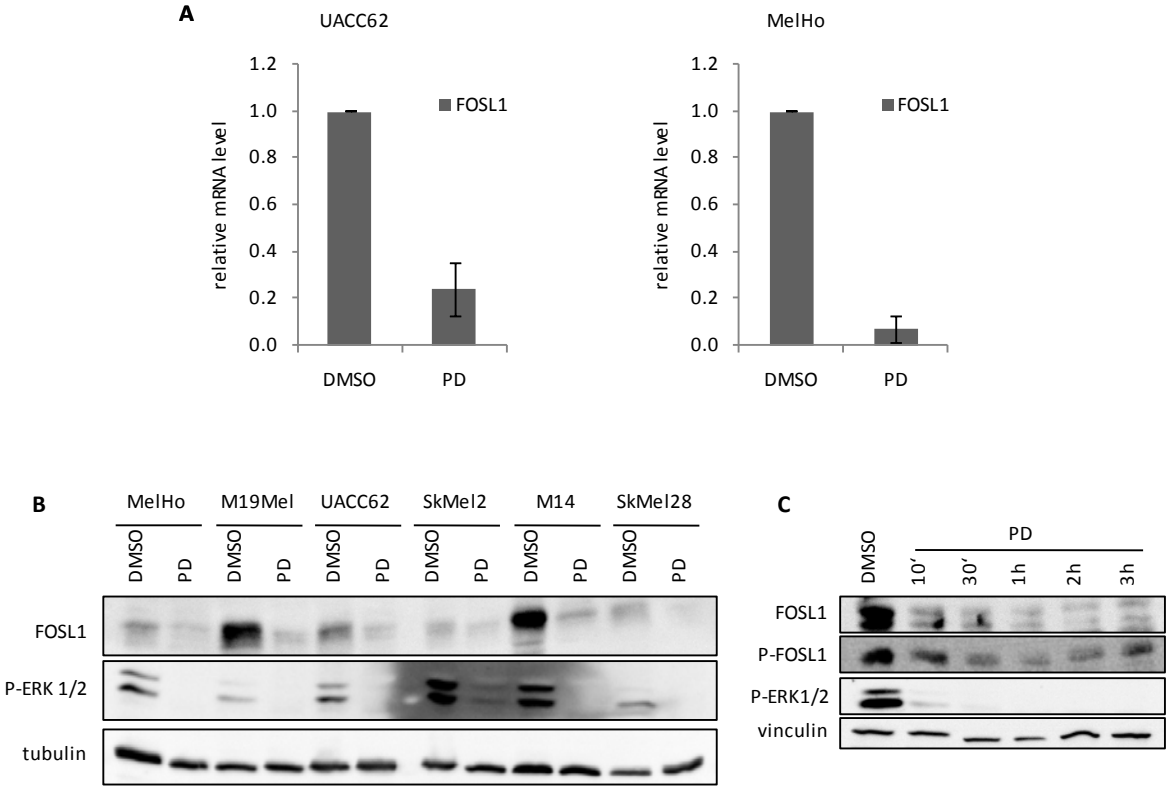

Figure 5: P-ERK1/2-dependent regulation of *FOSL1* mRNA and FOSL1 protein

A. RT-qPCR analysis of *FOSL1* after 24 hours of MEK inhibition with 2 µM PD184352 in UACC62 and MelHo cells. Calculations were made from 2 independent experiments, each performed in triplicates. **B**. FOSL1 and P-ERK1/2 (Thr202/Tyr204) levels as readout for MEK inhibition of different human melanoma cell lines after 24 hours of MEK inhibition with 2 µM PD184352. Tubulin served as a loading control. **C**. FOSL1, P-FOSL1 (Ser 265) and P-ERK1/2 levels after short time treatment of MelHo cells with 2 µM PD185243. Vinculin served as loading control.

I also used a P-FOSL1 antibody, which specifically detects serine 265- phosphorylated FOSL1. This site was previously described as direct phosphorylation target of P-ERK1/2 necessary for FOSL1 protein stability [85]. To check the phosphorylation state of FOSL1 at this site in dependency of MEK signaling P-FOSL1 was also detected in the short time experiment. In MelHo cells, dephosphorylation of serine 265 was observed after only 10 minutes of treatment and went along with decreasing total FOSL1 abundance.

3.1.2 PI3K- signaling- dependent regulation of FOSL1

Next to enhanced MAPK signaling, PI3K plays an important role in melanoma maintenance and progression. To test if this pathway has a possible impact on FOSL1, UACC62 and MelHo cells were treated with the PI3K inhibitor GDC0941 for 24h. *FOSL1* mRNA levels were clearly reduced after treatment in both cell lines (Figure 6A). Additionally, FOSL1 protein levels were analyzed after 24h of treatment in different human melanoma cell lines. All cell lines, irrespective of the endogenous levels of FOSL1, showed reduced FOSL1 levels after PI3K inhibition (Figure 6B). Here, the effect of the PI3K inhibitor was comparable to that of the MEK inhibitor. In contrast to the short time MEK inhibition, the inhibition of the PI3K pathway for 10 minutes up to 3 hours showed no obvious regulation of FOSL1 (Figure 6C). These findings indicate that FOSL1 is a transcriptional target of the PI3K pathway, but the protein stability is most likely not affected by this pathway.

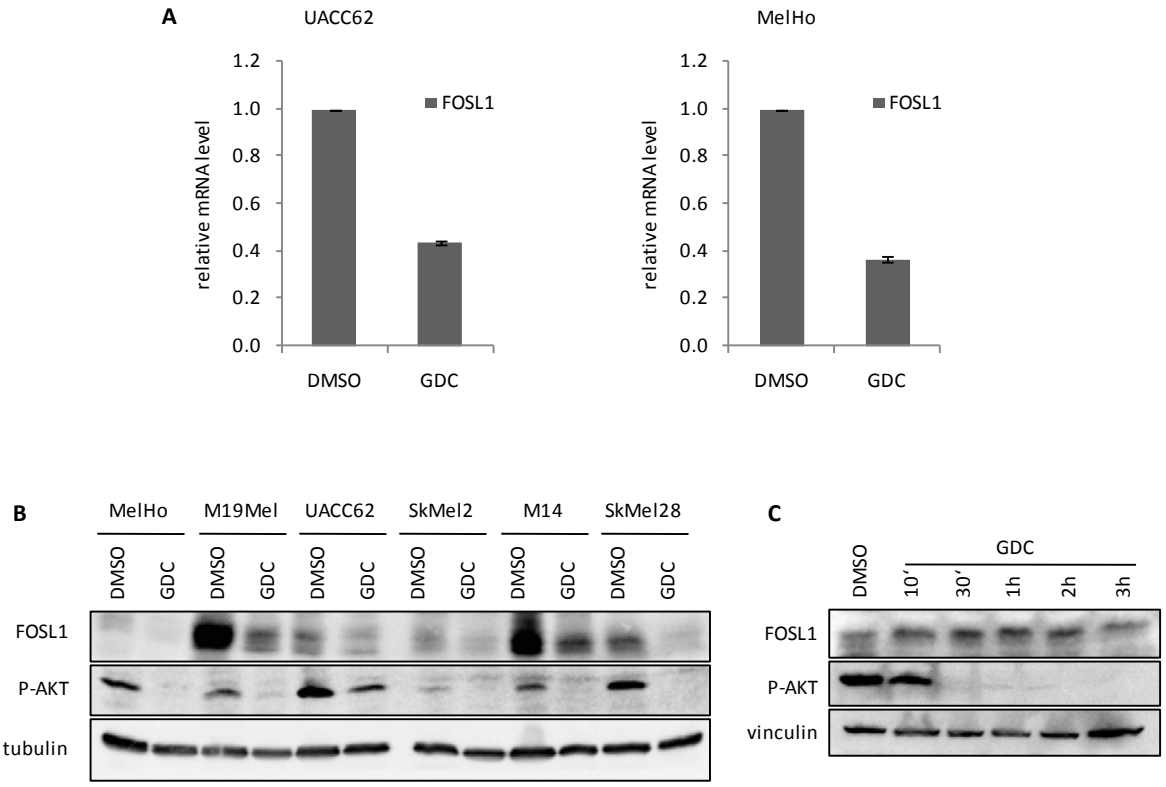

Figure 6: PI3K- dependent regulation of *FOSL1* mRNA and FOSL1 protein
A. RT-qPCR analysis of *FOSL1* after 24 hours of PI3K inhibition with 5 µM GDC0941 in UACC62 and MelHo cells. The experiment was performed two times, each time in triplicates. **B**. FOSL1 and P-AKT (Ser473) levels as readout for the PI3K inhibition of different human melanoma cell lines after 24 hours of PI3K inhibition with 5 µM GDC0941. Tubulin served as a loading control. **C**. FOSL1 and P-AKT (ser473) levels after short time treatment of MelHo cells with 5 µM GDC0941. Vinculin served as loading control.

3.1.3 P53- dependent regulation of FOSL1

Since it was described previously that FOSL1 is influenced by p53 signaling by an miRNA dependent mechanism involving miR-34a and miR-34c [86], this association was examined further in human melanoma cell lines. *TP53* is often mutated or massively downregulated by strongly enhanced levels of either MDM2 or especially MDM4 in many cases of human melanoma [51]. At first, Ma-Mel-47 human melanoma cells were transfected with control siRNA and miRNA mimics for miR-34a, miR-34b and miR-34c to find out if these miRNAs influence FOSL1 levels in human melanoma cells. Western blot analysis revealed clearly decreased FOSL1 protein levels in response to miR-34a and c, but not miR-34b and a control siRNA (Figure 7).

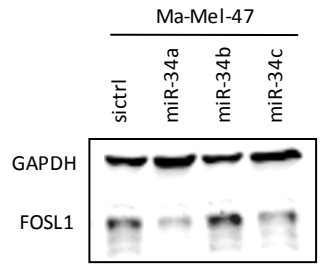

Figure 7: FOSL1 regulation in dependence of miR-34a and c
Western blot analysis of FOSL1 protein expression in Ma-Mel-47 melanoma cells after transfection with miR-34a/b/c miRNA mimics and control siRNA for 48 hours. GAPDH served as loading control. This analysis was done in collaboration with the group of A.Paschen (Molecular Tumor Biology Group, Department of Dermatology, University Hospital Essen), and the western blot was conducted by Dr. A. Heinemann.

To test whether these FOSL1-targeting miRNAs were regulated by p53 in melanoma, UACC62 cells were treated with the MDM2 inhibitor nutlin3a and the topoisomerase II inhibitor SN-38 to stabilize p53. The next step was the investigation of miR-34a and miR-34c levels in the two treatment situations. RT-TaqMan PCR was performed, and changes of miR-34a and miR-34c levels were calculated (Figure 8A). Endogenous levels of miR-34a in untreated control cells were higher than levels of miR-34c (data not shown). miR-34a was slightly, but significantly induced after 72 hours of nutlin3a treatment. miR-34c levels were dramatically increased after nutlin3a treatment for 48 and 72 hours and showed a weak, but significant increase after treatment with SN-38 for 48 hours (Figure 8A). In parallel, FOSL1 protein levels were reduced after both time points and both treatments and were inversely correlated to p53 levels (Figure 8B). Together, these results indicate that FOSL1 is regulated by miRNA-34a and miR-34c in a p53- dependent manner in human melanoma cell lines.

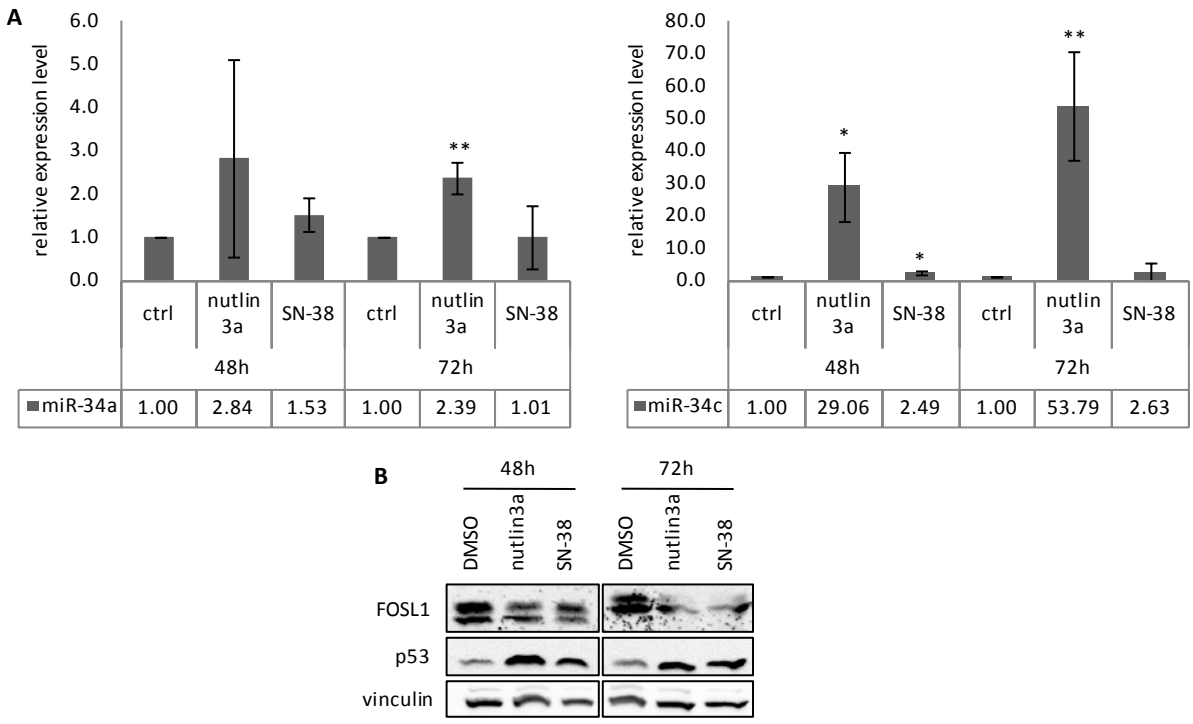

Figure 8: p53- dependent regulation of FOSL1
A. Relative expression level of miR-34a and miR-34c after 48 and 72 hours of 4 µM nutlin3a and 100 nM SN-38 treatment. After cell preparation RNA isolation, RNA was sent to our collaboration partners and TaqMan qPCR was performed by Dr. A. Heinemann in the group of A. Paschen (Molecular Tumor Biology Group, Department of Dermatology, University Hospital Essen) *: $p<0.05$; **: $p<0.01$ **B**. Western blot analysis of FOSL1, p53 as readout for inhibition of MDM2 and DNA damage of UACC62 cells after 4 µM nutlin3a and 100 nM SN-38 treatment for 48 and 72 hours. Vinculin served as loading control. The experiment was performed three times.

To investigate further the impact of p53- inducing DNA damage on miR-34a, miR-34c and FOSL1, the SN-38 treatment was performed in p53 negative cells. For this purpose, p53-negative human colon carcinoma HCT116 cells were treated for 48 hours with either DMSO or SN-38 and were compared to p53- proficient HCT116 wildtype cells. The p53-negative HCT116 cell line harbors targeted deletions of both *TP53* alleles and was generated by F. Bunz et al. [87].

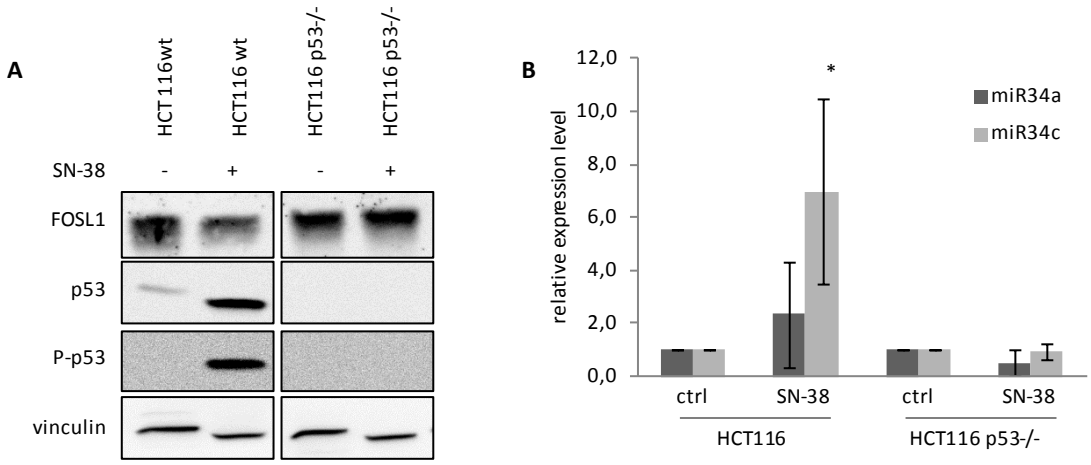

Figure 9: p53- dependent regulation of FOSL1 in human colon carcinoma cells
A. Western blot analysis of FOSL1, p53 and P-p53 (Ser15) of wildtype and p53-negative HCT116 after 48 hours of treatment with 100 nM SN-38. Vinculin served as a loading control. **B**. TaqMan qPCR analysis of miR-34a and miR-34c in wildtype and p53 negative HCT116 cells after 48 hours of 100 nM SN-38 treatment. After cell preparation and RNA isolation, RNA was sent to our collaboration partner for further analysis. TaqMan qPCR was performed by Dr. A. Heinemann in the group of A. Paschen (Molecular Tumor Biology, Department of Dermatology, University Hospital Essen). The experiment was repeated three times (*: $p<0.05$).

The Western blot of the treated cells showed clearly upregulated P-p53 (Ser15), indicting DNA damage, and total p53 levels after SN-38 treatment in the HCT116 wildtype cells, but not in the p53 deficient HCT116 cells. Simultaneously to upregulated p53 levels, downregulated FOSL1 levels could be observed in the wildtype cells. The FOSL1 level in p53-deficient HCT116 cells did not change after SN-38 treatment, indicating the p53- dependent regulation of FOSL1 (Figure 9A). The corresponding TaqMan qPCR showed a minimal upregulation of miR-34a, but a significant upregulation of miR-34c after SN-38 treatment in the HCT116 wiltype cells. The HCT116 p53 negative cells did not show altered miR-34a and miR-34c levels (Figure 9B). These results demonstrate that miR-34a and miR-34c are influenced by DNA damage treatment via p53 upregulation and that FOSL1 levels are reduced if miR-34a and miR-34c are present.

To directly compare the impact of the P-ERK1/2, PI3K and p53 pathways on FOSL1 protein level, all three pathways were manipulated with the respective inhibitors for 48 hours in the same cell line. Figure 10 displays that inhibition of MEK and PI3K show the strongest effect on FOSL1 levels, as the protein was massively downregulated in both situations. In contrast to that, stabilization of p53 only led to weakly reduced FOSL1 levels. Although inhibition of ERK1/2 and PI3K signaling resulted in diminished p53 level, what theoretically would lead to enhanced FOSL1 levels, FOSL1 levels were clearly decreased. This observation underlines the strong dependence of FOSL1 from ERK1/2 and PI3K signaling.

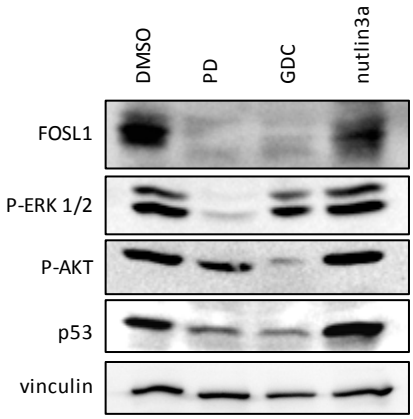

Figure 10: FOSL1 protein levels after manipulation of P-ERK1/2, PI3K and p53 signaling pathways
Western blot analysis of FOSL1, P-ERK1/2 (Thr202/Tyr204), P-AKT (Ser473) and p53 after treatment of UACC62 cells with 2 µM of the MEK1/2 inhibitor PD184352, 5 µM of the PI3K inhibitor GDC0941 and 4 µM of the MDM2 inhibitor nutlin3a for 48 hours. Vinculin served as a loading control.

3.2 FOSL1 mediated pro-tumorigenic effects in human melanoma

Since the ERK1/2 and PI3K signaling pathways are responsible for the induction of malignant features in human melanoma, FOSL1 as direct target of both pathways is a probable tumor-relevant candidate. Moreover, FOSL1 was described to enhance migrative and invasive phenotypes in several human tumors such as breast cancer, colon carcinoma and bladder cancer [86, 88, 89].

Interestingly, usage and analysis of a dataset of a systematically classified panel of 220 melanoma cell lines by phenotype-specific gene expression mapping, revealed that *FOSL1* expression correlates with a invasive phenotype (Figure 11) [90].

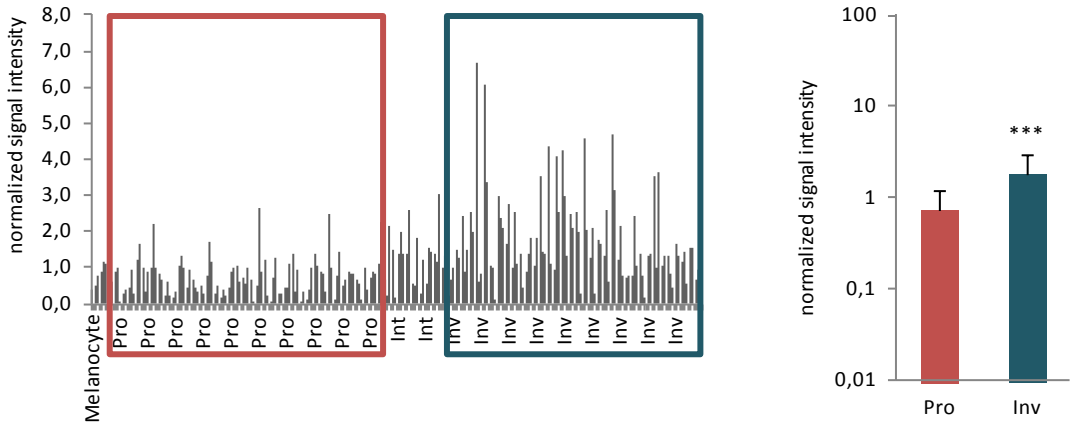

Figure 11: Classification of melanoma cells by phenotype-specific FOSL1 gene expression
Analysis of a probeset of 220 samples of melanoma cell lines reveals average expression signals of 0.75 (± 0.49) and 1.8 (± 1.24) for *FOSL1* in proliferative and invasive signature samples, respectively. This 2.4-fold difference is significant (P < 1.00E-05). Pro: proliferative, Int: intermediate, Inv: invasive [90].

Furthermore, the *FOSL1* gene is located on chromosome 11q13.1, a region, which is frequently amplified in melanoma and linked to poor prognosis [91].

Regarding FOSL1 protein levels during melanoma progression in patients (Figure 12) shows that the FOSL1 levels are increasing from benign nevi to primary tumors and are highest in metastases. These observations imply that FOSL1 might play an important role in the maintenance of late melanoma stages. To investigate the functional effects of gains in FOSL1 expression, I analyzed the effect of enhanced FOSL1 expression in melanoma cells with low intrinsic FOSL1 level.

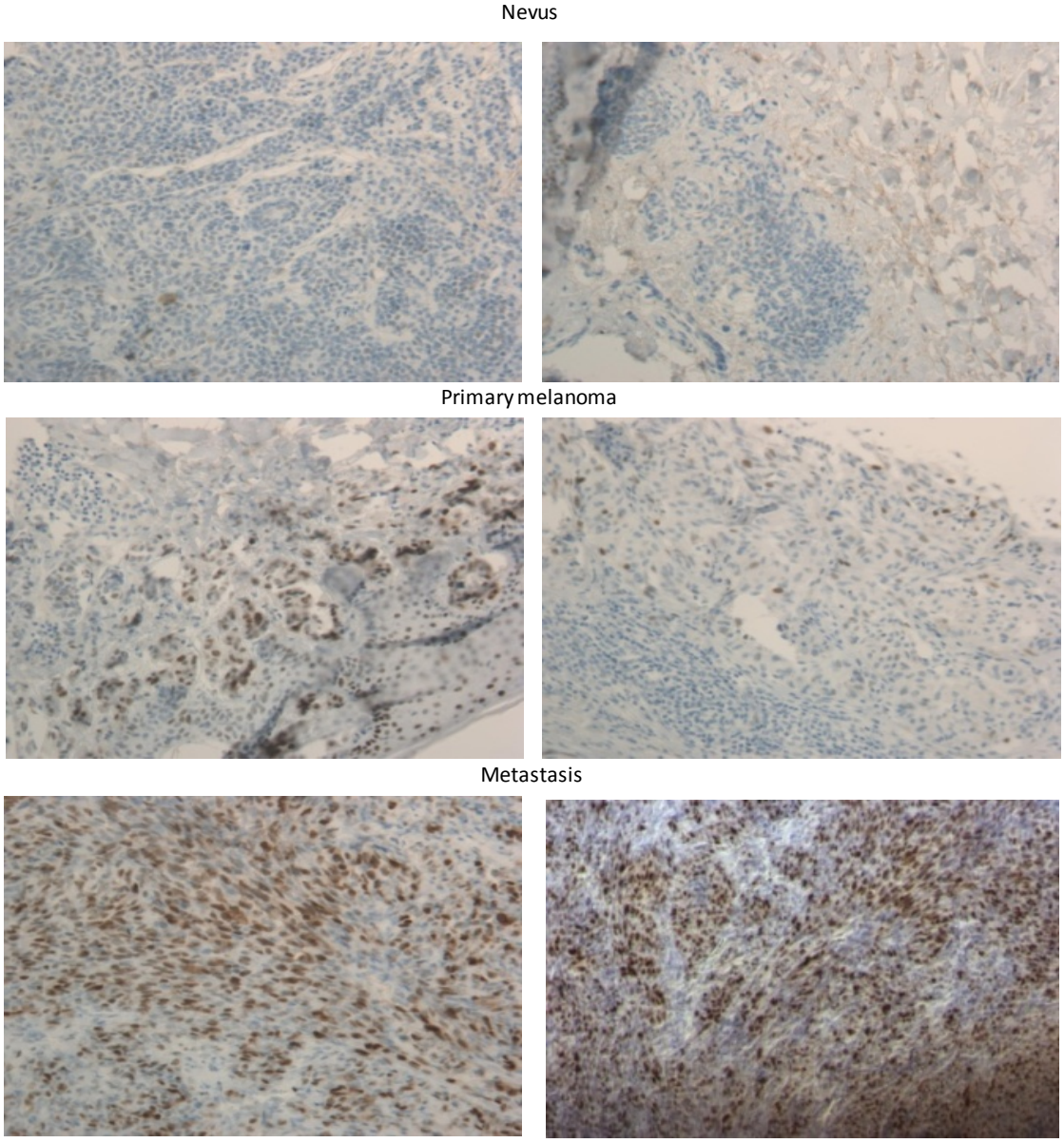

Figure 12: FOSL1 protein abundance during the progression of human melanoma
Representative images from a FOSL1 tissue microarray from different human melanoma progression stages. Brown staining indicates specific antibody binding. The tissue microarray was performed in the group of Anja Bosserhoff (Molecular Pathology, University of Regensburg, now Institute for Biochemistry, University of Erlangen).

3.2.1 Effects of FOSL1 on proliferation

The UACC62 and MelHo cell lines, both displaying low levels of endogenous FOSL1 as depicted in Figure 6B and Figure 7B, were infected with a virus containing a CMV-promoter- driven FOSL1 overexpression vector (p201-FOSL1). Additional FOSL1 expression was confirmed by western blot (Figure 13A). Although FOSL1 is endogenously expressed in UACC62 and MelHo cells, the endogenous FOSL1 signal was too weak to be visible in the context of the additional FOSL1 copies.

As it was previously described that FOSL1 knockdown reduces BrdU incorporation and thus proliferation of melanoma cells [84], it was interesting to investigate whether enhanced levels of FOSL1 would lead to higher proliferation rates. For this purpose, proliferation assays with the FOSL1-overexpressing UACC62 and MelHo cells were performed. Cells were counted after three and six days. In the UACC62 cell line, overexpression of FOSL1 led to a significantly enhanced proliferation rate after six days (Figure 13B). MelHo cells showed a higher overall proliferation rate than the UACC62 cells, but still the FOSL1 ovexpression resulted in a significantly increased proliferation rate which was already visible after three days of cultivation.

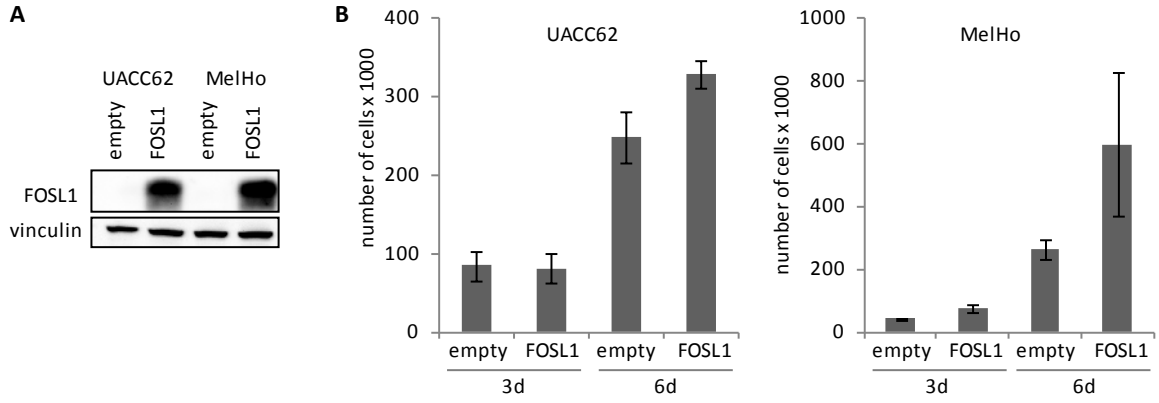

Figure 13: FOSL1- dependent proliferation of melanoma cells
A. Western blot analysis of FOSL1 in UACC62 and MelHo cells infected with constitutive FOSL1 overexpressing constructs (p201-FOSL1). Vinculin served as a loading control. **B**. Proliferation assay of FOSL1 overexpressing and empty vector cells. Cells were manually counted at day 3 and 6 after plating. Calculations were made from two independent experiments, each performed in triplicates.

3.2.2 Effects of FOSL1 on migration

To test whether FOSL1 overexpression enhances the migrative potential of human melanoma cell lines, transwell migration assays were performed. In MelHo cells, the constitutive overexpression of FOSL1 led to significantly increased migration rates after eight hours (Figure 14). In contrast, the UACC62 cell line did not show any migration through the standard transwell inlays with 8 µM pore size even after 24 hours of observation, which rendered them unsuitable for this type of assay.

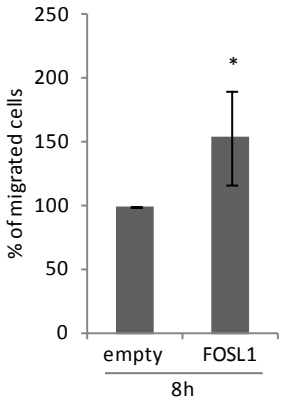

Figure 14: FOSL1- dependent migration in melanoma cells
Transwell migration assay of control MelHo cells (empty vector) and FOSL1 overexpressing cells. Cells were allowed to migrate for 8 hours. The assay was performed three times in triplicates (*: $p<0.05$).

3.2.3 Effects of FOSL1 on colony formation and anchorage independent growth

To gain more insight into the capability of FOSL1 to influence autonomous human melanoma cell growth, 2D colony formation assays were conducted. A small number of cells was plated onto cell dishes to establish stringent conditions for the single cells. Without the influence of directly adjacent cells, each cell has to form an autonomous colony on its own and without the benefit of secreted growth factors of the surrounding cells. In case of UACC62 and MelHo cells, only few control cells were able to form colonies within 12 days. In contrast, colony formation of FOSL1 overexpressing cells was strongly enhanced (Figure 15A). Taken together, FOSL1 overexpression enables single cells to form 2D-colonies.

To analyze *in vitro* whether FOSL1 overexpression also confers metastasis associated features, soft agar 3D colony forming assays were performed. In this *in vitro* transformation assay, cells have to survive and grow in a medium- agar mixture without any habitual matrix offered to them. Hence, this assay measures the anoikis resistance of cells. Again, UACC62 and MelHo FOSL1 overexpressing cells were compared to the respective empty vector control. After seven days of culture, similar numbers of colonies were observed in UACC62 and MelHo cells irrespective of FOSL1 expression, demonstrating that the control cells were already capable of thriving under anchorage independent conditions (Figure 15B). To check whether endogenous FOSL1 is necessary for the ability to form colonies in control cells, siRNA- mediated knockdown experiments were performed. Cells were transfected with either control siRNA or siRNA targeting *FOSL1* and seven days after plating the transfected cells into the agar-medium mixture, control cells were compared to FOSL1 knockdown cells. The knockdown of FOSL1 resulted in a strongly reduced number of colonies (Figure 15C), thus demonstrating that endogenous FOSL1 is indeed needed in melanoma cells to form anchorage independent colonies.

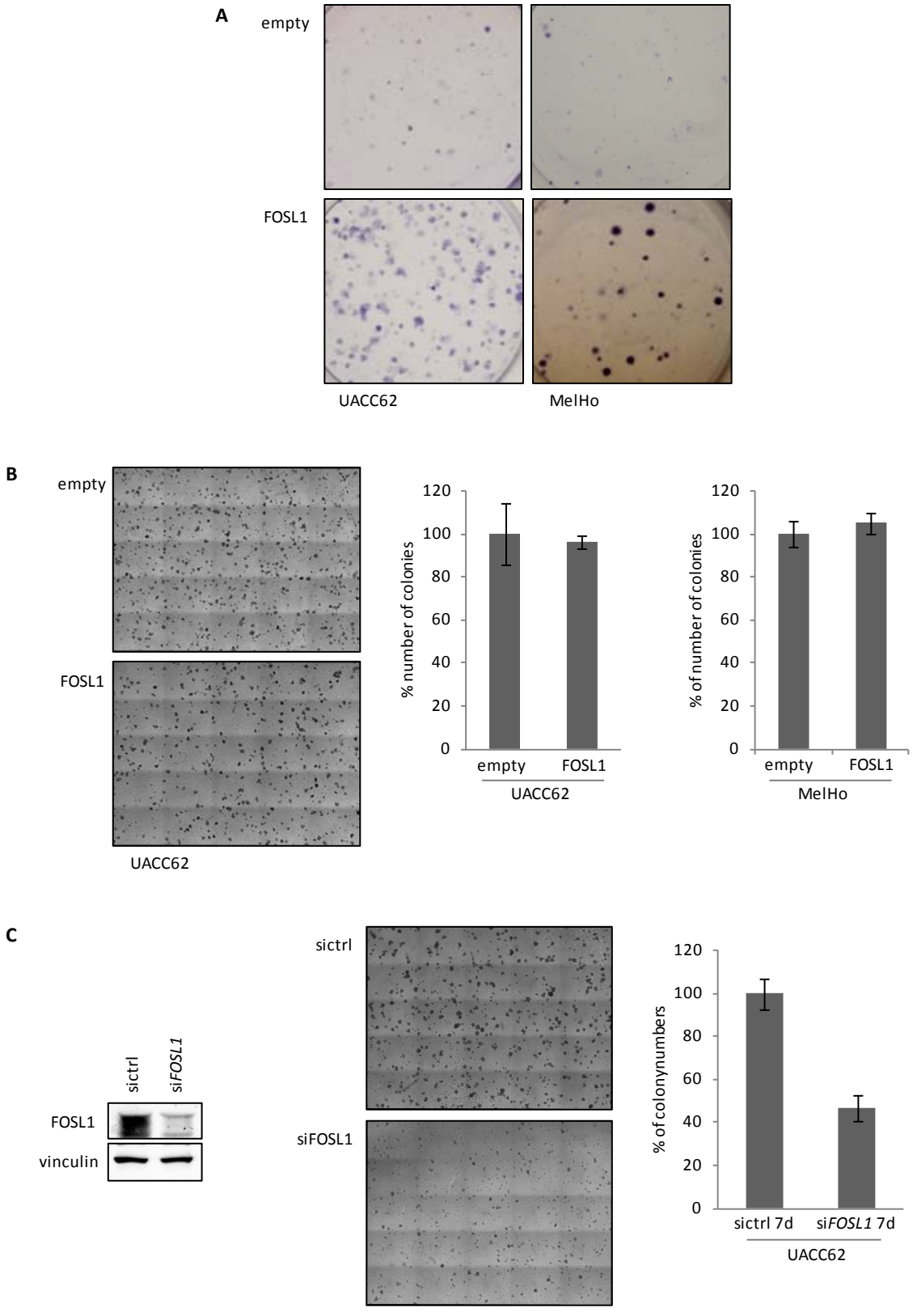

Figure 15: FOSL1- dependent colony forming ability in human melanoma cells

A. Colony formation assay. In case of UACC62 cells, 400 cells were seeded at the start of the experiment per well of a 6-well dish; for MelHo cells 150 cells were used. Cells were allowed to form colonies for 12 days and were thereafter stained with 2% crystal violet solution, before pictures were taken. The experiment was done 2 times in triplicates and representative images are shown. **B**. Soft agar assays after of UACC62 control and FOSL1 overexpressing cells and the corresponding quantification. Additionally, quantification of MelHo cells after 7 days

of soft agar growth is shown. The analysis was done 2 times in triplicates for UACC62 cells and once in triplicates for MelHo cells. **C**. Western blot of *FOSL1* siRNA- mediated knockdown for 3 days and soft agar colonies after 7 days in UACC62 cells in sictrl and si*FOSL1* treated cells with associated quantification. Vinculin served as a loading control. Experiments were performed two times in triplicates.

3.3 Downstream effectors of FOSL1 in melanoma

So far, I could show that enhanced FOSL1 levels increase the tumorigenic features even of fully transformed melanoma cells such as UACC62 and MelHo. To decipher these effects of FOSL1 on the cells, I aimed at determining the scope of FOSL1- dependent target genes in melanoma.

3.3.1 Microarray analysis

The transcription factor FOSL1 has many direct target genes which can potentially be revealed by microarray analysis. For this purpose, a GeneChip® Human Genome U133 Plus 2.0 Array (Affymetrix) was performed. To get more sensitive results, I chose to investigate target gene expression in cells which underwent *FOSL1* knockdown instead of FOSL1 overexpression. siRNA- mediated *FOSL1* knockdown was performed in UACC62 cells and was compared to cells treated with non-targeting siRNA.

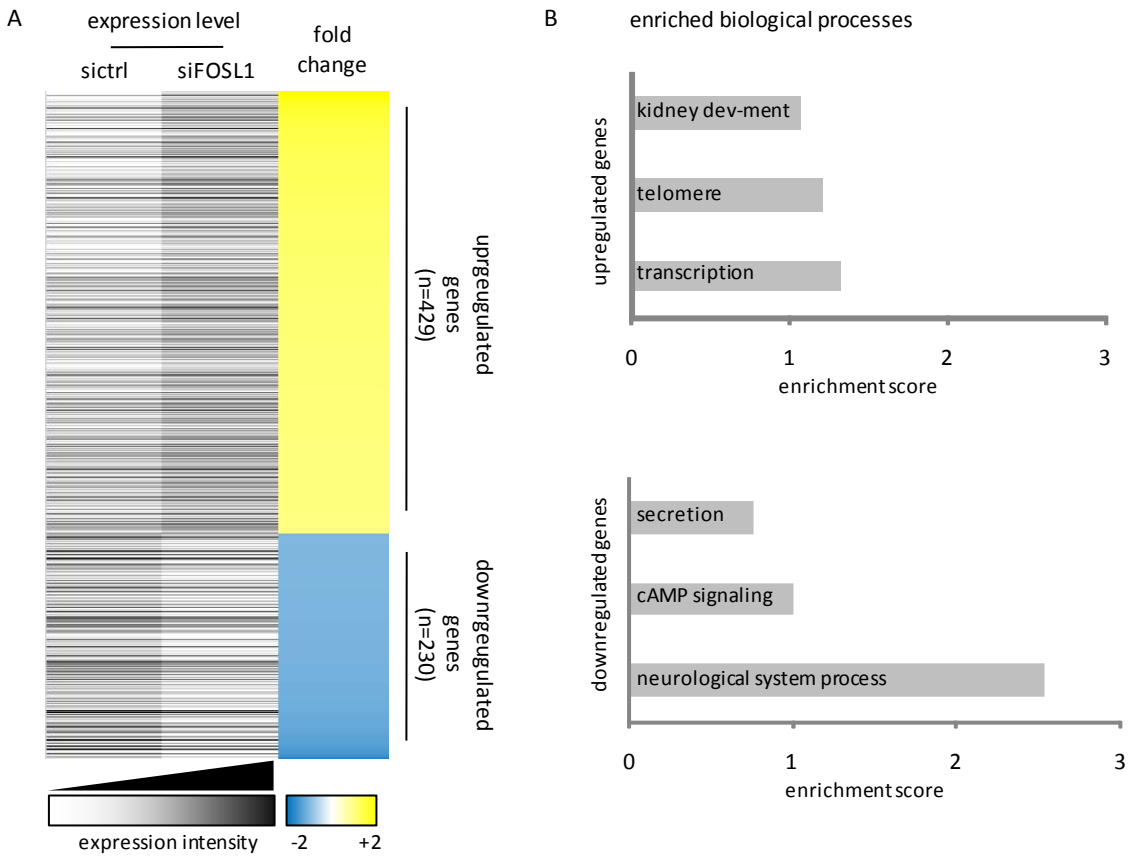

Figure 16: Regulated genes in UACC62 after siRNA-mediated *FOSL1* knockdown
A. Heatmap of up- and downregulated genes (fold change ≥ 1.5, min log2 RMA signal intensity ≥ 6 (Robust Multi-array Average)). In grey, RMA signal intensities are shown. Fold changes are shown in yellow-blue gradation. **B**. The three most enriched biological processes for up- and downregulated genes. Values above 1.3 are considered significant, in accordance with DAVID recommendations [92].

In total, 659 genes were regulated by *FOSL1* knockdown (Figure 16A). Gene Ontology (GO)-Term clustering of biological processes with the Database for Annotation, Visualization and Integrated Discovery (*DAVID*) (version 6.7) revealed different annotation clusters for up- and downregulated genes [93]. In Figure 16B the three most enriched clusters are shown.

The only significant enriched annotation cluster was “neurological system process” for the downreguated genes (Figure 16B). Interestingly, melanocytes, the precursors of melanoma cells, and several neuronal cell types arise from the same origin during embryonal development, namely the neural crest [94]. The regulation of neuronal genes could thus point to possible de- or transdifferentiation characteristics of the melanoma cells. The neural crest is a highly migrative embryonic tissue with high self renewal capacities [95]. A dedifferentiation of melanoma cells towards their ontogenetic origin could possibly provide stemness and migration features.

3.3.2 FOSL1- dependent regulation of neuronal genes

The genes from the neuron related GO-Terms are detailed in Figure 17. To validate the FOSL1-dependent expression of neuronal genes in melanoma cells, I chose three strongly regulated genes

from these groups, namely the structural neuronal genes β3-tubulin (*TUBB3*) and neurofilament (*NEFL*), as well as neuropilin1 (*NRP1*), a gene encoding a membrane-bound co-receptor.

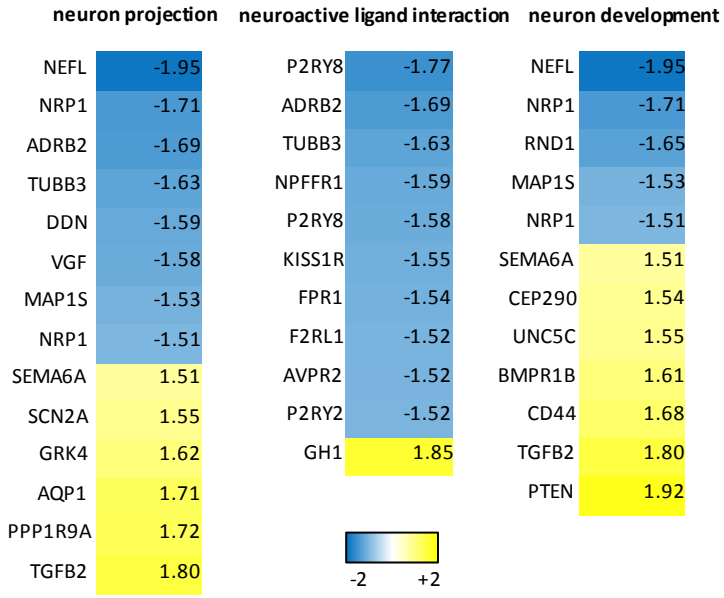

Figure 17: Neuronal GO-Terms of regulated genes in response to FOSL1 knockdown (fold change ≥ 1.5)

RT-qPCR was performed with UACC62 and MelHo cells transfected with control or *FOSL1* specific siRNA. All three genes were found to be clearly downregulated in both cell lines (Figure 18A) when *FOSL1* was knocked down. To investigate whether enhanced FOSL1 protein levels could also affect expression of the neuronal genes, RT-qPCR analysis was also conducted from UACC62 and MelHo cells overexpressing FOSL1. In both cell lines FOSL1 overexpression led to at least 2-fold upregulation of *TUBB3*, 4-fold upregulation of *NEFL* and 8-fold upregulation of *NRP1* compared to the empty vector cells (Figure 18B).

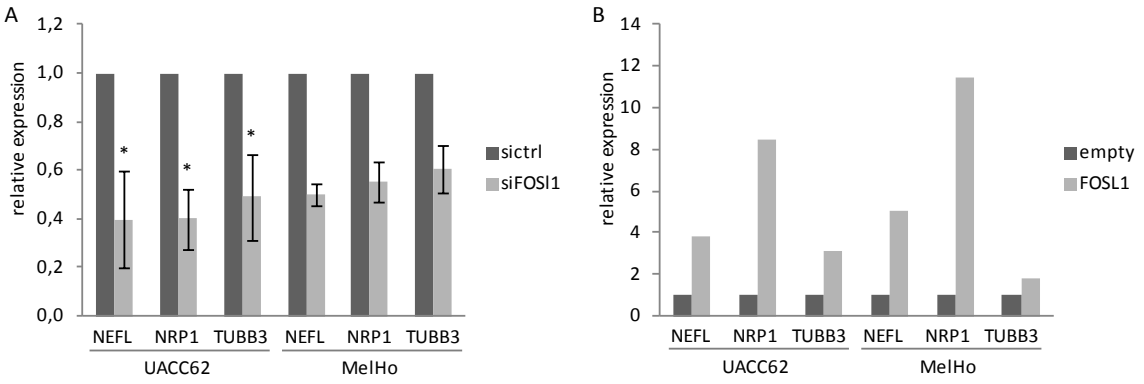

Figure 18: Validation of neuron related genes regulated by FOSL1
A. RT-qPCR of indicated neuronal genes in UACC62 cells and MelHo cells after siRNA- mediated knockdown of *FOSL1* for 3 days. Values for UACC62 cells were calculated form three different experiments performed in triplicates. Values for MelHo cells were calculated from two independent biological replicates **B**. RT-qPCR of neuronal genes in UACC62 and MelHo cells in FOSL1 overexpressing cells compared to control cells (empty

vector). Experiments were performed 4 times. The extent of upregulation of the three target genes differed a lot between the four experiments. Although the mean value derived from all four experiments was not significant for all genes, the upregulating trend was seen in all four experiments (*: $p<0.05$). For the UACC62 cells, the upregulation of *TUBB3* was seen in 3 of 4 experiments.

As I showed before, that FOSL1 is strongly affected by ERK1/2 and PI3K signaling (Figure 5 and Figure 6), it was interesting if this is reflected in the transcriptional level of the three neuronal genes. Thus, regulation of *NEFL*, *NRP1* and *TUBB3* mRNA expression was analyzed in dependence of P-ERK1/2 and PI3K signaling. For this purpose, UACC62 cells were treated with the MEK inhibitor PD184352 or the PI3K inhibitor GDC0941 for 24 hours. All three neuronal targets were found to be downregulated in response to both inhibitors (Figure 19A).

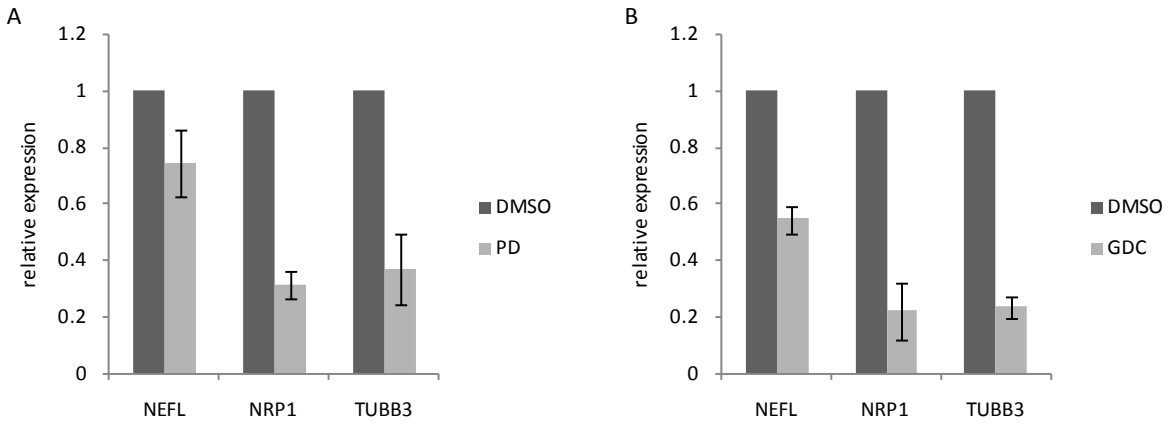

Figure 19: MEK1/2- and PI3K- dependent regulation of *NEFL*, *NRP1* and *TUBB3*
A, B. RT-qPCR analysis of *NEFL*, *NRP1* and *TUBB3* in UACC62 cells after treatment with 2 µM MEK inhibitor PD184352 (**A**) and 5 µM PI3K inhibitor GDC0941 (**B**) for 24 hours. Calculations were made from two independent experiments, each done in triplicates.

3.3.3 Expression of neuronal target genes in melanoma cells with different differentiation states

Our data suggest that FOSL1 might be able to regulate a trans- or dedifferentiation program in human melanoma. To better address this question, it was necessary to investigate whether there is a connection between FOSL1 expression and differentiation state. For this purpose, Western blot analysis with different human melanoma cell lines was performed to determine their MITF level in comparison to FOSL1 (Figure 20A). MITF is a melanocyte lineage specific transcription factor which is, among others, responsible for inducing the genes encoding pigment-generating enzymes. Interestingly, the only pigmented cell line UACC257 with the highest MITF level shows a very low level of FOSL1. In contrast, A375, which is considered as a dedifferentiated cell line shows the lowest MITF expression, but the highest FOSL1 level. However, an inverse correlation between MITF and FOSL1 expression was not consistently observed in the other cell lines.

Furthermore, the expression of the MITF target genes dopachrome tautomerase (*DCT*) and tyrosinase (*TYR*), both involved in the first steps of eumelanin production, were investigated by RT-qPCR. Δct values were calculated indicating the expression of *DCT* and *TYR* compared to the *RPS14* housekeeping

gene. Figure 20B shows the basal expression levels of the pigmentation genes in UACC62 cells, the cell line we used for the microarray analyses, as well as the most dedifferentiated melanoma cell line A375 and the most differentiated cell line UACC257. Expression of the pigment genes among the three cell lines correlated with differentiation state and MITF abundance (Figure 20A). However, there was no clear correlation between basal expression of the neuronal genes *NEFL*, *NRP1* and *TUBB3* and differentiation (Figure 20C).

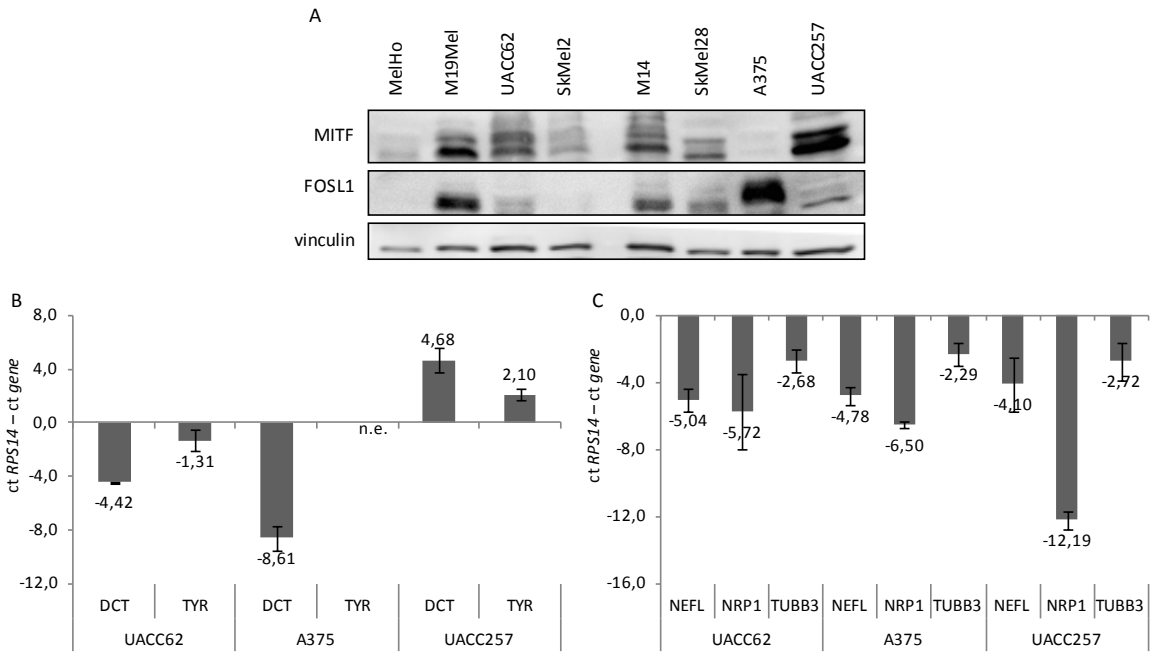

Figure 20: Investigation of the differentiation state of human melanoma cells
A. Western blot analysis of MITF and FOSL1 expression levels in human melanoma cell lines. Vinculin served as loading control. **B**. Calculation of Δct values of pigmentation markers normalized to *RPS14* housekeeping gene representing the basal expression level of the examined genes in the respective cell lines: ct *RPS14* – ct *gene* (n.e. not expressed). **C**. Calculation of Δct values of validated neuronal related genes normalized to *RPS14* housekeeping gene. Calculations were made from two independent experiments, each performed in triplicates. Normalization: ct *RPS14*- ct *gene.*

To determine whether FOSL1 overexpression can alter the balance between differentiation genes and neuronal genes, I generated FOSL1 overexpressing cell lines from the dedifferentiated cell line A375 and the differentiated cell line UACC257. These cells were analyzed together with the described UACC62 cells, which show an intermediate differentiation state. RT-qPCR was accomplished using mRNA of control and FOSL1 overexpressing cells. In addition to the three neuronal genes *NEFL*, *NRP1* and *TUBB3,* mRNA expression levels of the pigment markers *DCT* and *TYR* were determined. In control UACC62 cells, where the neuronal genes were upregulated in the FOSL1 overexpressing cells (Figure 18B), *DCT* was downregulated and *TYR* mRNA levels were unaffected by FOSL1 overexpression (Figure 21A). Regarding the dedifferentiated cell line A375 it was striking that the neuronal gene expression was not induced by FOSL1 overexpression, but *DCT* was downregulated similarly to the UACC62 cells

(Figure 21B). As described in Figure 20, *TYR* was not expressed in A375 cells. In the differentiated UACC257 cells neuronal gene expression was enhanced as observed for UACC62 cells, but *DCT* or *TYR* mRNA expression levels were not altered by FOSL1 overexpression (Figure 21C). Taken together, I demonstrated that FOSL1 is able to shift the balance towards cellular dedifferentiation by upregulating neuron related genes and by downregulating pigment cell specific genes in human melanoma cell lines. This regulation differed between cell lines and likely, depends on the cellular differentiation state.

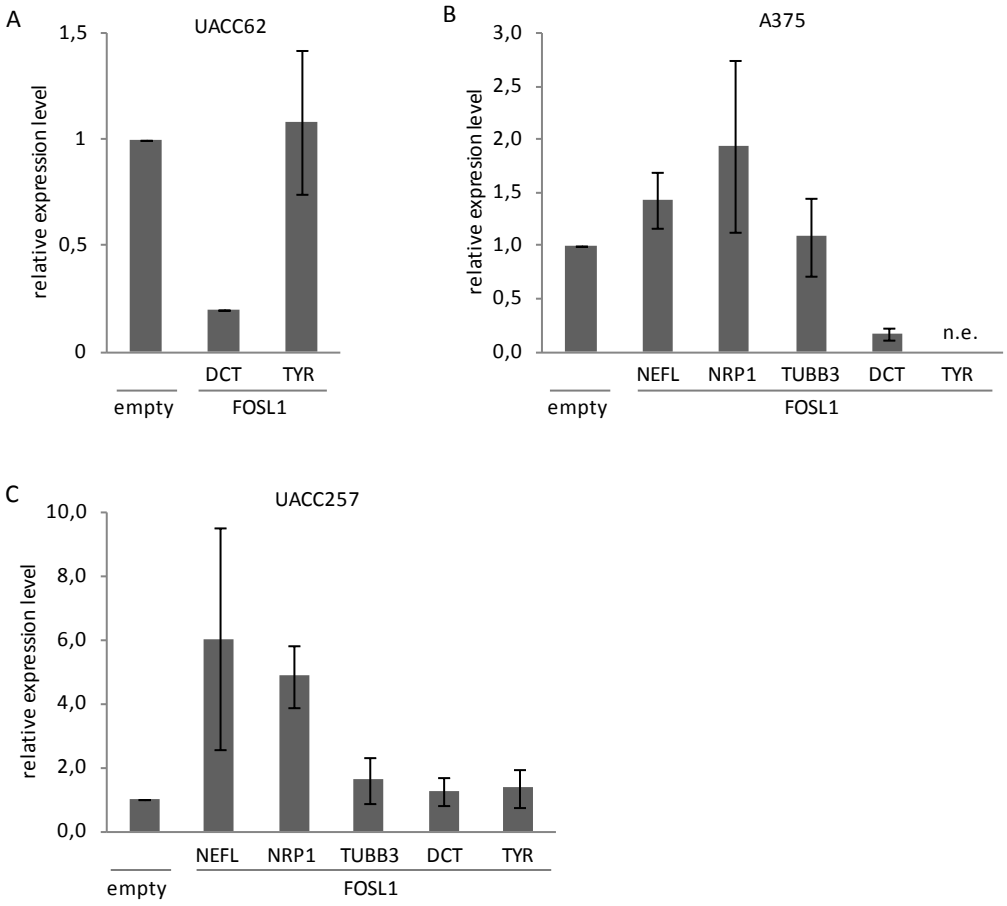

Figure 21: Influence of FOSL1 overexpression on the regulation of neuronal genes and pigment genes in differently differentiated melanoma cells
A-C. RT-qPCR analysis of the indicated genes in UACC62 (**A**), A375 (**B**) and UACC257 cells (**C**) in response to FOSL1 overexpression (n.e. not expressed). Calculations were made from two independent experiments, each performed in triplicates.

3.3.4 Transcriptional regulators downstream of FOSL1

In addition to the observed group of neuronal genes, I was also interested in FOSL1 downstream transcription regulators, which could probably be involved in mediating the biological consequences of FOSL1 expression. DAVID functional annotation clustering with the downregulated genes from

Figure 16 also revealed the GO-Term 'transcription activator activity'. This GO-Term contained four genes: *FOSL1* itself, *HMGA1*, *HOXA9* and *CEBPE* (Table 15).

Table 15: GO-Term 'transcription activator activity' with associated genes
Functional annotation clustering with DAVID of 1.5 fold downregulated genes

GO-Term	transcription activator activity
genes	*FOSL1*
	HMGA1
	HOXA9
	CEBPE

As there is evidence for a role of HMGA1 and HOXA9 in cellular reprogramming and the regulation of stem cell related genes, respectively, I focused on these two genes for further studies [96, 97]. The FOSL1-dependent regulation of *HMGA1*, but not *HOXA9* could be validated in RT-qPCR experiments (Figure 22A und B). The high mobility group AT-hook 1 (HMGA1) protein is involved in chromatin remodeling processes [98]. Its role in cellular reprogramming was described in adult mesenchymal stem cells, where HMGA1 is able to restore stem cell properties by activating stem cell specific transcription networks [96]. I conducted western blot analysis of different human melanoma cell lines to test for HMGA1 and FOSL1 protein expression. HMGA1 was expressed at different levels in all human melanoma cell lines as well as in the NHEM melanocyte cell line (Figure 22C). In four out of seven melanoma cell lines, HMGA1 expression was higher than in NHEM cells. Of note, HMGA1 protein levels seemed to correlate with FOSL1 levels. Additionally, the FOSL1-dependent protein expression of HMGA1 was shown in western blot analysis of different human melanoma cell lines after siRNA-mediated knockdown of *FOSL1* (Figure 22D).

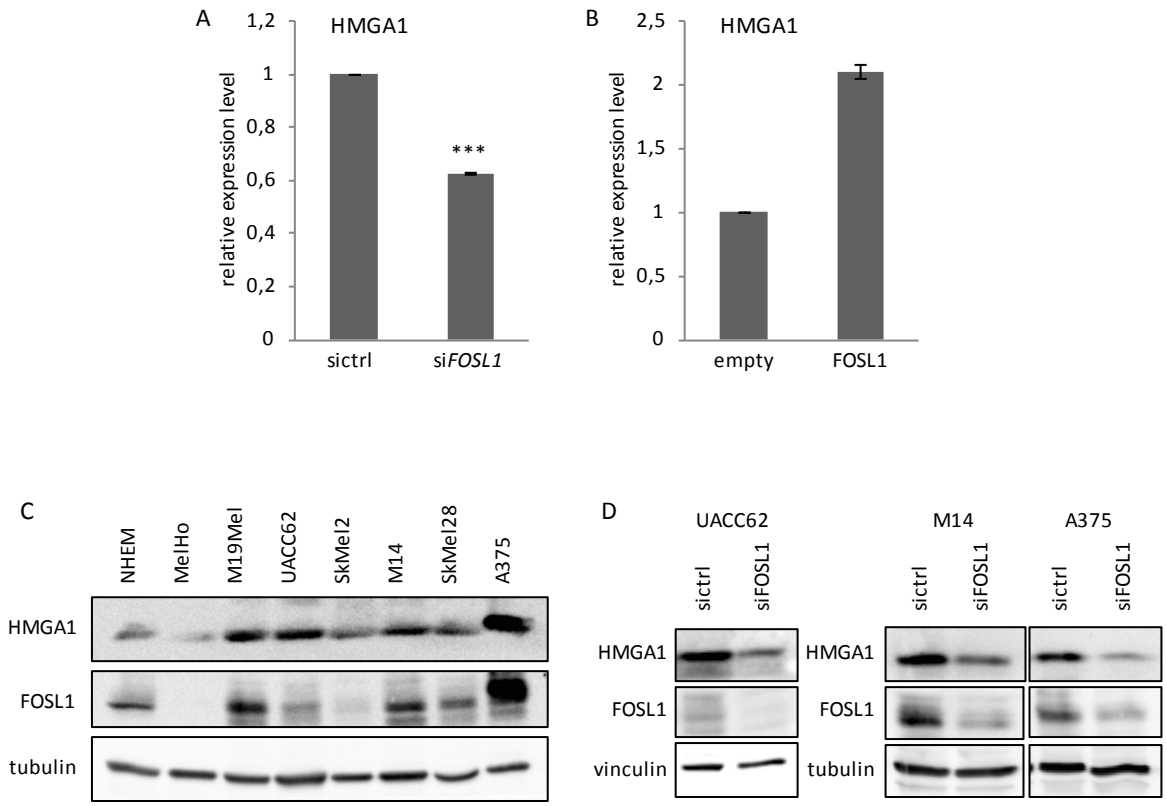

Figure 22: HMGA1 expression in melanocytes (NHEM) and human melanoma cell lines in correlation to FOSL1 expression

A. RT-PCR of *HMGA1* in UACC62 cells after siRNA- mediated knockdown of *FOSL1* for 3 days. Values were calculated from three independent experiments, each performed in triplicates (***: p<0.001). **B**. RT-qPCR of *HMGA1* in FOSL1 overexpressing UACC62 cells. Values were calculated from 2 independent experiments, each performed in triplicates. **C.** Western blot analysis of HMGA1 and FOSL1 protein expression in normal human epidermal melanocytes (NHEM) and different melanoma cell lines. Although FOSL1 is expressed on protein level in MelHo cells, as shown in Figure 1C, the band was too weak to be visible in the context of cellular extract of cells with strong FOSL1 expression **D.** Western blot of HMGA1 and FOSL1 levels in different human melanoma cell lines after siRNA- mediated *FOSL1* knockdown. UACC62 were harvested 3 days after transfection. M14 and A375 cells were harvested 2 days after transfection. Vinculin and tubulin served as loading controls.

3.3.5 FOSL1-ChIP analysis of the HMGA1 genomic region

Next, I asked if HMGA1 is a direct transcriptional target of FOSL1. For this purpose, ChIP analysis was performed. I used UACC62 cells with a FOSL1-flag-tagged overexpression construct (p201-FOSL1flag) and compared them to empty vector cells (Figure 23A). The flag-tagged FOSL1 construct was employed as the flag antibody was expected to give a more specific signal than a FOSL1 antibody. Subsequently, I checked *HMGA1* mRNA levels in these cells, as I wanted to be sure that the flag-tag does not impair the transcriptional activity of FOSL1 (Figure 23B). HMGA1 was significantly upregulated after FOSL1flag overexpression.

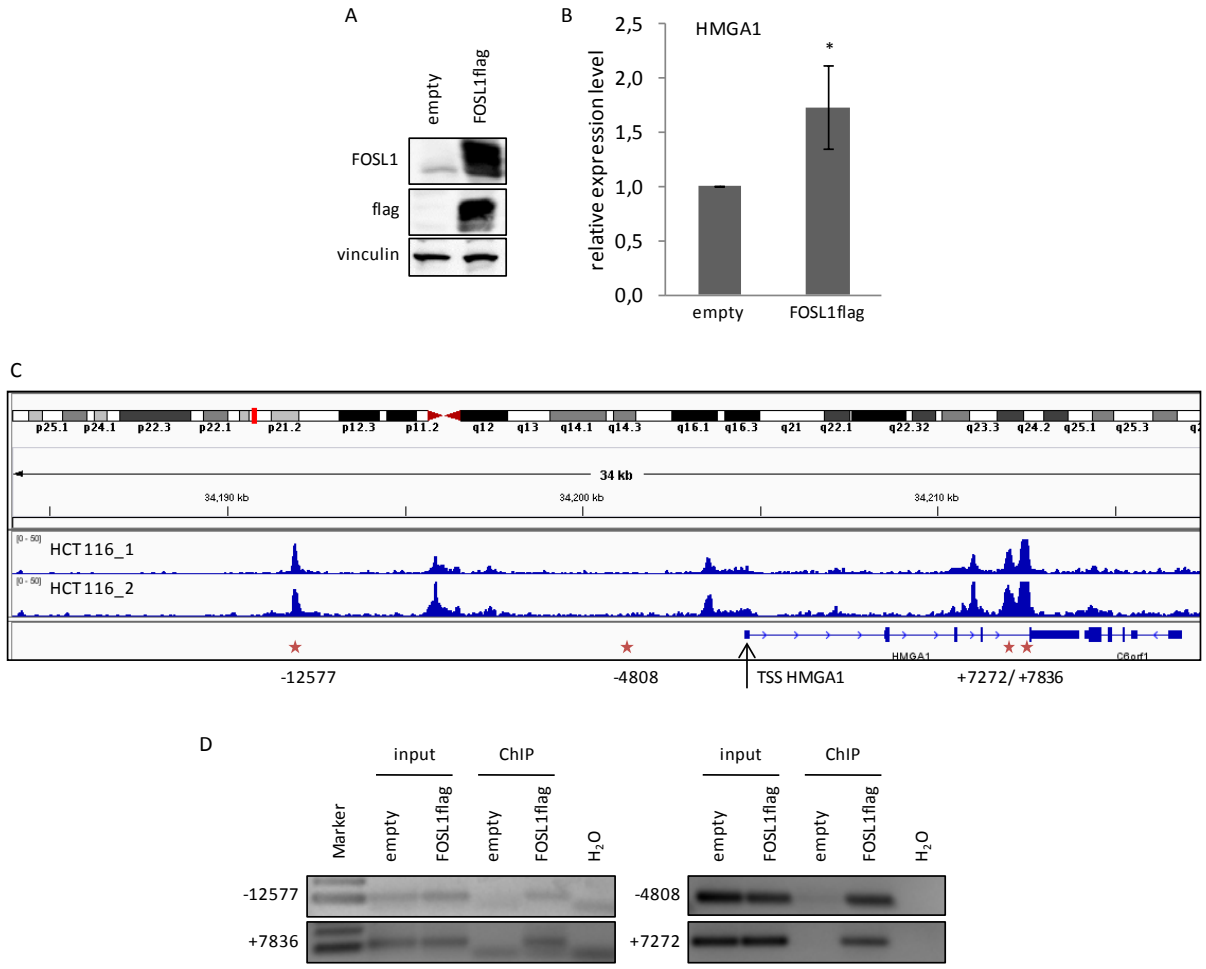

Figure 23: FOSL1 ChIP analysis
A. Western blot analysis of FOSL1 and the flag-tag of FOSL1-flag expressing UACC62 cells and empty vector cells as control. Vinculin served as a loading control. **B**. RT-qPCR expression analysis of *HMGA1* in UACC62 FOSL1flag expressing cells (p201-FOSL1flag). The experiment was performed three times in triplicates (*: $p<0.05$). **C**. Overview of the HMGA1 genomic region on chromosome 6p21 and ChIP sequencing data for FOSL1 in HCT116 cells. The peaks show the enrichment of FOSL1 in the respective genomic region. The ChIP sequencing was performed twice in HCT116 cells from the HudsonAlpha Institute for Biotechnology (http://hudsonalpha.org/). Primers for our ChIP experiment were designed against four genomic regions indicated by the red asterisks. The black arrowhead marks the transcriptional start site of *HMGA1*. The three chosen peaks -12577, + 7272, and +7836 contain predicted binding sites for FOSL1 (http://www.sabiosciences.com/chipqpcrsearch.php?species_id=0&factor=Fra1&gene=HMGA1&nfactor=n&ninfo=n&ngene=n&B2=Search). Their numbers indicate the distance of the first base of the designed forward primer to the TSS. -4808 was chosen as a negative control, as no enrichment was observable at this site in the HCT116 cells. **D**. PCR from genomic DNA after ChIP of UACC62 cells overexpressing FOSL1flag compared to control cells. Input means the isolated, sonicated genomic DNA, which is subsequently applied for the ChIP procedure.

In a publicly available dataset from the HudsonAlpha Institute for Biotechnology (http://hudsonalpha.org/), using different cell lines and ChIP-seq, I found that FOSL1 binds to the HMGA1 promoter in the cancer cell line HCT116. Figure 23C shows the enrichment of FOSL1 in the HMGA1 genomic DNA region on chromosome 6p21 after ChIP-sequencing analysis in HCT116 cells. The identified peaks and the information about predicted FOSL1 binding sites in the genomic region served as indication for the primer design for our approach in the UACC62 cells. The prediction of the target

sites for FOSL1 is based on a database named DECODE: DECipherment Of DNA Elements, which combines data of a text mining application and data from the UCSC Genome Browser (http://www.sabiosciences.com/chipqpcrsearch.php?species_id=0&factor=Fra1&gene=HMGA1&nfactor=n&ninfo=n&ngene=n&B2=Search). For my analysis of FOSL1 binding to the HMGA1 genomic region in melanoma cells, I chose four primer pairs. Three of them amplify target regions within high peaks, which additionally contain predicted FOSL1 binding sites (-12577, +7272, +7835). One primer pair covers a region without a peak in HCT116 cells or a predicted target site as a possible negative control (-4808) (Figure 23C). Figure 23D shows the results of the PCR after ChIP. A signal was observed in all four cases. Moreover, the signal was specific for FOSL1flag binding, as empty vector cells show no binding. This observation points to specific FOSL1 binding in the HMGA1 genomic region, indicating that *HMGA1* is a direct transcriptional target of FOSL1 in melanoma cells.

3.4 HMGA1 and its role in melanoma

3.4.1 HMGA1 regulation in melanoma

To further investigate the regulation of the FOSL1 target HMGA1 in human melanoma, UACC62 cells were treated with a MEK1/2 and a PI3K inhibitor, respectively. In this cell line, HMGA1 was significantly regulated on mRNA and protein level by both signaling pathways (Figure 24A, B). Interestingly, analyses of a larger melanoma cell line panel revealed that MEK inhibition only reduced the HMGA1 protein amount in some cases, whereas PI3K inhibition consistently led to decreased HMGA1 abundance (Figure 24C).

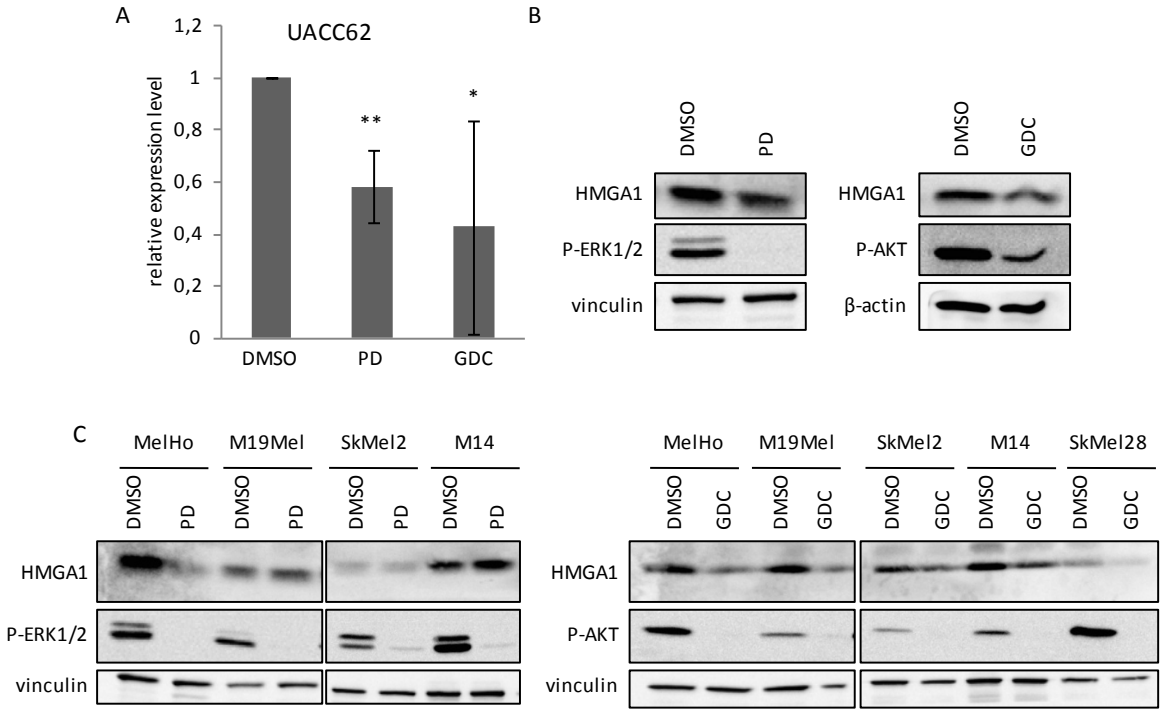

Figure 24: Regulation of HMGA1 after MEK and PI3K inhibition
A. RT-qPCR analysis of *HMGA1* mRNA levels after MEK inhibition with 2 µM PD184352 and PI3K inhibition with 5 µM GDC0941 for 24 hours in UACC62 cells (*: $p<0.05$; **: $p<0.01$) **B**. Western blot analysis of HMGA1, P-ERK1/2 (Thr202/Tyr204) and P-AKT (Ser473) levels after MEK inhibition with PD184352 and PI3K inhibition with GDC0941 for 24 hours in UACC62 cells. **C**. HMGA1, P-ERK1/2 (Thr202/Tyr204) and P-AKT (Ser473) protein levels after inhibition of MEK and PI3K in different melanoma cell lines. Vinculin and β-actin served as loading controls.

3.4.2 The influence of HMGA1 on neuronal genes

Since HMGA1 was formerly described as a transcription factor with the ability to reprogram somatic cells it was interesting to investigate whether HMGA1 regulates the neuronal FOSL1 target genes [96]. Unexpectedly, HMGA1 knockdown rather went along with a slight upregulation of *NEFL*, *NRP1* and *TUBB3* (Figure 25).

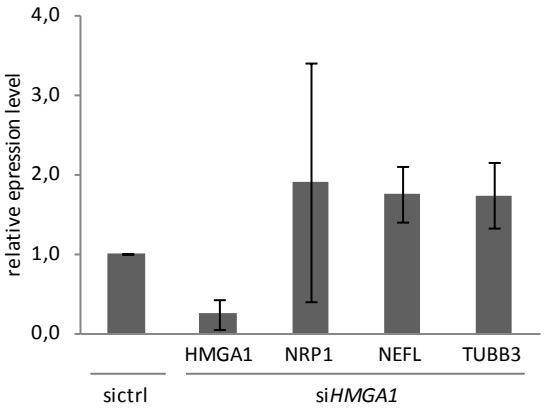

Figure 25: HMGA1 influence on neuronal genes
RT-qPCR of UACC62 cells after siRNA- mediated knockdown of *HMGA1* for 3 days compared to control siRNA transfected cells. Values were calculated from 2 independent experiments, each performed in triplicates.

This method did not confirm that HMGA1 mediates the FOSL1- dependent regulation of the neuronal genes. In spite of this indication, I was interested if HMGA1 imparts the several pro-tumorigenic effects of FOSL1.

3.4.3 Functional effects of HMGA1 in melanoma

Similar to FOSL1, HMGA1 expression is correlated to the invasive phenotype according to the analysis of the cell line specific gene expression datasets provided by Widmer et al. (Figure 26).

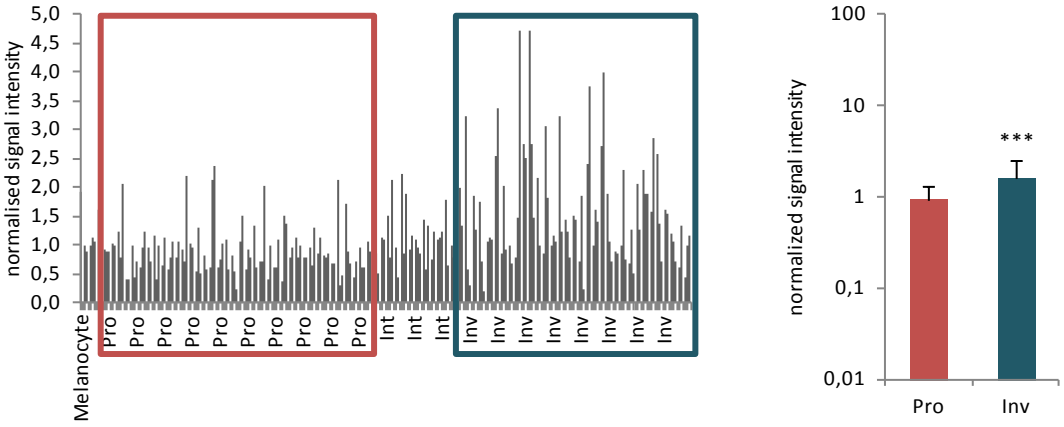

Figure 26: Classification of melanoma cells by phenotype-specific *HMGA1* gene expression
Analysis of a probeset of data of 220 samples of melanoma cell lines reveals average expression signals of 0.93 (± 0.42) and 1.54 (± 0.94) for *HMGA1* in proliferative and invasive signature samples, respectively. This difference is significant (P < 1.00E-05), but it is small (1.7-fold). Pro: proliferative, Int: intermediate, Inv: invasive [90].

Thus, it was necessary to investigate if HMGA1 affects the same pro-tumorigenic features as FOSL1 in human melanoma. Therefore, siRNA- mediated knockdown of *HMGA1* was performed. Firstly, proliferation assays were conducted. Cells with *HMGA1* knockdown were counted after three and six days and were compared to control siRNA transfected cells. Figure 27A shows that the *HMGA1* knockdown was very efficient, and displayed a massively reduced proliferation rate (Figure 27B). Secondly, it was determined whether HMGA1 is also necessary for anchorage independent growth of the melanoma cells. Hence, control siRNA cells and *HMGA1* knockdown cells were seeded in soft agar and were allowed to grow for seven days. Subsequently, colonies were counted. Knockdown of *HMGA1* led to significantly reduced number of colonies at a similar rate as *FOSL1* knockdown (compare Figure 27C and Figure 15).

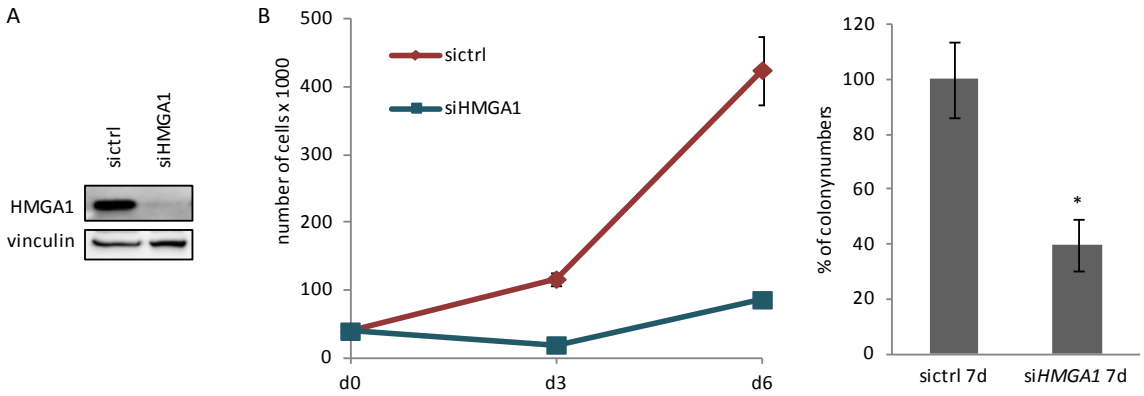

Figure 27: HMGA1- dependent proliferation and anchorage independent growth in human melanoma
A. Western blot of HMGA1 in UACC62 cells after siRNA- mediated gene knockdown after 3 days. Vinculin served as loading control **B**. Proliferation of UACC62 cells after siRNA- mediated knockdown of HMGA1 compared to control siRNA transfected cells. Cells were counted after 3 and 6 days. The experiment was performed two times in triplicates. **C**. Soft agar assay growth of UACC62 cells after siRNA- mediated knockdown of *HMGA1*. Cells were allowed to grow in soft agar for 7 days. Afterwards, colonies consisting of more than 8 cells were manually counted. Calculations were made from two different biological experiments, each performed in triplicates.

3.4.4 HMGA1 as mediator of FOSL1-driven pro-tumorigenic effects

To investigate whether HMGA1 is responsible for the pro-tumorigenic effects of FOSL1 overexpression, I performed a siRNA- induced *HMGA1* knockdown in FOSL1 overexpressing cells. The HMGA1 knockdown was very efficient in the control cells and in FOSL1 overexpressing cells (Figure 28A). At first, a proliferation assay was conducted. As expected, the proliferation inducing effect of FOSL1 overexpression could be observed. When HMGA1 was knocked down, proliferation was strongly impaired irrespective of the presence of the FOSL1 overexpression construct (Figure 28).

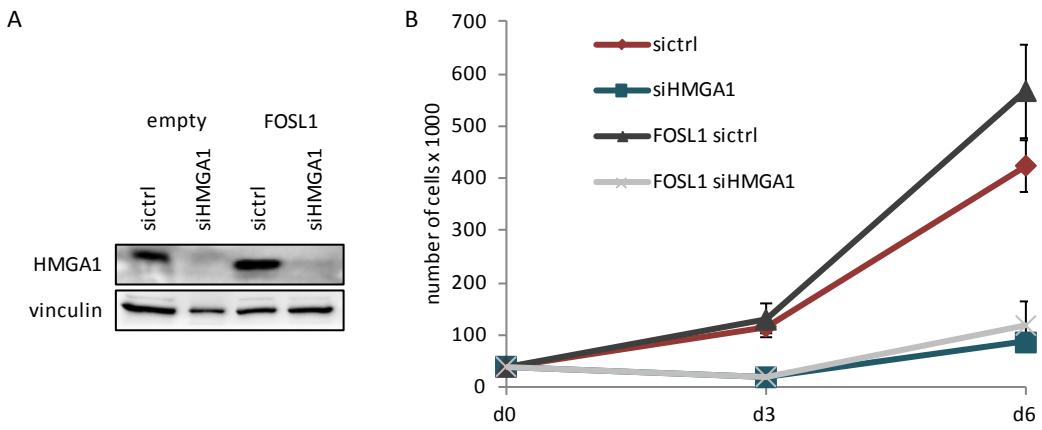

Figure 28: HMGA1 influence on FOSL1- induced proliferation in human melanoma cells
A. Western blot analysis of empty vector and FOSL1 expressing UACC62 cells after siRNA- induced knockdown of *HMGA1* for 3 days. Vinculin served as a loading control. **B**. Proliferation assay of empty vector and FOSL1 overexpressing UACC62 cells after siRNA- mediated knockdown of *HMGA1*. Cells were counted after 3 and 6 days. The results for the empty vector cells are the same as shown in Figure 27B and they are included here for the sake of completeness. The assay was performed two times in triplicates.

In addition, I monitored colony formation potential of these cells. For this purpose, 2D colony formation assay with a starting cell number of 150 cells per 6-well was performed. As previously described, FOSL1 overexpression enhanced the colony forming ability clearly, but siRNA caused knockdown of *HMGA1* reduced the colony number of both empty vector and FOSL1 overexpressing cells (Figure 29A). The soft agar assay also showed that whereas 3D colony forming potential was vastly reduced under conditions of HMGA1 knockdown, it was not rescued by FOSL1 overexpression (Figure 29B).

Taken together, these findings show that HMGA1 knockdown abolished FOSL1- dependent cellular processes. In control cells, HMGA1 knockdown even had a stronger effect compared to FOSL1 knockdown, which might be attributed to the higher siRNA efficiency (compare Figure 27A and Figure 22C).

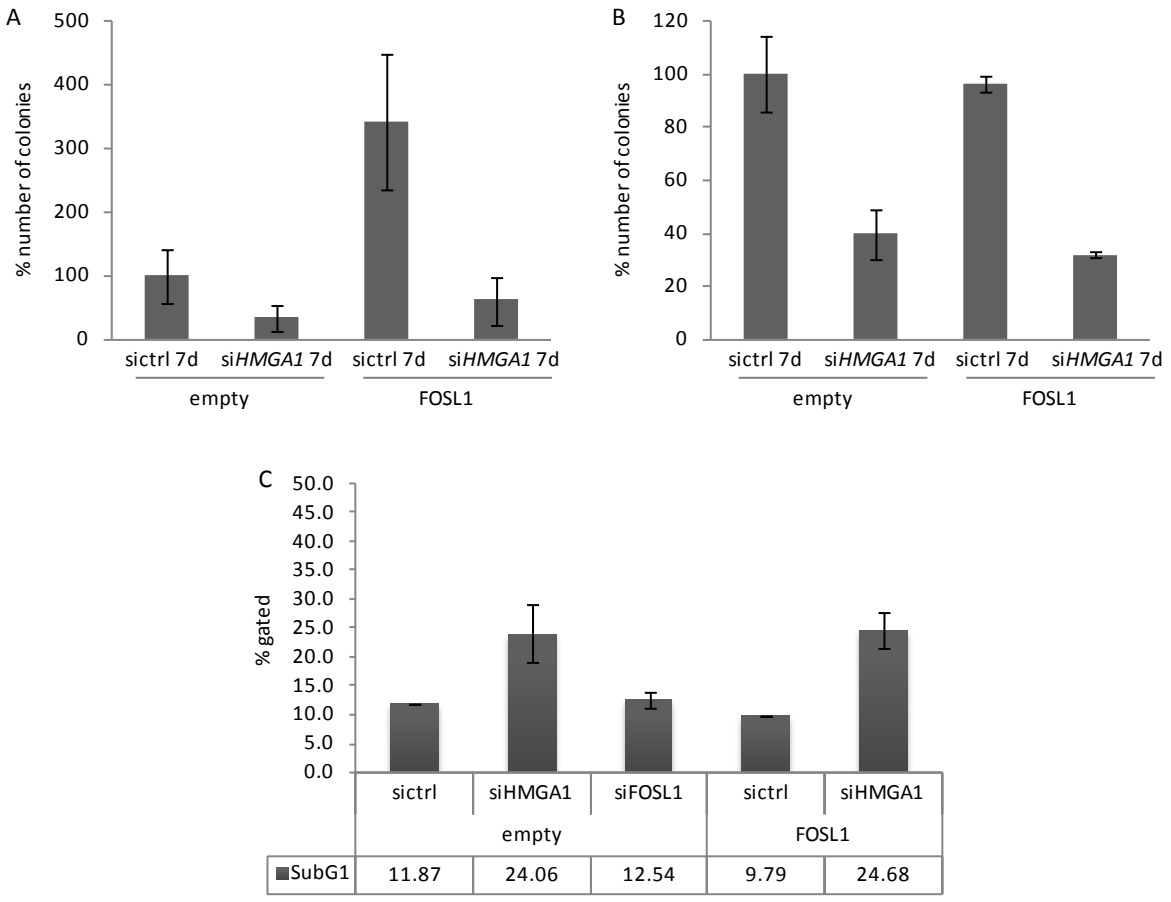

Figure 29: HMGA1 effect on FOSL1-induced colony forming ability and HMGA1-dependent cell death of human melanoma cells

A. Quantification of 2D-colony formation assay of empty vector and FOSL1 overexpressing UACC62 cells after siRNA- mediated knockdown of *HMGA1*. **B**. Quantification of soft agar assays of empty vector and FOSL1 overexpressing UACC62 cells after siRNA- mediated knockdown of *HMGA1* compared to control siRNA treated cells, respectively. Cells were allowed to grow for 7 days. The results for the soft agar assay in empty vector cells are the same as shown in Figure 27B and they are shown here for the sake of completeness. **C**. Cell death in UACC62 control and FOSL1 overexpressing cells after siRNA- mediated knockdown of *HMGA1*. Cells were fixed 3 days after siRNA-mediated knockdown, stained with propidium iodide and FACS analysis was performed. The experiment was performed two times.

As I could observe a slight decrease in cell number after 3 days in UACC62 empty vector and FOSL1 overexpressing cells after siRNA- mediated knockdown of *HMGA1* (Figure 27 and Figure 28), I checked whether enhanced cell death was involved in this effect. FACS analyses were performed to determine SubG1 levels of the mentioned cells. Figure 29C shows that the siRNA- mediated knockdown of *HMGA1* in UACC62 empty vector cells and FOSL1 overexpressing cells induced an increased number of cells in the subG1 phase, indicating cell death. However, cell death was not induced by siRNA-mediated knockdown of *FOSL1*.

Conclusively, a gain of FOSL1 in human melanoma cells, as e.g. observed in patients with metastatic melanoma by 11q13 amplifications, resulted in an advantage of melanoma maintenance, which was strongly influenced by FOSL1- dependent HMGA1 induction.

4. Discussion

4.1 FOSL1 and cellular plasticity

4.1.1. FOSL1 as pro-tumorigenic and tumor-maintaining transcription factor

In a variety of human tumors of epithelial origin, FOSL1 is linked to tumorigenic processes, especially metastasis. Different groups could show that FOSL1 is responsible for the induction of invasion and cellular processes similar to EMT [73, 74, 77, 88, 99]. EMT was originally described to occur during embryogenesis. In general, the cells undergoing EMT lose cell adhesion and their epithelial phenotype and gain motility features and a more mesenchymal phenotype. The metastatic spread of a cancer cell is strongly reminiscent of the cellular behavior of a cell during EMT [100], and comparable events were also observed in melanoma, a non-epithelial tumor [101]. In several human tumors, such as breast and bladder cancer, the FOSL1 downstream effectors were identified. In most cases, these effectors are inducers of metastatic cellular features. Among these FOSL1 targets are well described EMT inducing transcription factors, such as ZEB1/2 [74], receptor tyrosine kinases, such as AXL, which regulates cell motility [88] and regulators of cell invasion, such as the matrix metalloproteinase MMP1 [102] or CD44, a cell surface glycoprotein involved in migration and adhesion [99, 103].

The present thesis reveals that in human melanoma cells, FOSL1 overexpression in cells with a low endogenous level of FOSL1 also led to pro-tumorigenic features which included migration, but mainly affected proliferation and colony formation. As the cell lines used in this study are already fully transformed, it is difficult to address whether this proliferative feature plays a role during growth and establishment of the primary tumor. As FOSL1 expression is highest in metastases, it is tempting to assume that the enhanced FOSL1 levels enable the maintenance of metastases due to the high proliferative characteristics.

4.1.2 FOSL1 and dedifferentiation in melanoma

Next, it was interesting to investigate the FOSL1 downstream effectors in the context of melanoma and to determine if invasion or EMT-related genes play a role. Microarray analysis revealed several target genes of FOSL1, but the common EMT inducers were not substantially regulated. Hence, this result indicates that FOSL1 dependent melanoma progression must be regulated in an alternative way compared to the epithelial tumors, where FOSL1 acts as an EMT activator. Strikingly, FOSL1 levels influenced the regulation of many neuron-related genes, such as *NEFL*, *NRP1* and *TUBB3*, which is interesting due to the embryonic origin of melanocytes. Melanocytes and neurons, as well as craniofacial cells, neuroendocrine cells and glia cells derive from the neural crest, a highly migratory

embryonic tissue [104]. It depends on the strictly regulated program whether a neural crest cell differentiates into the one or the other direction. The melanocytic lineage is dependent on WNT and NOTCH signaling, leading finally to the expression of MITF, the transcriptional master regulator for melanocyte specification and differentiation [105]. The acquisition of neuron-related gene expression of melanoma cells could point to de- or transdifferentiation processes. Dedifferentiation in cancer cells has been observed in different human tumor types such as breast cancer, glioblastomas, bladder and colon carcinomas. In these tumors the dedifferentiation can lead to stem cell associated features of cells within the tumors and is linked to strong heterogeneity, aggressiveness or poor prognosis [106, 107]. In melanoma, the cancer stem cell theory is controversially discussed, but dedifferentiation events were investigated in different models. Landsberg et al. could observe dedifferentiation of melanoma cells after successful T-cell immunotherapy. These dedifferentiated melanoma cells highly expressed the typical neural crest marker NGFR (nerve growth factor receptor) and showed a dedifferentiation-associated tumor relapse. Cheli et al. demonstrated, that knockdown of the differentiation-relevant transcription factor MITF in melanoma cells results in the re-expression of pluripotency markers and enhanced invasiveness [108, 109]. A comparable modulation of differentiation is performed by FOSL1. Besides regulating neuron-related genes, I found that FOSL1 was also able to influence the melanocyte specific pigment gene *DCT*. Whereas *TYR* levels, another pigment marker gene, did not change in response to alterations of FOSL1 levels, *DCT* was downregulated in the strongly dedifferentiated and depigmented cell lines A375 and UACC62. In the most differentiated and pigmented cell line UACC257, FOSL1 overexpression did not affect *DCT* expression levels. However, the effect on the neuron-related genes was highest in this cell line. The reduced expression of pigment genes supports the theory, that FOSL1 has dedifferentiating effects on melanoma cells.

Interestingly, the neuron-related genes, which were analyzed during this study, were previously connected to enhanced invasion or aggressiveness of melanoma cells. *Nefl* was recently shown to be included into a group of dedifferentiation genes, which are upregulated in highly aggressive, anoikis-resistant, NRAS-transformed melanocytes [110]. NRP1 is a co-receptor of VEGF-A, which mediates signaling through VEGFR-2 and thereby strongly enhances migration of melanoma cells in a syngeneic mouse model. Additionally, NRP1 promotes MMP2 secretion, resulting in increased invasiveness of melanoma cells [111]. Furthermore, *NRP1*, along with *FOSL,* is strongly associated with an invasive signature according to phenotype-specific gene expression mapping of a panel of 220 melanoma cell lines [90]. TUBB3 is a class III member of the beta tubulin protein family and constitutes a commonly used neuronal marker. In a publication of 2006, TUBB3 expression was linked to reprogramming of malignant melanoma cells. The group worked on the transplantation of human melanoma cells into the area surrounding the neural crest in an embryonic chick model. They observed that a

subpopulation of cells, which invaded the chick tissue, acquired expression of TUBB3 [112]. Beside the neuron related genes *NEFL*, *NRP1* and *TUBB3*, I detected the high mobility group AT-hook 1 (*HMGA1*) as novel target of FOSL1 in melanoma.

4.2 HMGA1- a novel player in melanoma?

HMGA1 is a non-histone chromatin protein that contains 3 AT-hooks. With these positively charged motifs it is able to bind AT-rich regions in the minor groove of the DNA, thereby changing the chromatin conformation and increasing the affinity of other DNA-binding proteins for their binding sites. Moreover, HMGA1 is able to establish protein-protein interactions with transcription factors. Thus, HMGA1 harbors no intrinsic transcriptional activation capacity, but highly contributes to induction of transcription by influencing the structural architecture of chromosomes and recruiting further activating regulators [113].

Whereas HMGA1 is highly and ubiquitously expressed during embryonic development, it is only weakly expressed in normal adult tissue [114].

The *HMGA1* transcript is processed into three different *HMGA1* splice variants: *HMGA1a*, *HMGA1b* and *HMGA1c*. HMGA1a and HMGA1b only differ in eleven amino acids, which are present in HMGA1a (107 amino acids), but absent in HMGA1b (96 amino acids). HMGA1c was reported to be generated by non-canonical splicing, leading to a frame shift compared to the HMGA1a and HMGA1b variant, therefore containing only 2 AT- hooks to bind DNA. HMGA1c (179 amino acids) resembles HMGA1a and HMGA1b in the first 65 amino acids, but then it differs [115]. In more recent publications, HMGA1c is not mentioned anymore as relevant isoform of the *HMGA1* transcript and is not listed in the transcript table of the *HMGA1* gene overview on the genome browser ENSEMBL, indicating that this isoform is considered as biologically irrelevant.

Potential differences in the function and activity between the HMGA1a and b isoform are barely investigated. Previously published data suggested differing functions of HMGA1a and b, as the two proteins underwent different posttranslational modifications, but no evidence was produced [116]. Furthermore, another group determined only slight differences in the DNA- binding affinities of the two isoforms [117]. A direct comparison of the downstream regulated target genes of HMGA1a and b using microarray analysis illustrated, that more than a half of the 2-fold upregulated genes after overexpression of either HMGA1a or HMGA1b in fbroblasts are overlapping [118]. The same group could monitor a transformed phenotype of fibroblasts and B lymphoid cells, if either HMGA1a or b was ectopically expressed. Moreover, the transformed fibroblasts formed tumors in athymic, nude mice. However, metastasis to the lung was only observed in mice, which were injected with HMGA1a overexpressing fibroblasts [119].

In all experiments shown in this work, HMGA1a and b were affected by the siRNA- mediated knockdown. Moreover, the used HMGA1 antibody detected both isoforms. This is also the case for the vast majority of HMGA1 publications, as the commonly available antibodies against HMGA1 are not able to distinguish the small difference of 11 amino acids between the two isoforms.

The variety of biological functions of HMGA1 goes along with the multilateral modes of action of HMGA1. Whereas FOSL1 knockdown mice are embryonic lethal, HMGA1 knockdown mice are viable and show physiological and anatomical aberrations. *HMGA1*$^{-/+}$ and *HMGA1*$^{-/-}$ mice suffer from cardiac hypertrophy and develop myelo-lymphoproliferative disorders in 78% of heterozygous and 80% of homozygous knockout mice, respectively, which becomes apparent at 12 months of age. The myelo-lymphoproliferative disorders include myeloid/ lymphoid hyperplasia, B-type lymphoma and myeloid leukemia [120]. Moreover, the lack of HMGA1 in mice leads to a phenotype similar to type 2 diabetes mellitus. The mice display insulin resistance as well as reduced insulin secretion [121].

The constitutional CMV-driven overexpression of HMGA1 in several examined organs of transgenic mice including muscle, lung, testis, heart, hypophysis, spleen, liver, white adipose tissue, and kidney leads to development of pituitary adenomas and natural killer cell lymphomas. Furthermore, in several animals hyperplasia of the pancreas and the adrenal gland were diagnosed [122].

Consistent with the malignant phenotype of HMGA1 transgenic mice, HMGA1 is also closely linked to malignancy in humans. In several tumors, HMGA1 was found to be overexpressed. Most of these tumors belong to the group of malignant epithelial tumors, such as tumors of the prostate, colorectum, lung, breast, pancreas and thyroid [123-128]. In all described tumors, increasing levels of HMGA1 are correlated to increasing degrees of malignancy or metastatic potential. In uveal melanoma, HMGA1 expression was found in 44% of 89 examined tumors in a study from 2013. In these tumors, HMGA1 expression was directly correlated to mitoses counts, and high HMGA1 protein expression was associated to shorter survival of the patients [129].

4.2.1 Tumor promoting effects of HMGA1

In the present work, it was demonstrated that the siRNA mediated knockdown of HMGA1 in melanoma cells had anti-tumorigenic consequences. Similar to *FOSL1* knockdown, *HMGA1* knockdown strongly reduced proliferation rate and soft agar growth. These cellular processes are also influenced by HMGA1 in other tumors. Proliferation rates of bladder cancer cells were diminished after HMGA1 reduction via a miRNA-dependent process. HMGA1 is a direct target of miR-26a, which directly binds to the 3'UTR of *HMGA1* mRNA. Hence, elevated levels of miR-26a resulted in diminished HMGA1 levels and proliferation rates [130]. Moreover, in human gliomas and pituitary adenomas HMGA1 upregulation was correlated to enhanced proliferation [131, 132]. Anchorage independent growth was

also altered in several tumor types in a HMGA1 dependent manner. In breast cancer cells and large cell lung carcinoma the knockdown of HMGA1 led to decreased anchorage independent growth. The same result was seen for pancreatic adenocarcinoma cells. Furthermore, anoikis resistance was enhanced if HMGA1 levels were increased in these cells. In all of these mentioned tumor entities HMGA1 expression is closely linked to metastasis and HMGA1 is considered to be a prognostic marker. In melanoma cells HMGA1 knockdown had clear tumor suppressive effects, but did not contribute to the FOSL1 dedifferentiating capability as examined by the expression of the neuronal genes *NEFL*, *NRP1* and *TUBB3*. Nonetheless, it was observed that the most dedifferentiated cell line A375 contained the highest amount of HMGA1. As HMGA1 is also demonstrated to be necessary for FOSL1-mediated pro-tumorigenic effects in melanoma cells, HMGA1 likely acts in parallel to the neuronal gene induction.

A recent publication from 2013 revealed a HMGA1 gene expression signature in breast cancer, which was activated in a large subset of tumors and was linked to poor prognosis. Additionally, the group observed induced mesenchymal- to- epithelial transition (MET), decreased stemness and reduced self renewal of breast cancer cells after HMGA1 knockdown. This resulted in decreased migration and invasion *in vitro* and in the diminished formation of metastases in lungs *in vivo*. This observed phenotype was in line with the HMGA1 regulated genes being closely related to EMT processes and the formation of stem cells. As the HMGA1 gene expression signature included several genes, which serve as biomarkers for prognosis, relapse and metastasis in breast cancer, HMGA1 was again classified as crucial indicator for tumor progression [133]. However, a link to genes which are associated with breast cancer dedifferentiation was not observed.

In colon cancer, an association of HMGA1- induced tumor progression and induction of stem cell properties could be identified [134].

In general, HMGA1 has several mechanisms of action and a broad spectrum of target genes in cancer cells. One mechanism is mediated by direct interaction of HMGA1 with other proteins. HMGA1 was shown to bind the small pocket domain of retinoblastoma protein in glioblastoma cells. The interaction of the two proteins abolishes the inhibitory effect of retinoblastoma protein on E2F1 and allows transcriptional activation of target genes. In glioblastoma cells, the cyclin E gene expression was induced via this signaling axis if HMGA1 was overexpressed, leading to the abrogation of a serum-starvation induced G0 arrest [135]. As E2F1 plays a crucial role in melanoma progression and metastasis, this HMGA1 dependent influence on E2F1 might also be an interesting process in melanoma [136]. HMGA1 was also reported to bind to p53, a second important tumor suppressor in melanoma. In colon carcinoma and non small cell lung cancer cells it was demonstrated that HMGA1 directly binds to p53 and in turn diminishes p53- dependent apoptosis. This phenotype is mediated by

the HMGA1 induced modulation of p53 transcriptional activity. HMGA1 suppresses the inhibitory effect of p53 on *BCL-2* expression, resulting in diminished apoptosis induction [137].

Besides the direct binding of effector proteins, HMGA1 was also demonstrated to affect nucleotide excision repair (NER) after DNA damage. In breast cancer cells HMGA1 inhibited NER after DNA damage induced by UVB exposure. Due to the lack of DNA repair, chromosomal rearrangements, resulting in the acquisition of genomic and chromosomal instability, were observed. The authors proposed two mechanisms for the influence of HMGA1 on NER. One the one hand, there was indication that HMGA1 directly binds to the UVB induced cyclobutane pyrimidines (CPD) and shields the NER machinery from the DNA. On the other hand, they observed the HMGA1 dependent alteration of the expression of NER genes, such as the downregulation of *XPA* (Xeroderma pigmentosum, complementation group A) [138]. CPDs, if unrepaired, can result in cytosine to thymidine transitions, thus giving rise to the UVB signature which is typical for human melanoma, Consequently, a connection between HMGA1 and NER might also be relevant for this tumor type [139].

HMGA1 is also able to exert its influence on cells by assisting in target gene induction. The spectrum of affected genes is broad. In a cancerous background, *MMP2*, *MMP9, MMP13* and *MMP16* were regulated in a HMGA1 dependent manner. *MMP2* was upregulated by HMGA1 in undifferentiated, large-cell lung cancer and promoted transformation [140]. In pancreatic adenocarcinoma cells, *MMP9* was shown to be upregulated if HMGA1 was overexpressed and was linked to cellular invasiveness [141]. In human epithelial cells, HMGA1 overexpression caused *MMP13* and *MMP16* upregulation and was associated to epithelial-to-mesenchymal transition [142]. Besides the invasion related MMP genes, cell cycle and growth regulators were also regulated by HMGA1. In medulloblastoma, *HMGA1* knockdown led to diminished cdc25A (M-phase inducer phosphatase 1) levels, which was highly correlated with reduced cell growth [143].

Furthermore, enzymes involved in different metabolic pathways are regulated by HMGA1. One melanoma relevant factor might be the cyclooxygenase-2 (COX-2), a bifunctional enzyme, which is involved in prostaglandin and thromboxane production, as it catalyzes the conversion of arachidonic acid to PGG_2 (prostaglandin G_2) and subsequently the further conversion of PGG_2 to PGH_2 (prostaglandin H_2). This enzyme is highly expressed in malignant melanoma cells and metastatic lesions, but not in nevi or primary skin melanoma cells [144]. In uterine tumors and pancreatic adenocarcinomas, HMGA1 increased COX-2 expression. In the pancreatic cancer system, COX-2 inhibitors abolished tumorigenic potential of xenografts with high endogenous levels of HMGA1 [145]. In the uterine tumors of transgenic mice, which overexpress HMGA1 under the control of a H-2K promoter and an immunoglobulin μ intronic enhancer, COX-2 mRNA and protein levels were upregulated being in line with enhanced HMGA1 and COX-2 expression levels in human high-grade

uterine leiomyosarcoma tumors. Complementarily, *COX-2* was identified as direct target gene of HMGA1 by ChIP analysis [146].

4.2.2 The FOSL1/HMGA1 signaling axis in cutaneous melanoma

The present work shows that FOSL1 and HMGA1 are both expressed in human melanoma cell lines. Interestingly, the levels are differing between the investigated cell lines, but the expression levels of both proteins show a clear tendency of correlation. Regarding different human tumors, it was striking that both transcription factors are overexpressed in a variety of tumor entities, mainly of epithelial origin. Furthermore, FOSL1 and HMGA1 were both found to be associated with metastasis and poor clinical outcome in patients with diverse kinds of tumors, as for example colorectal cancer and breast cancer [133, 147-149].

In melanoma cells, HMGA1 mRNA and protein levels were diminished after FOSL1 knockdown and increased in FOSL1 overexpressing melanoma cells, showing the FOSL1 dependent transcriptional regulation of HMGA1. Moreover, the ChIP analyses in my study indicate that HMGA1 is a direct transcriptional target of FOSL1.

The pro-tumorigenic effects of FOSL1 and HMGA1 are overlapping in melanoma cells. Both transcription factors regulate proliferation, colony forming ability and anchorage independent growth. Moreover, FOSL1 enhanced migration ability of melanoma cells. As the used UACC62 cells are unable to migrate in the transwell migration assay used in this study, I did not investigate HMGA1 dependent migration. Nevertheless, HMGA1 influenced migration capacity of several examined tumor cell lines, such as basal-like breast cancer and bladder cancer, hence it is possible that HMGA1 may also affect melanoma cell migration [130, 133]. Finally, for all FOSL1 induced pro-tumorigenic effects HMGA1 was shown to be absolutely necessary. Enhanced FOSL1 dependent proliferation and colony forming ability was reversed by HMGA1, revealing a functional FOSL1/HMGA1 tumor promoting signaling axis in melanoma. However, knockdown of *HMGA1* led to the induction of apoptosis, which was not observed when *FOSL1* levels were reduced. A possible explanation for this observation might be the stronger knockdown efficiency of HMGA1 compared to FOSL1 (compare Figure 11C and Figure 23A).

Additionally, the influence of upstream signals on FOSL1 and HMGA1 in melanoma was determined. The data revealed that FOSL1 mRNA and protein levels are strongly dependent on MEK1/2 signaling. In contrast, HMGA1 responds to a much lesser extent to MEK inhibition than FOSL1, at least on protein level. More precisely, HMGA1 protein expression was diminished in two of the five tested melanoma cell lines after MEK inhibition. In contrast to that, after PI3K inhibition, HMGA1 was downregulated to lower levels compared to MEK inhibition in all six examined melanoma cell lines. Thus, HMGA1 levels are modulated to a higher degree by PI3K signaling than by ERK1/2 signaling. As FOSL1 and HMGA1

show these different dependencies on the upstream signaling, there is indication that HMGA1 regulation in melanoma underlies additional mechanisms in addition to FOSL1 mediated regulation.

Analyses of the *HMGA1* promoter region and the regulation of this gene in other cell systems provide insight into the complex modulation of *HMGA1* expression. The promoter region contains several binding motifs for classical transcription factors, which are also interesting for melanoma tumors. In the proximal regulatory region an AP1 binding site was discovered and found to be responsible for TPA induced activation of *HMGA1* expression in immortalized leukemia cells [150]. Together with a close SP1 binding site, this AP1 site was demonstrated to be important for the basal transcription of *HMGA1*. In contrast, a distal AP1 binding site and three vicinal SP1-like binding sites are responsible for oncogenic RAS mediated induction of *HMGA1* expression [151]. These AP1 binding sites were not investigated in the ChIP analysis of this work, as only a moderate accumulation of FOSL1 at this site was measured in the referenced HCT116 ChIP experiment and no predicted FOSL1 binding site was indicated by the DECODE database. Moreover, an E-box was located at -1353 bp of the HMGA1 promoter and was shown to be essential for c-MYC-dependent induction of *HMGA1* expression in Burkitt's lymphoma and HEK293 cells [152]. Also MYCN was identified as regulator of *HMGA1* transcription. In neuroblastoma cells, MYCN mediated expression via multiple *cis*-acting MYCN response elements, which were found near the transcriptional start sites of the *HMGA1* gene [153]. Interestingly, also E2F1 was demonstrated to stimulate the transcription of *HMGA1*. The authors uncovered a putative E2F1 binding site and found that E2F1 functionally interacted with SP1 to stimulate *HMGA1* transcriptional induction [154]. The overexpression of E2F1 is frequently found in high-grade tumors and is also associated with an aggressive phenotype in melanoma [136].

Moreover, further signaling pathways have been described to mediate HMGA1 levels. HMGA1 was found to be regulated by miRNAs. As described above, miR-26a was shown to influence HMGA1 levels in bladder cancer [130]. In prostate cancer it was demonstrated that *HMGA1* mRNA is a direct target of miR-296. Frequently diminished levels of miR-296 in pancreatic tumors were highly linked to strongly enhanced HMGA1 levels. Moreover, ectopic expression of miRNA296 resulted in HMGA1 downregulation and reversed proliferation and invasion [155]. Intriguingly, both miRNAs, miR-26a and miR-296, are strongly downregulated in metastatic melanoma [156, 157].

4.3 Conclusion

The present study demonstrates that FOSL1 induces several tumor promoting effects in human melanoma by the activation of dedifferentiating properties. As FOSL1 expression strongly depends on activated ERK1/2- signaling and PI3K- signaling, the pharmacological interruption of the FOSL1-dependent tumorigenic mediation of melanoma is possible. Moreover, the investigation of the novel FOSL1 target gene HMGA1, an activating transcription factor with reprogramming abilities, elucidates a mechanism for the conversion of FOSL1 into the observed pro-tumorigenic effects. Taken together, this work identifies FOSL1 as a crucial regulator of melanoma maintenance and activator of dedifferentiation processes of melanoma cells.

Appendix

1. *fosl1* and *jun* in the *mitf:xmrk* medaka melanoma model

To investigate the role of Fosl1 and its dimerization partner Jun in an in vivo melanoma model, I planned to generate transgenic fish lines for *fosl1* and *jun* from a *mitf:xmrk* transgenic medaka. These fishes express Xmrk (Xiphophorus melanoma receptor kinase), a constitutively activated and oncogenic version of Egfr (epidermal growth factor receptor) under the control of the pigment cell specific mitfa promoter. Consequently, these fishes suffer from pigment cell tumors, including black melanomas (Appendix Figure 1A) and yellowish xanthoerythrophoromas (Appendix Figure 1B) [158].

Appendix Figure 1: Representative *mitf:xmrk* transgenic medaka fishes
A. 4-week-old-juvenile medaka with invasive extracutaneous melanotic melanoma. **B**. 10-week-old medaka with exophytically growing xanthoerythrophoroma. (Images from [158]).

At the beginning of the project, it was important to investigate the existence and number of orthologue *fosl1* and *jun* medaka genes. The Ensembl genome browser revealed one medaka *fosl1* gene (ENSORLG00000002045) and two medaka *jun* genes (ENSORLG00000014541 and ENSORLG00000010096)[62]. For the sake of simplification, the *jun* gene ENSORLG00000014541 was named *jun-a* and the second *jun* gene ENSORLG00000010096 was named *jun-b*. Next, the mRNA expression levels of the *fosl1* and the two *jun* genes were determined in different wildtype medaka tissues and different xanthoerythrophoroma and melanoma tumors of *mitf:xmrk* transgenic medaka. Appendix Figure 2 shows that *fosl1* and *jun-b* were ubiquitously expressed in the examined tissues, while *jun-a* was not expressed in liver. In most tissues *fosl1* was expressed to a higher extent than the two *jun* isoforms.

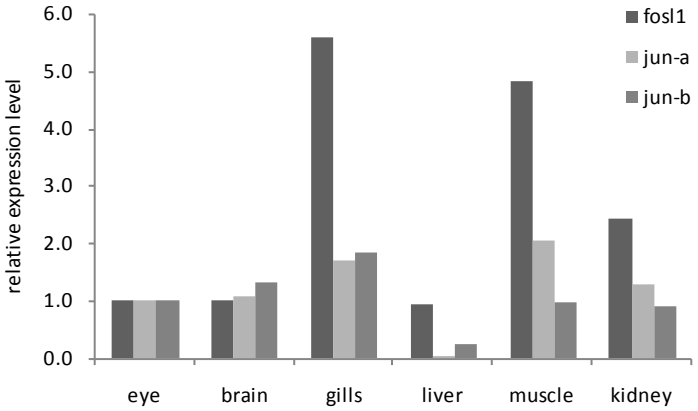

Appendix Figure 2: Expression levels of *fosl1, jun-a* and *jun-b* in medaka wildtype tissues
RT-qPCR of *fosl1*, *jun-a* and *jun-b* in different medaka wildtype tissues normalized to β-actin levels and eye tissue. RT- qPCR was performed once in triplicates.

Fosl1, *jun-a* and *jun-b* were also expressed in the different tumor samples. Interestingly, the expression of all three genes was very heterogenous, irrespective of the tumor type (Appendix Figure 3).

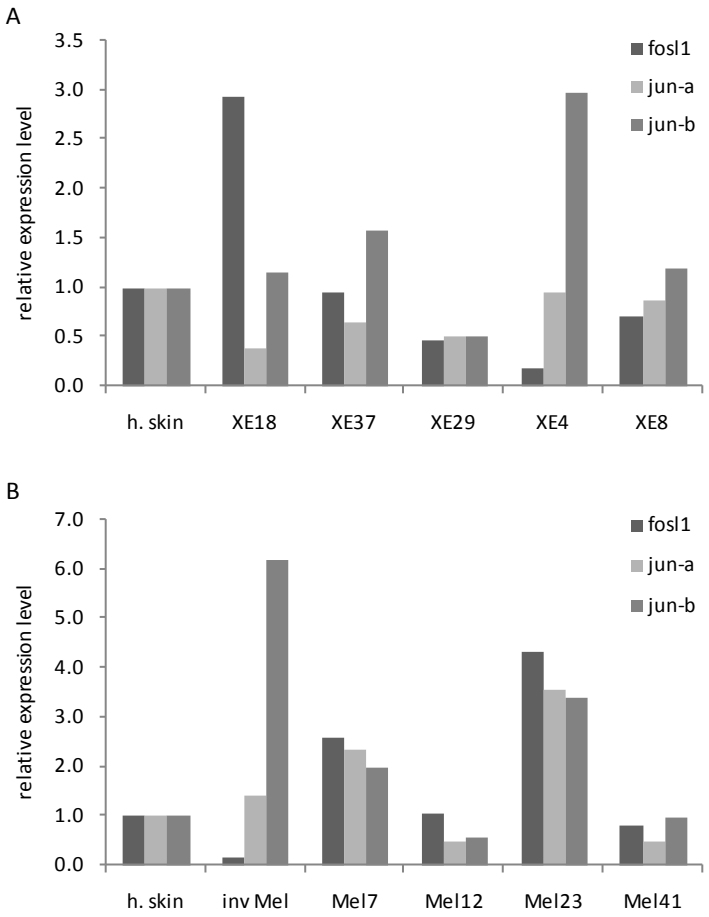

Appendix Figure 3: Expression levels of *fosl1, jun-a* and *jun-b* in *mitf:xmrk* transgenic medaka pigment cell tumors

RT-qPCR of *fosl1*, *jun-a* and *jun-b* in **A**. yellowish xanthoerythrophoroma tumors and **B**. black melanoma tumors (inv Mel: invasive melanoma). mRNA levels were normalized to hyperpigmented skin (h. skin) and β-actin. RT-qPCR was performed once in triplicates.

To better understand the contribution of *fosl1* and the two *jun* genes to the *mitf:xmrk* induced tumors, I planned to generate novel transgenic fish lines harboring different wildtype and truncated version of these genes in the *mitf:xmrk* background. Next experimental steps to generate these *fosl1* and *jun* transgenic fish lines would have been the microinjection of the respective constructs, coinjected with the meganuclease enzyme into the one cell stage of *mitf:xmrk* transgenic medaka embryos. The meganuclease enzyme I-SceI is an endonuclease from S. cerevisiae which linearizes transgenes of interest flanked by recognition sites for a more efficient integration into the genome [159].
For the purpose of generating transgenic fish lines, different versions of *fosl1* and the *jun* genes were amplified by PCR from wildtype medaka tissue and cloned into a meganuclease recognition site containing vector under the control of the mitfa promoter (Appendix Figure 4).

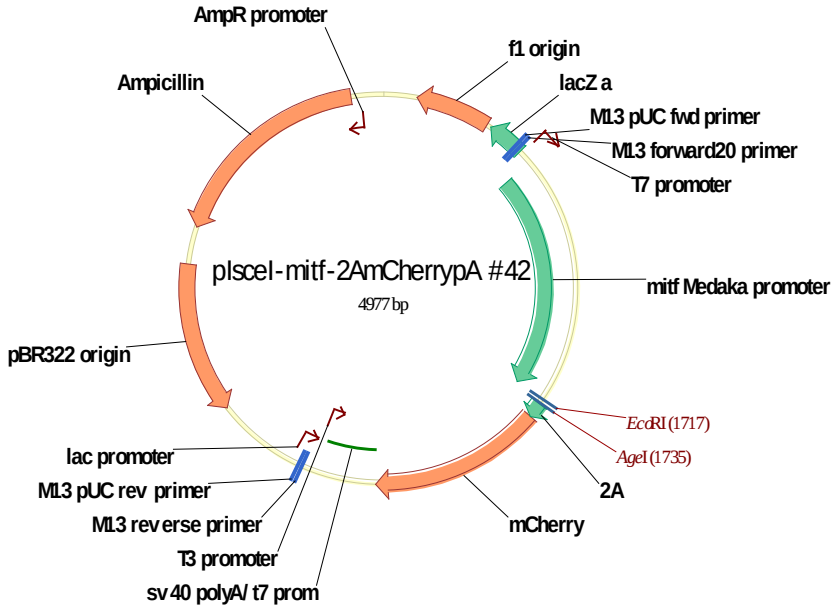

Appendix Figure 4: Meganuclease vector pI-sceI-mitf2A-mcherry
Scheme of the meganuclease vector pIsceI-mitf2A-mcherry containing the *mitfa* promoter of medaka to drive the expression of a gene of interest and the downstream 2A-m-cherry construct. Indicated restriction sites for EcoRI and AgeI mark the integration site for medaka *fosl1*, *fosl1* interaction domain and *jun-a and jun-b*.

I cloned full length *fosl1* to accomplish a Fosl overexpressing situation in the pigment cells of medaka. Additionally, I cloned the bZip domain of Fosl1 as a dominant-negative competitor to the endogenous Fosl1, lacking the amino acids 155-191 (in humans: Δ131-167 [160])(Appendix Figure 5 A). For the two Jun proteins the previously described dominant-negative versions Tam-67 were planned to clone. These Jun versions lack their transactivation domains (Δ 3-121), resulting in the formation of transcriptionally inactive AP1 complexes (Appendix Figure 5B) [161].

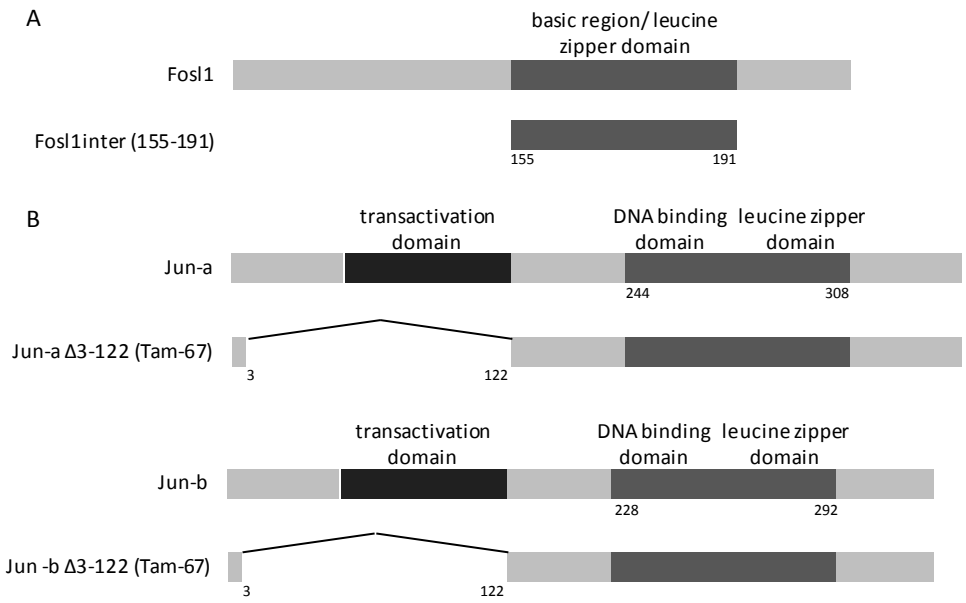

Appendix Figure 5: Schematic map of different medaka Fosl (A) and Jun (B) versions for generating transgenic fish lines

The meganuclease vector already contained a T2A site directly upstream of a m-cherry fluorescence reporter gene. This T2A self-cleavage site ensures the transcription of the upstream gene of interest and the downstream m-cherry reporter to almost identical amount [162].

For the dominant-negative version of JUN, TAM-67, and its effect in melanoma, several groups showed reduced target gene expression and reduced tumorigenicity [163, 164]. However, further literature research and discussion with our collaborators revealed that TAM67 is too unspecific to surely investigate the role of only JUN and not generally JUN-containing, whole AP1 complexes. FOSL1 dependent features for example would be hidden by the overexpression of JUN, as FOSL1 needs to bind as a JUN:FOSL1 heterodimer to DNA to activate transcription [63].

2. Dominant-negative FOSL1 and JUN in human melanoma

In addition to the medaka melanoma system, the role of dominant-negative version of *FOSL1* was also investigated in a human melanoma cell line. As the constitutive overexpression of full length FOSL1 has a distinctly positive effect on proliferation, the sequence of the JUN interaction domain of the human FOSL1 (FOSL1inter) was also cloned in the p201-iEP vector and expressed in MelHo cells (Appendix Figure 6).

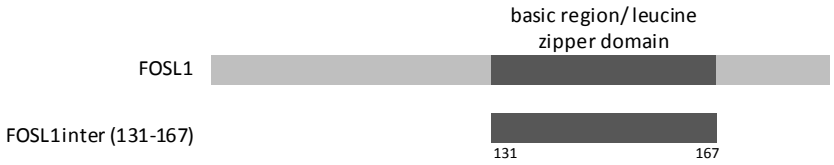

Appendix Figure 6: Schematic map of human full length FOSL1 and FOSL1inter, the bZip region of FOSL1 (amino acids 131-167*),* for generating transgenic melanoma cell lines

Subsequently, the cells were checked for proliferation. Unexpectedly, the overexpression of the dominant-negative *FOSL1* construct had no effect on cellular proliferation (Appendix Figure 7).

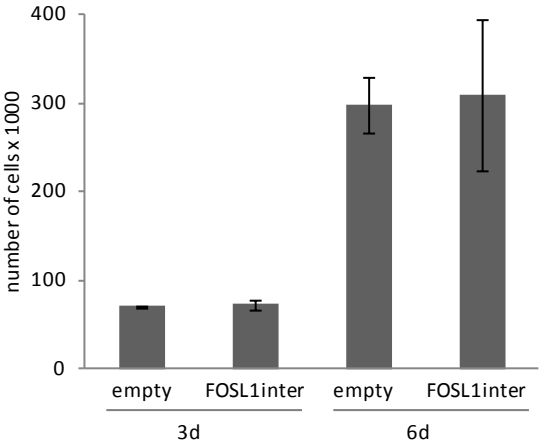

Appendix Figure 7: Proliferation of human MelHo melanoma cells overexpressing the interaction domain of *FOSL1*
Calculation was made from one experiment performed in triplicates.

As soft agar growth of melanoma cells was severely reduced after siRNA mediated knockdown of *FOSL1*, soft agar assay was performed with the MelHo cells overexpressing the FOSL1 interaction domain and compared to empty vector cells. The dominant-negative version of FOSL1 was not able to decrease the anchorage independent growth of the MelHo cells (Appendix Figure 8).

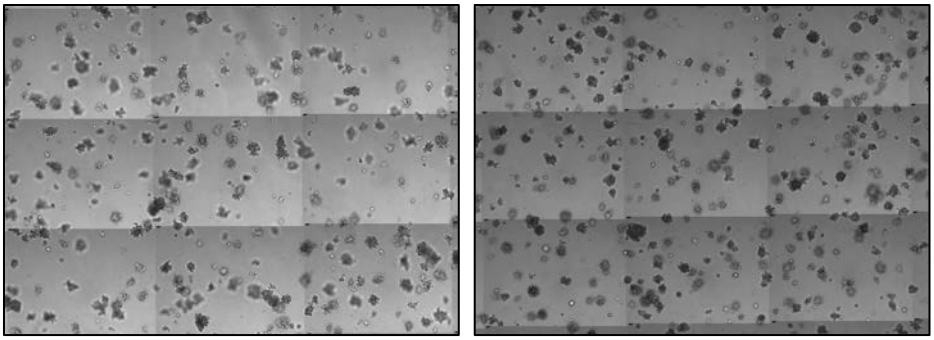

Appendix Figure 8: Soft agar assay of human MelHo melanoma cells overexpressing the JUN interaction domain of FOSL1
Cells were grown in soft agar for 7 days. The experiment was performed once in triplicates.

Due to the negative results of the *FOSL1inter* transgenic MelHo cells and the missing specificity of the TAM67 version of JUN, we decided to discontinue the project.

Bibliography

1. *Zentrum für Krebsregisterdaten* Available from: http://www.krebsdaten.de/Krebs/DE/Content/Krebsarten/Melanom/melanom_node.html.

2. *American Cancer Society. Melanoma Skin Cancer Overview.*; Available from: http://www.cancer.org/cancer/skincancer-melanoma/index.

3. Liu, J.J. and D.E. Fisher, *Lighting a path to pigmentation: mechanisms of MITF induction by UV.* Pigment Cell Melanoma Res, 2010. **23**(6): p. 741-5.

4. Gray-Schopfer, V., C. Wellbrock, and R. Marais, *Melanoma biology and new targeted therapy.* Nature, 2007. **445**(7130): p. 851-7.

5. Sagebiel, R.W., *Melanocytic nevi in histologic association with primary cutaneous melanoma of superficial spreading and nodular types: effect of tumor thickness.* J Invest Dermatol, 1993. **100**(3): p. 322S-325S.

6. Crucioli, V. and J. Stilwell, *The histogenesis of malignant melanoma in relation to pre-existing pigmented lesions.* J Cutan Pathol, 1982. **9**(6): p. 396-404.

7. *Surveillance, Epidemiology, and End Results Program*. Available from: http://seer.cancer.gov/statfacts/html/melan.html.

8. *Deutsche dermatologische Gesellschaft: Ergebnisse des Zentralregisters Malignes Melanom*. Available from: http://www.derma.de/de/daten/leitlinien/leitlinien/malignes-melanom/.

9. Singh, A.D., L. Bergman, and S. Seregard, *Uveal melanoma: epidemiologic aspects.* Ophthalmol Clin North Am, 2005. **18**(1): p. 75-84, viii.

10. *Melanoma Research Foundation*. Available from: http://www.melanoma.org/understand-melanoma/what-is-melanoma/mucosal-melanoma.

11. Kamb, A., et al., *Analysis of the p16 gene (CDKN2) as a candidate for the chromosome 9p melanoma susceptibility locus.* Nat Genet, 1994. **8**(1): p. 23-6.

12. Goldstein, A.M., et al., *High-risk melanoma susceptibility genes and pancreatic cancer, neural system tumors, and uveal melanoma across GenoMEL.* Cancer Res, 2006. **66**(20): p. 9818-28.

13. Quelle, D.E., et al., *Alternative reading frames of the INK4a tumor suppressor gene encode two unrelated proteins capable of inducing cell cycle arrest.* Cell, 1995. **83**(6): p. 993-1000.

14. Serrano, M., G.J. Hannon, and D. Beach, *A new regulatory motif in cell-cycle control causing specific inhibition of cyclin D/CDK4.* Nature, 1993. **366**(6456): p. 704-7.

15. Hussussian, C.J., et al., *Germline p16 mutations in familial melanoma.* Nat Genet, 1994. **8**(1): p. 15-21.

16. Walker, G.J., et al., *Virtually 100% of melanoma cell lines harbor alterations at the DNA level within CDKN2A, CDKN2B, or one of their downstream targets.* Genes Chromosomes Cancer, 1998. **22**(2): p. 157-63.

17. Valverde, P., et al., *Variants of the melanocyte-stimulating hormone receptor gene are associated with red hair and fair skin in humans.* Nat Genet, 1995. **11**(3): p. 328-30.

18. Ranadive, N.S. and I.A. Menon, *Role of reactive oxygen species and free radicals from melanins in photoinduced cutaneous inflammations.* Pathol Immunopathol Res, 1986. **5**(2): p. 118-39.

19. Mitra, D., et al., *An ultraviolet-radiation-independent pathway to melanoma carcinogenesis in the red hair/fair skin background.* Nature, 2012. **491**(7424): p. 449-53.

20. Lopez-Bergami, P., *The role of mitogen- and stress-activated protein kinase pathways in melanoma.* Pigment Cell Melanoma Res, 2011. **24**(5): p. 902-21.

21. Giehl, K., *Oncogenic Ras in tumour progression and metastasis.* Biol Chem, 2005. **386**(3): p. 193-205.

22. Sumimoto, H., et al., *The BRAF-MAPK signaling pathway is essential for cancer-immune evasion in human melanoma cells.* J Exp Med, 2006. **203**(7): p. 1651-6.

23. McKay, M.M. and D.K. Morrison, *Integrating signals from RTKs to ERK/MAPK.* Oncogene, 2007. **26**(22): p. 3113-21.

24. Davies, H., et al., *Mutations of the BRAF gene in human cancer.* Nature, 2002. **417**(6892): p. 949-54.

25. Wan, P.T., et al., *Mechanism of activation of the RAF-ERK signaling pathway by oncogenic mutations of B-RAF.* Cell, 2004. **116**(6): p. 855-67.

26. Dumaz, N., et al., *In melanoma, RAS mutations are accompanied by switching signaling from BRAF to CRAF and disrupted cyclic AMP signaling.* Cancer Res, 2006. **66**(19): p. 9483-91.

27. Fedorenko, I.V., G.T. Gibney, and K.S. Smalley, *NRAS mutant melanoma: biological behavior and future strategies for therapeutic management.* Oncogene, 2013. **32**(25): p. 3009-18.

28. *The cancer genome atlas*

29. Willmore-Payne, C., et al., *Human malignant melanoma: detection of BRAF- and c-kit-activating mutations by high-resolution amplicon melting analysis.* Hum Pathol, 2005. **36**(5): p. 486-93.

30. Minor, D.R., et al., *Sunitinib therapy for melanoma patients with KIT mutations.* Clin Cancer Res, 2012. **18**(5): p. 1457-63.

31. Bastian, B.C., *Understanding the progression of melanocytic neoplasia using genomic analysis: from fields to cancer.* Oncogene, 2003. **22**(20): p. 3081-6.

32. Koprowski, H., et al., *Expression of the receptor for epidermal growth factor correlates with increased dosage of chromosome 7 in malignant melanoma.* Somat Cell Mol Genet, 1985. **11**(3): p. 297-302.

33. Prickett, T.D., et al., *Analysis of the tyrosine kinome in melanoma reveals recurrent mutations in ERBB4.* Nat Genet, 2009. **41**(10): p. 1127-32.

34. Van Raamsdonk, C.D., et al., *Mutations in GNA11 in uveal melanoma.* N Engl J Med, 2010. **363**(23): p. 2191-9.

35. Van Raamsdonk, C.D., et al., *Frequent somatic mutations of GNAQ in uveal melanoma and blue naevi.* Nature, 2009. **457**(7229): p. 599-602.

36. Sarbassov, D.D., et al., *Phosphorylation and regulation of Akt/PKB by the rictor-mTOR complex.* Science, 2005. **307**(5712): p. 1098-101.

37. Toker, A. and A.C. Newton, *Akt/protein kinase B is regulated by autophosphorylation at the hypothetical PDK-2 site.* J Biol Chem, 2000. **275**(12): p. 8271-4.

38. Manning, B.D. and L.C. Cantley, *AKT/PKB signaling: navigating downstream.* Cell, 2007. **129**(7): p. 1261-74.

39. Tzivion, G., M. Dobson, and G. Ramakrishnan, *FoxO transcription factors; Regulation by AKT and 14-3-3 proteins.* Biochim Biophys Acta, 2011. **1813**(11): p. 1938-45.

40. Chin, L., L.A. Garraway, and D.E. Fisher, *Malignant melanoma: genetics and therapeutics in the genomic era.* Genes Dev, 2006. **20**(16): p. 2149-82.

41. Goel, V.K., et al., *Examination of mutations in BRAF, NRAS, and PTEN in primary cutaneous melanoma.* J Invest Dermatol, 2006. **126**(1): p. 154-60.

42. Tsao, H., et al., *Genetic interaction between NRAS and BRAF mutations and PTEN/MMAC1 inactivation in melanoma.* J Invest Dermatol, 2004. **122**(2): p. 337-41.

43. Omholt, K., et al., *Mutations of PIK3CA are rare in cutaneous melanoma.* Melanoma Res, 2006. **16**(2): p. 197-200.

44. Vousden, K.H. and C. Prives, *Blinded by the Light: The Growing Complexity of p53.* Cell, 2009. **137**(3): p. 413-31.

45. Murray-Zmijewski, F., E.A. Slee, and X. Lu, *A complex barcode underlies the heterogeneous response of p53 to stress.* Nat Rev Mol Cell Biol, 2008. **9**(9): p. 702-12.

46. *IARC TP53 DATABASE*.

47. Mar, V.J., et al., *BRAF/NRAS wild-type melanomas have a high mutation load correlating with histologic and molecular signatures of UV damage.* Clin Cancer Res, 2013. **19**(17): p. 4589-98.

48. Honda, R., H. Tanaka, and H. Yasuda, *Oncoprotein MDM2 is a ubiquitin ligase E3 for tumor suppressor p53.* FEBS Lett, 1997. **420**(1): p. 25-7.

49. Wadgaonkar, R. and T. Collins, *Murine double minute (MDM2) blocks p53-coactivator interaction, a new mechanism for inhibition of p53-dependent gene expression.* J Biol Chem, 1999. **274**(20): p. 13760-7.

50. Shvarts, A., et al., *MDMX: a novel p53-binding protein with some functional properties of MDM2.* EMBO J, 1996. **15**(19): p. 5349-57.

51. Gembarska, A., et al., *MDM4 is a key therapeutic target in cutaneous melanoma.* Nat Med, 2012. **18**(8): p. 1239-47.

52. Zhang, Y.P., Y. Xiong, and W.G. Yarbrough, *ARF promotes MDM2 degradation and stabilizes p53: ARF-INK4a locus deletion impairs both the Rb and p53 tumor suppression pathways.* Cell, 1998. **92**(6): p. 725-734.

53. McLure, K.G. and P.W. Lee, *How p53 binds DNA as a tetramer.* EMBO J, 1998. **17**(12): p. 3342-50.

54. Grossman, S.R., *p300/CBP/p53 interaction and regulation of the p53 response.* Eur J Biochem, 2001. **268**(10): p. 2773-8.

55. Avantaggiati, M.L., et al., *Recruitment of p300/CBP in p53-dependent signal pathways.* Cell, 1997. **89**(7): p. 1175-84.

56. Gu, W. and R.G. Roeder, *Activation of p53 sequence-specific DNA binding by acetylation of the p53 C-terminal domain.* Cell, 1997. **90**(4): p. 595-606.

57. Angel, P., et al., *Phorbol ester-inducible genes contain a common cis element recognized by a TPA-modulated trans-acting factor.* Cell, 1987. **49**(6): p. 729-39.

58. Nakabeppu, Y. and D. Nathans, *The basic region of Fos mediates specific DNA binding.* EMBO J, 1989. **8**(12): p. 3833-41.

59. Kaminska, B., et al., *Modulation of the composition of AP-1 complex and its impact on transcriptional activity.* Acta Neurobiol Exp (Wars), 2000. **60**(3): p. 395-402.

60. van Dam, H. and M. Castellazzi, *Distinct roles of Jun : Fos and Jun : ATF dimers in oncogenesis.* Oncogene, 2001. **20**(19): p. 2453-64.

61. O'Shea, E.K., R. Rutkowski, and P.S. Kim, *Mechanism of specificity in the Fos-Jun oncoprotein heterodimer.* Cell, 1992. **68**(4): p. 699-708.

62. *e! ENSEMBL* Available from: http://www.ensembl.org/Homo_sapiens/Gene/Splice?db=core;g=ENSG00000175592;r=11:65892049-65900573.

63. Milde-Langosch, K., *The Fos family of transcription factors and their role in tumourigenesis.* Eur J Cancer, 2005. **41**(16): p. 2449-61.

64. Chinenov, Y. and T.K. Kerppola, *Close encounters of many kinds: Fos-Jun interactions that mediate transcription regulatory specificity.* Oncogene, 2001. **20**(19): p. 2438-52.

65. Pognonec, P., et al., *Cross-family interaction between the bHLHZip USF and bZip Fra1 proteins results in down-regulation of AP1 activity.* Oncogene, 1997. **14**(17): p. 2091-8.

66. Schreiber, M., et al., *Placental vascularisation requires the AP-1 component fra1.* Development, 2000. **127**(22): p. 4937-48.

67. Eferl, R., et al., *The Fos-related antigen Fra-1 is an activator of bone matrix formation.* EMBO J, 2004. **23**(14): p. 2789-99.

68. Jochum, W., et al., *Increased bone formation and osteosclerosis in mice overexpressing the transcription factor Fra-1.* Nat Med, 2000. **6**(9): p. 980-4.

69. Luther, J., et al., *Elevated Fra-1 expression causes severe lipodystrophy.* J Cell Sci, 2011. **124**(Pt 9): p. 1465-76.

70. Bergers, G., et al., *Transcriptional activation of the fra-1 gene by AP-1 is mediated by regulatory sequences in the first intron.* Mol Cell Biol, 1995. **15**(7): p. 3748-58.

71. Mechta, F., et al., *Transformation by ras modifies AP1 composition and activity.* Oncogene, 1997. **14**(7): p. 837-47.

72. Vallone, D., et al., *Neoplastic transformation of rat thyroid cells requires the junB and fra-1 gene induction which is dependent on the HMGI-C gene product.* EMBO J, 1997. **16**(17): p. 5310-21.

73. Kustikova, O., et al., *Fra-1 induces morphological transformation and increases in vitro invasiveness and motility of epithelioid adenocarcinoma cells.* Mol Cell Biol, 1998. **18**(12): p. 7095-105.

74. Bakiri, L., et al., *Fra-1/AP-1 induces EMT in mammary epithelial cells by modulating Zeb1/2 and TGFbeta expression.* Cell Death Differ, 2014.

75. Verde, P., et al., *Deciphering AP-1 function in tumorigenesis: fra-ternizing on target promoters.* Cell Cycle, 2007. **6**(21): p. 2633-9.

76. Zajchowski, D.A., et al., *Identification of gene expression profiles that predict the aggressive behavior of breast cancer cells.* Cancer Res, 2001. **61**(13): p. 5168-78.

77. Belguise, K., et al., *FRA-1 expression level regulates proliferation and invasiveness of breast cancer cells.* Oncogene, 2005. **24**(8): p. 1434-44.

78. Zhao, C., et al., *Genome-wide profiling of AP-1-regulated transcription provides insights into the invasiveness of triple-negative breast cancer.* Cancer Res, 2014. **74**(14): p. 3983-94.

79. Gall, T.M. and A.E. Frampton, *Gene of the month: E-cadherin (CDH1).* J Clin Pathol, 2013. **66**(11): p. 928-32.

80. Song, Y., et al., *An association of a simultaneous nuclear and cytoplasmic localization of Fra-1 with breast malignancy.* BMC Cancer, 2006. **6**: p. 298.

81. Chiappetta, G., et al., *FRA-1 protein overexpression is a feature of hyperplastic and neoplastic breast disorders.* BMC Cancer, 2007. **7**: p. 17.

82. Joseph Sambrook, D.W.R., *Molecular Cloning- a laboratory manual*. Vol. 3. 2001.

83. Wei, C.L., et al., *A global map of p53 transcription-factor binding sites in the human genome.* Cell, 2006. **124**(1): p. 207-19.

84. Teutschbein, J., et al., *Gene expression analysis after receptor tyrosine kinase activation reveals new potential melanoma proteins.* BMC Cancer, 2010. **10**: p. 386.

85. Pakay, J.L., et al., *A 19S proteasomal subunit cooperates with an ERK MAPK-regulated degron to regulate accumulation of Fra-1 in tumour cells.* Oncogene, 2012. **31**(14): p. 1817-24.

86. Yang, S., et al., *MicroRNA-34 suppresses breast cancer invasion and metastasis by directly targeting Fra-1.* Oncogene, 2013. **32**(36): p. 4294-303.

87. Bunz, F., et al., *Requirement for p53 and p21 to sustain G2 arrest after DNA damage.* Science, 1998. **282**(5393): p. 1497-501.

88. Sayan, A.E., et al., *Fra-1 controls motility of bladder cancer cells via transcriptional upregulation of the receptor tyrosine kinase AXL.* Oncogene, 2012. **31**(12): p. 1493-503.

89. Wu, J., et al., *MicroRNA-34a inhibits migration and invasion of colon cancer cells via targeting to Fra-1.* Carcinogenesis, 2012. **33**(3): p. 519-28.

90. Widmer, D.S., et al., *Systematic classification of melanoma cells by phenotype-specific gene expression mapping.* Pigment Cell Melanoma Res, 2012. **25**(3): p. 343-53.

91. Vincek, V., S. Xu, and Y.S. Fan, *Comparative genome hybridization analysis of laser-capture microdissected in situ melanoma.* J Cutan Pathol, 2010. **37**(1): p. 3-7.

92. Huang da, W., B.T. Sherman, and R.A. Lempicki, *Systematic and integrative analysis of large gene lists using DAVID bioinformatics resources.* Nat Protoc, 2009. **4**(1): p. 44-57.

93. Dennis, G., Jr., et al., *DAVID: Database for Annotation, Visualization, and Integrated Discovery.* Genome Biol, 2003. **4**(5): p. P3.

94. Le Douarin, N.M., et al., *Neural crest cell plasticity and its limits.* Development, 2004. **131**(19): p. 4637-50.

95. Bhatt, S., R. Diaz, and P.A. Trainor, *Signals and switches in Mammalian neural crest cell differentiation.* Cold Spring Harb Perspect Biol, 2013. **5**(2).

96. Shah, S.N., et al., *HMGA1 reprograms somatic cells into pluripotent stem cells by inducing stem cell transcriptional networks.* PLoS One, 2012. **7**(11): p. e48533.

97. Ferrell, C.M., et al., *Activation of stem-cell specific genes by HOXA9 and HOXA10 homeodomain proteins in CD34+ human cord blood cells.* Stem Cells, 2005. **23**(5): p. 644-55.

98. Reeves, R. and L. Beckerbauer, *HMGI/Y proteins: flexible regulators of transcription and chromatin structure.* Biochim Biophys Acta, 2001. **1519**(1-2): p. 13-29.

99. Ramos-Nino, M.E., et al., *Fra-1 governs cell migration via modulation of CD44 expression in human mesotheliomas.* Mol Cancer, 2007. **6**: p. 81.

100. Hugo, H., et al., *Epithelial--mesenchymal and mesenchymal--epithelial transitions in carcinoma progression.* J Cell Physiol, 2007. **213**(2): p. 374-83.

101. Lin, K., et al., *The Role of B-RAF Mutations in Melanoma and the Induction of EMT via Dysregulation of the NF-kappaB/Snail/RKIP/PTEN Circuit.* Genes Cancer, 2010. **1**(5): p. 409-420.

102. Kimura, R., et al., *Phosphorylated c-Jun and Fra-1 induce matrix metalloproteinase-1 and thereby regulate invasion activity of 143B osteosarcoma cells.* Biochim Biophys Acta, 2011. **1813**(8): p. 1543-53.

103. Ramos-Nino, M.E., et al., *Microarray analysis and RNA silencing link fra-1 to cd44 and c-met expression in mesothelioma.* Cancer Res, 2003. **63**(13): p. 3539-45.

104. Pavan, W.J. and D.W. Raible, *Specification of neural crest into sensory neuron and melanocyte lineages.* Dev Biol, 2012. **366**(1): p. 55-63.

105. Liu, J., et al., *Developmental pathways activated in melanocytes and melanoma.* Arch Biochem Biophys, 2014. **563C**: p. 13-21.

106. Ben-Porath, I., et al., *An embryonic stem cell-like gene expression signature in poorly differentiated aggressive human tumors.* Nat Genet, 2008. **40**(5): p. 499-507.

107. Vermeulen, L., et al., *Wnt activity defines colon cancer stem cells and is regulated by the microenvironment.* Nat Cell Biol, 2010. **12**(5): p. 468-76.

108. Landsberg, J., et al., *Melanomas resist T-cell therapy through inflammation-induced reversible dedifferentiation.* Nature, 2012. **490**(7420): p. 412-6.

109. Cheli, Y., et al., *Mitf is the key molecular switch between mouse or human melanoma initiating cells and their differentiated progeny.* Oncogene, 2011. **30**(20): p. 2307-18.

110. Leikam C, H.A., Otto C, Murphy DJ, Mühling B, Kneitz S, Nanda I, Schmid M, Wagner TU, Haferkamp S, Bröcker EB, Schartl M, Meierjohann S *In vitro evidence for senescent multinucleated melanocytes as a source for tumor-initiating cells.* Cell Death Dis (accepted), 2015.

111. Ruffini, F., S. D'Atri, and P.M. Lacal, *Neuropilin-1 expression promotes invasiveness of melanoma cells through vascular endothelial growth factor receptor-2-dependent and -independent mechanisms.* Int J Oncol, 2013. **43**(1): p. 297-306.

112. Kulesa, P.M., et al., *Reprogramming metastatic melanoma cells to assume a neural crest cell-like phenotype in an embryonic microenvironment.* Proc Natl Acad Sci U S A, 2006. **103**(10): p. 3752-7.

113. Bianchi, M.E. and A. Agresti, *HMG proteins: dynamic players in gene regulation and differentiation.* Curr Opin Genet Dev, 2005. **15**(5): p. 496-506.

114. Sgarra, R., et al., *Nuclear phosphoproteins HMGA and their relationship with chromatin structure and cancer.* FEBS Lett, 2004. **574**(1-3): p. 1-8.

115. Cleynen, I. and W.J. Van de Ven, *The HMGA proteins: a myriad of functions (Review).* Int J Oncol, 2008. **32**(2): p. 289-305.

116. Edberg, D.D., et al., *Dynamic and differential in vivo modifications of the isoform HMGA1a and HMGA1b chromatin proteins.* J Biol Chem, 2005. **280**(10): p. 8961-73.

117. Watanabe, M., et al., *Characterization of the Stoichiometry of HMGA1/DNA Complexes.* Open Biochem J, 2013. **7**: p. 73-81.

118. Resar, L., et al., *STAT3: A Direct HMGA1 Gene Target Important in Lymphoid Malignancy.* ASH Annual Meeting Abstracts, 2006. **108**(11): p. 2222-.

119. Wood, L.J., et al., *The oncogenic properties of the HMG-I gene family.* Cancer Res, 2000. **60**(15): p. 4256-61.

120. Fedele, M., et al., *Haploinsufficiency of the Hmga1 gene causes cardiac hypertrophy and myelo-lymphoproliferative disorders in mice.* Cancer Res, 2006. **66**(5): p. 2536-43.

121. Foti, D., et al., *Lack of the architectural factor HMGA1 causes insulin resistance and diabetes in humans and mice.* Nat Med, 2005. **11**(7): p. 765-73.

122. Fedele, M., et al., *Transgenic mice overexpressing the wild-type form of the HMGA1 gene develop mixed growth hormone/prolactin cell pituitary adenomas and natural killer cell lymphomas.* Oncogene, 2005. **24**(21): p. 3427-35.

123. Tamimi, Y., et al., *Increased expression of high mobility group protein I(Y) in high grade prostatic cancer determined by in situ hybridization.* Cancer Res, 1993. **53**(22): p. 5512-6.

124. Kim, D.H., et al., *Expression of the HMGI(Y) gene in human colorectal cancer.* Int J Cancer, 1999. **84**(4): p. 376-80.

125. Sarhadi, V.K., et al., *Increased expression of high mobility group A proteins in lung cancer.* J Pathol, 2006. **209**(2): p. 206-12.

126. Flohr, A.M., et al., *High mobility group protein HMGA1 expression in breast cancer reveals a positive correlation with tumour grade.* Histol Histopathol, 2003. **18**(4): p. 999-1004.

127. Abe, N., et al., *Pancreatic duct cell carcinomas express high levels of high mobility group I(Y) proteins.* Cancer Res, 2000. **60**(12): p. 3117-22.

128. Chiappetta, G., et al., *The expression of the high mobility group HMGI (Y) proteins correlates with the malignant phenotype of human thyroid neoplasias.* Oncogene, 1995. **10**(7): p. 1307-14.

129. Qu, Y., et al., *Overexpression of high mobility group A1 protein in human uveal melanomas: implication for prognosis.* PLoS One, 2013. **8**(7): p. e68724.

130. Lin, Y., et al., *miR-26a inhibits proliferation and motility in bladder cancer by targeting HMGA1.* FEBS Lett, 2013. **587**(15): p. 2467-73.

131. Pang, B., et al., *HMGA1 expression in human gliomas and its correlation with tumor proliferation, invasion and angiogenesis.* J Neurooncol, 2012. **106**(3): p. 543-9.

132. Wang, E.L., et al., *Increased expression of HMGA1 correlates with tumour invasiveness and proliferation in human pituitary adenomas.* Histopathology, 2010. **56**(4): p. 501-9.

133. Pegoraro, S., et al., *HMGA1 promotes metastatic processes in basal-like breast cancer regulating EMT and stemness.* Oncotarget, 2013. **4**(8): p. 1293-308.

134. Belton, A., et al., *HMGA1 induces intestinal polyposis in transgenic mice and drives tumor progression and stem cell properties in colon cancer cells.* PLoS One, 2012. **7**(1): p. e30034.

135. Ueda, Y., et al., *High mobility group protein HMGA1 inhibits retinoblastoma protein-mediated cellular G0 arrest.* Cancer Sci, 2007. **98**(12): p. 1893-901.

136. Alla, V., et al., *E2F1 in melanoma progression and metastasis.* J Natl Cancer Inst, 2010. **102**(2): p. 127-33.

137. Esposito, F., et al., *High-mobility group A1 proteins regulate p53-mediated transcription of Bcl-2 gene.* Cancer Res, 2010. **70**(13): p. 5379-88.

138. Adair, J.E., et al., *Inhibition of nucleotide excision repair by high mobility group protein HMGA1.* J Biol Chem, 2005. **280**(37): p. 32184-92.

139. Rass, K. and J. Reichrath, *UV damage and DNA repair in malignant melanoma and nonmelanoma skin cancer.* Adv Exp Med Biol, 2008. **624**: p. 162-78.

140. Hillion, J., et al., *Upregulation of MMP-2 by HMGA1 promotes transformation in undifferentiated, large-cell lung cancer.* Mol Cancer Res, 2009. **7**(11): p. 1803-12.

141. Liau, S.S., A. Jazag, and E.E. Whang, *HMGA1 is a determinant of cellular invasiveness and in vivo metastatic potential in pancreatic adenocarcinoma.* Cancer Res, 2006. **66**(24): p. 11613-22.

142. Reeves, R., D.D. Edberg, and Y. Li, *Architectural transcription factor HMGI(Y) promotes tumor progression and mesenchymal transition of human epithelial cells.* Mol Cell Biol, 2001. **21**(2): p. 575-94.

143. Lau, K.M., et al., *Overexpression of HMGA1 deregulates tumor growth via cdc25A and alters migration/invasion through a cdc25A-independent pathway in medulloblastoma.* Acta Neuropathol, 2012. **123**(4): p. 553-71.

144. Goulet, A.C., et al., *Analysis of cyclooxygenase 2 (COX-2) expression during malignant melanoma progression.* Cancer Biol Ther, 2003. **2**(6): p. 713-8.

145. Hillion, J., et al., *The HMGA1-COX-2 axis: a key molecular pathway and potential target in pancreatic adenocarcinoma.* Pancreatology, 2012. **12**(4): p. 372-9.

146. Tesfaye, A., et al., *The high-mobility group A1 gene up-regulates cyclooxygenase 2 expression in uterine tumorigenesis.* Cancer Res, 2007. **67**(9): p. 3998-4004.

147. Diesch, J., et al., *Widespread FRA1-dependent control of mesenchymal transdifferentiation programs in colorectal cancer cells.* PLoS One, 2014. **9**(3): p. e88950.

148. Abe, N., et al., *Determination of high mobility group I(Y) expression level in colorectal neoplasias: a potential diagnostic marker.* Cancer Res, 1999. **59**(6): p. 1169-74.

149. Desmet, C.J., et al., *Identification of a pharmacologically tractable Fra-1/ADORA2B axis promoting breast cancer metastasis.* Proc Natl Acad Sci U S A, 2013. **110**(13): p. 5139-44.

150. Ogram, S.A. and R. Reeves, *Differential regulation of a multipromoter gene. Selective 12-O-tetradecanoylphorbol-13-acetate induction of a single transcription start site in the HMG-I/Y gene.* J Biol Chem, 1995. **270**(23): p. 14235-42.

151. Cleynen, I., et al., *Transcriptional control of the human high mobility group A1 gene: basal and oncogenic Ras-regulated expression.* Cancer Res, 2007. **67**(10): p. 4620-9.

152. Wood, L.J., et al., *HMG-I/Y, a new c-Myc target gene and potential oncogene.* Mol Cell Biol, 2000. **20**(15): p. 5490-502.

153. Giannini, G., et al., *High mobility group A1 is a molecular target for MYCN in human neuroblastoma.* Cancer Res, 2005. **65**(18): p. 8308-16.

154. Massimi, I., et al., *The HMGA1 protoncogene frequently deregulated in cancer is a transcriptional target of E2F1.* Mol Carcinog, 2013. **52**(7): p. 526-34.

155. Wei, J.J., et al., *Regulation of HMGA1 expression by microRNA-296 affects prostate cancer growth and invasion.* Clin Cancer Res, 2011. **17**(6): p. 1297-305.

156. Mueller, D.W., M. Rehli, and A.K. Bosserhoff, *miRNA expression profiling in melanocytes and melanoma cell lines reveals miRNAs associated with formation and progression of malignant melanoma.* J Invest Dermatol, 2009. **129**(7): p. 1740-51.

157. Reuland, S.N., et al., *MicroRNA-26a is strongly downregulated in melanoma and induces cell death through repression of silencer of death domains (SODD).* J Invest Dermatol, 2013. **133**(5): p. 1286-93.

158. Schartl, M., et al., *A mutated EGFR is sufficient to induce malignant melanoma with genetic background-dependent histopathologies.* J Invest Dermatol, 2010. **130**(1): p. 249-58.

159. Thermes, V., et al., *I-SceI meganuclease mediates highly efficient transgenesis in fish.* Mech Dev, 2002. **118**(1-2): p. 91-8.

160. Glover, J.N. and S.C. Harrison, *Crystal structure of the heterodimeric bZIP transcription factor c-Fos-c-Jun bound to DNA.* Nature, 1995. **373**(6511): p. 257-61.

161. Brown, P.H., et al., *Dominant-negative mutants of cJun inhibit AP-1 activity through multiple mechanisms and with different potencies.* Cell Growth Differ, 1996. **7**(8): p. 1013-21.

162. Kim, J.H., et al., *High cleavage efficiency of a 2A peptide derived from porcine teschovirus-1 in human cell lines, zebrafish and mice.* PLoS One, 2011. **6**(4): p. e18556.

163. Lopez-Bergami, P., et al., *Rewired ERK-JNK signaling pathways in melanoma.* Cancer Cell, 2007. **11**(5): p. 447-60.

164. Matthews, C.P., et al., *Dominant-negative activator protein 1 (TAM67) targets cyclooxygenase-2 and osteopontin under conditions in which it specifically inhibits tumorigenesis.* Cancer Res, 2007. **67**(6): p. 2430-8.

Publications

1. Thoma, E.C., et al., *Ectopic expression of neurogenin 2 alone is sufficient to induce differentiation of embryonic stem cells into mature neurons.* PLoS One, 2012. **7**(6): p. e38651.

2. Thoma, E.C., et al., *Parallel differentiation of embryonic stem cells into different cell types by a single gene-based differentiation system.* Cell Reprogram, 2012. **14**(2): p. 106-11.

3. Haydn, J.M., et al., *The MAPK pathway as an apoptosis enhancer in melanoma.* Oncotarget, 2014. **5**(13): p. 5040-53.

4. Schartl, M., et al., *Whole Body Melanoma Transcriptome Response in Medaka.* PLoS One, 2015. **10**(12): p. e0143057.

5. Maurus, K., et al., *The AP-1 transcription factor FOSL1 causes melanocyte reprogramming and transformation.* Cancer Res, 2016. submitted

Acknowledgements

I would like to thank Prof. Dr. Svenja Meierjohann for supervising me with unlimited encouragement, enthusiasm and patience as my first supervisor. She kindly guided me through my work and was always there when help and advice was needed.

Moreover, I would like to thank Prof. Dr. Christian Stigloher for acting as my second supervisor and for his interest in my work.

I also would like to thank Prof. Dr. Dr. Manfred Schartl, who always provided help and support and who enabled my work on this interesting project at all.

Sincere thanks needs to be given to the Meierjohann-group, including all former and present lab members (Anita Hufnagel, Hannes Haydn, Dani Haug, Alex Schmitt, Max Schaafhausen, Madlen Staus, Johannes Grimm, Claudia Leikam), and of course to all my colleagues and friends of the departments of the PC and the EBC not only for the constructive scientific discussions, but also for the nice working atmosphere and the great lunch breaks.

Finally, I would like to thank Steffen, my family and friends, who also supported me whenever it was necessary and for always believing in me.